University of South-Eastern Norway

www.usn.no

FMH606 Master's Thesis 2023

Energy and Environmental Technology

Optimum conditions and maximum capacity at the amine-based CO_2 capture plant at TCM Mongstad

Shahin Haji Kermani

Faculty of Technology, Natural Sciences, and Maritime Sciences

Campus Porsgrunn

University of South-Eastern Norway

www.usn.no

Course: FMH606 Master's Thesis, 2023

Title: Optimum conditions and maximum capacity at the amine-based CO_2 capture plant at TCM Mongstad

Number of pages: 107

Keywords: TCM, Aspen Plus, Aspen EDR, CO_2 capture, MEA, Simulation, Limitation

Student name: Shahin Haji Kermani

Supervisor: Lars Erik Øi

Co-supervisor: Koteswara Rao Putta

External partner: CO_2 Technology Centre Mongstad (TCM)

Availability Open

Summary:

Using amine-based solutions is a mature method for CO_2 capture. The study simulates this process for Technology Centre Mongstad (TCM) using a rate-based model in Aspen Plus. The main purpose is to develop a rigorous model for TCM and find the operation limits, maximum utilization capacity, and maximum achievable CO_2 removal efficiency at the plant.

The model accuracy is verified by using different scenarios from the test campaign reports at TCM with four main configurations: Combined Heat and Power (CHP) flue gas, Refinery Residue Fluid Catalytic Cracker (RFCC) flue gas, lean vapour compression, and cold rich-solvent bypass. The deviation between the experimental data and simulation results is compared. The model shows more accuracy with more detailed input data and accurate practical parameters.

The verified model is used with scenario MHP with all the TCM configurations to simulate the plant. Aspen EDR is also used to design real heat exchangers. To avoid flooding, the maximum gas flow to the direct-contact cooler and absorber column is 78500 and 52000 Sm^3/hr respectively. There is a maximum reboiler duty of 8.4 and 3.4 MW for RFCC and CHP stripper at the plant respectively. The optimum operating condition to achieve a CO_2 removal efficiency of 90% after amine lean loading adjustment by using maximum gas flow, both strippers, and 15% of rich-solvent bypass gives a total SRD of 3.0 $MJ/kgCO_2$.

By using a maximum amine flow rate of 230 ton/hr, a CO_2 removal efficiency of 98% can be achieved. The optimum modification gives a bypass fraction of 19% and SRD of 3.63 $MJ/kgCO_2$. Moreover, sending the condensed water to the CHP stripper will give an SRD of 3.65 $MJ/kgCO_2$, which is less energy efficient than the previous configuration.

Preface

This report was written during the spring of 2023 as my master's thesis and is part of the master's program in Energy and Environmental technology at the Department of Process, Energy and Environment at the University of South-Eastern Norway (USN).

The focus of this project is to perform a literature review on performance data of amine-based CO_2 capture using MEA at TCM, develop a rate-based model in Aspen Plus on the CO_2 capture process at TCM, verify the model with previous test campaigns, extend and modify the model with TCM plant configurations to find the maximum flow capacity and the plant limitations, and optimize the operating condition to achieve the maximum CO_2 removal efficiency at the plant.

Sincere thanks to my supervisors, Lars Erik Øi and Koteswara Rao Putta, for their supervision, guidance, patience, and support during this thesis. The learning outcome of this study will guide me on my future path, and I will always appreciate these moments. I would also like to express my gratitude towards my family and my girlfriend for their support and encouragement during these months. Your presence warms my heart and gives me the strength to reach my dreams.

The software and tools used during this project were:

Aspen Plus V12, Aspen Exchanger and Design (Aspen EDR) V12, and Microsoft 365 (MS Word 2016, MS Excel 2016, MS Visio 2016).

Porsgrunn, 15th of May 2023

Shahin Haji Kermani

Contents

Nomenclature

Abbreviation	Description
TCM	Technology Centre Mongstad
MEA	Monoethanolamine
DEA	Diethanolamine
TEA	Amino methyl propanol
MDEA	Methyl diethanolamine
CO_2	Carbon dioxide
H_2O	Water
HCO_3	Bicarbonate
CO_3	Carbonate
H_2CO_3	Carbonic acid
NH_3	Ammonia
ID	Induced Draft
CHP	Combined Heat and Power
RFCC	Residue Fluid Catalytic Cracking
CCGT	Combined Cycle Gas Turbine
DCC	Direct-contact cooler
LVC	Lean Vapour Compression
AIC	Absorber intercooling
SRD	Specific Reboiler Duty
USN	University of South-eastern Norway
CAPEX	Capital expenditure
OPEX	Operational expenditures
EDR	Exchanger Design and Rating
LL	Lean CO_2 Loading
MWt	Molecular weight
NRTL	Non-Random Two-Liquid
RK	Redlich-Kwong
STP	Standard Temperature and Pressure
MW	Megawatt
MJ	Megajoule
hr	Hour

1 Introduction

Technology Centre Mongstad (TCM) is the world's largest and most flexible test centre for developing and improving CO_2 capture technologies and a leading competence centre for carbon capture. It is located at one of Norway's most complex industrial facilities, Mongstad in Vestland county, and it was started in 2006 when the Norwegian government and Statoil (now Equinor) agreed to establish the world's largest full-scale CO_2 capture and storage project [1]. It is necessary to have good and robust simulation models to analyze the process behaviour.

There have been performed several projects at the University of South-Eastern Norway (USN) on process simulation of amine-based CO_2 capture. Most of the simulations have been performed with the program Aspen HYSYS and Aspen Plus. In several Master Thesis projects both programs have been used to simulate the amine-based CO_2 capture process at TCM.

The focus of this project is to perform a literature review on performance data of amine-based CO_2 capture using MEA at TCM, develop a rate-based model in Aspen Plus on the CO_2 capture process for the TCM plant operational data, verify the model with previous test campaigns, extend and modify the model with the advanced configurations at the TCM plant to find the maximum utilization capacity of the installed equipment and the operation limits, and optimize the operating condition to achieve the maximum CO_2 removal efficiency by using the maximum gas and amine flow rate and advanced configurations at TCM.

Outline of the thesis

In chapter 2, a history of CO_2 emission levels and the carbon-related health and environmental effects are presented together with the carbon capture technology and different types of solvents including amine solution technology. A brief description of the chemistry of the absorption process is also reviewed. Moreover, the process description of the TCM plant including each piece of equipment and the necessary specifications is presented. This chapter finishes with a thorough literature review and the problem description.

In chapter 3, the simulation model and methodology are presented, including the different simulation tools and necessary calculations. Simulation and model specification including property method, together with the equipment specification of the simulated equipment, is presented in this chapter.

Chapter 4 presents the model validation with different scenarios and performance data from the previous test campaigns and compares them with the simulation results. The scenarios presented in this thesis are categorized into four different configurations: Combined Heat and Power (CHP) flue gas, Refinery Residue Fluid Catalytic Cracker (RFCC) flue gas, lean vapour compression, and rich-solvent bypass.

In chapter 5, the verified rate-based model is extended to simulate the TCM plant with a more detailed heat exchanger simulation and using a specific scenario named MHP. Moreover, simulation modification and the TCM plant utilization limitations for each piece of the installed equipment are discussed and obtained in this chapter. Optimization of the model to obtain maximum plant capacity and the operating condition to achieve the maximum CO_2 removal efficiency are also presented in this chapter.

Chapter 6 presents the results of the model verification for different configurations, a summary of the practical TCM plant limits and modifications, and a discussion about the model accuracy, plant optimization, and energy consumption. Recommended future works are also mentioned in the last section of the chapter.

Chapter 7 presents the conclusion of the thesis.

The task description of this thesis is attached in appendix A.

2 Background and task description

This chapter gives a brief introduction to climate change due to CO_2 emission, CO_2 capture technologies and chemistry, a description of the process at TCM, a summary of earlier work on the subject, and in the end a problem description and the aim of this project.

2.1 CO_2 emission and climate change

Carbon dioxide (CO_2) is one of the major greenhouse gases, and it has been produced in massive quantities in the last decades. The rapid development of modern civilization has increased the number of industries contributing to CO_2 emissions, for example, combustion of coal, coke, and natural gas, fermentation of carbohydrate materials, manufacture of cement and lime, etc. As a result, over thirty billion tons of CO_2 are added to the atmosphere each year [2]. Different sources for the emission of CO_2 are illustrated in table 2.1 [3].

Table 2.1: Profile by process or industrial activity of worldwide large stationary CO_2 sources with emissions of more than 0.1 million tons of CO_2 ($MtCO_2$) per year [3].

Process	Number of sources	Emissions ($MtCO_2\ yr^{-1}$)
Fossil fuels		
Power	4,942	10,539
Cement production	1,175	932
Refineries	638	798
Iron and steel industry	269	646
Petrochemical industry	470	379
Oil and gas processing	Not available	50
Other sources	90	33
Biomass		
Bioethanol and bioenergy	303	91
Total	**7,887**	**13,466**

The emission of carbon dioxide has raised big concerns about the relationship between anthropogenic CO_2 and an increase in global temperature, commonly referred to as global warming. This can bring issues like the melting of snow cover and ice caps, rising sea levels, and more severe weather patterns [4]. Acid rain, smog, and change in the food supply are other negative effects of CO_2 emission on the environment [2].

Furthermore, CO_2 emission poses direct risks to human health, even at low levels. Inflammation reduces cognitive performance, and kidney and bone problems are some of the health problems that are caused by exposure to CO_2 levels as low as 1000 parts per million (ppm) [5].

Figure 2.1 shows atmospheric CO_2 levels measured at Mauna Loa Observatory, Hawaii, in recent years, with natural, seasonal changes removed. The latest level measurement was 420 ppm in December 2022 [6]. Carbon dioxide emissions have increased in recent years and will probably continue to increase in the years to come, and preventing the emissions is important.

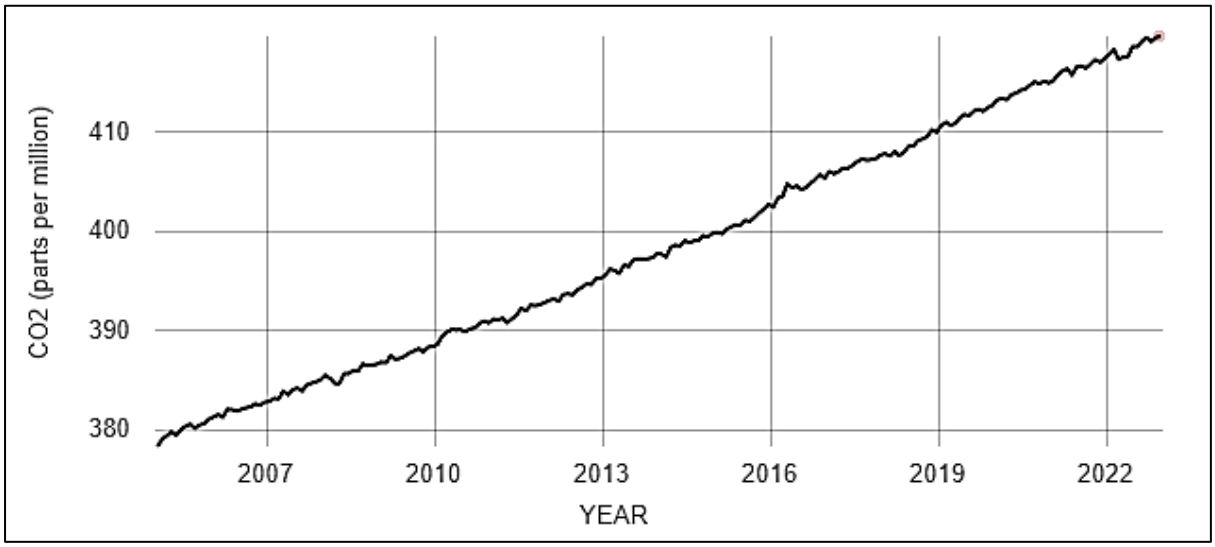

Figure 2.1: Atmospheric CO_2 levels measured at Mauna Loa Observatory, Hawaii [6].

2.2 Carbon capture technologies

A variety of methods have been studied and performed to remove and separate CO_2 from industrial waste in the last decades. Different technologies to remediate CO_2 are mainly classified as precombustion CO_2 capture, post-combustion CO_2 capture, and oxyfuel combustion [4].

2.2.1 Oxyfuel combustion CO_2 capture methods

In oxyfuel combustion, pure O_2 is used for combustion, and as a result, CO_2 and H_2O are the products of the combustion, and separating them can be done easily after the combustion [4].

2.2.2 Pre-combustion CO_2 capture methods

In pre-combustion capture, the fossil fuel is gasified and reacted in a water gas shift reactor to produce H_2 and CO_2. Produced H_2 can be used as an energy carrier; meanwhile, CO_2 is captured [4].

2.2.3 Post-combustion CO_2 capture methods

In post-combustion capture, CO_2 is captured from the effluent gas after the fossil fuels are combusted in conventional energy generation. CO_2 can be stored underground, used for enhancing oil recovery, and as carbon resources to be converted into other useful compounds after capture [4].

Today's technology to capture and separate CO_2 after combustion includes solvents, sorbents, and membranes. In general, the mechanism of carbon capture depends on the chemistry of capturing material. Using solvent and solid sorbent is more common since more types of materials can be used in these technologies. For example, ethanolamine, ammonia, alkali metal solutions, amino acid salts, polyglycol ether, and ionic liquids can be used as solvents; and

soda-lime, active carbon, zeolite, molecular sieve, silica gel, solid amine sorbents, metallic compounds can be used as solid sorbents. Only a few materials can be used in CO_2 capture membranes in comparison with other methods. The general materials for membranes are polyimides, zeolites, and fluoropolymers. Table 2.2 shows the post-combustion technology advantages and challenges [2].

Table 2.2: Post-combustion technology advantages and challenges [2].

CO_2 capture technology	Advantages	Challenges
Solvent	• Chemical solvents provide a high chemical potential (or driving force) necessary for selective capture from streams with low CO_2 partial pressure • Wet-scrubbing allows good heat integration and ease of heat management (useful for exothermic absorption reactions)	• Trade off between heat of reaction and kinetics. Current solvents require a significant amount of steam to reverse chemical reactions and regenerate the solvent, which de-rates power plant • Energy required to heat, cool, and pump nonreactive carrier liquid (usually water) is often significant • Vacuum stripping can reduce regeneration steam requirements, but is expensive
Solid sorbent	• Chemical sites provide large capacities and fast kinetics, enabling capture from streams with low CO_2 partial pressure • Higher capacities on a per mass or volume basis than similar wet-scrubbing chemicals • Lower heating requirements than wet-scrubbing in many cases (CO_2 and heat capacity dependent) • Dry process—less sensible heating requirement than wet scrubbing process	• Heat required to reverse chemical reaction (although generally less than in wet-scrubbing cases) • Heat management in solid systems is difficult, which can limit capacity and/or create operational issues when absorption reaction is exothermic • Pressure drop can be large in flue gas applications • Sorbent attrition
Membrane	• No steam load • No chemicals • Simple and modular designs • 'Unit operation' vs. complex 'process'	• Membranes tend to be more suitable for high-pressure processes such as IGCC • Trade off between recovery rate and product purity (difficult to meet both high recovery rate and high purity) • Requires high selectivity (due to CO_2 concentration and low pressure ratio) • Poor economy of scale • Multiple stages and recycle streams may be required

Several studies are being done on post-combustion CO_2 capture since separating CO_2 at the exhaust gas can be retrofitted to existing power plants. On the other hand, specific types of oxyfuel combustion can also be retrofitted, but it can decrease the efficiency of the furnace, and pre-combustion CO_2 capture needs a gasifier, and it cannot be applied to old facilities. As a result, this project will only focus on post-combustion CO_2 capture technologies [4].

2.3 Different types of solvents

The selection of the appropriate solvent is the most important part of the solvent-based CO_2 capture process. The desired solvent characteristics for the CO_2 capture process shown in table 2.3 affect the total cost and the efficiency of the capture process. The high capacity and the low heat absorption of the solvent are mainly focused as the most important facts. The efficiency of the post-combustion CO_2 capture process can be increased by key process enhancements like "novel solvent regeneration". Such improvements also need some specific features of the solvent [7].

Table 2.3: Desired solvent characteristics for the CO_2 capture process [7].

Desired Solvent Characteristic	Comments
1. High capacity and low heat of absorption	This characteristic is most important as it directly relates to the energy expended (megawatt-hours per metric ton of CO_2), but the laws of thermodynamics connect the absorption capacity and heat,[5] and thus independent variation may be restricted.
2. High mass transfer and chemical kinetics	This characteristic is desirable because it reduces equipment sizes, and for the same equipment and flow will increase capacity because the system will operate closer to the equilibrium limit.
3. Low viscosity	Lower viscosity reduces pumping costs, and usually leads to faster mass transfer and higher heat-transfer rate.[6]
4. Low degradation tendency	Lower degradation tendency reduces the need for solvent replacement or reclaiming, and allows the regenerator to operate at higher pressure (i.e., higher temperature), which increases thermal efficiency.
5. Low volatility	Lower solvent volatility decreases solvent slip in the absorber, and hence reduces the capacity required for the wash system.
6. Toxicity/environmental	Of particular concern here is the formation of toxic by-products like nitrosamines,[7] or environmental impacts from volatility losses.
7. Cost and availability	A readily available chemical that has other uses is often preferred.
8. Low Fouling Tendency	This characteristic is closely related to the solvent melting point and indicates whether it may precipitate as a solid. Solvent degradation may also cause fouling.

Usually, solvents can be categorized into three groups: chemical, physical, and mixture solvents. When chemical solvents are used, CO_2 and solvent undergo a chemical reaction in the liquid phase. This reaction reduces the partial equilibrium pressure and increases the driving force for mass transfer because this chemical reaction consumes the CO_2 in the liquid-gas interface. As a result of that, the CO_2 concentration gradient at the interface increases. Thus, chemical solvents are considered more efficient in CO_2 absorption [8].

The high absorption and desorption mass transfer coefficients, relative insensitivity to acid gases (H_2S) partial pressure, and a high capture level of acid gases are the main advantages of chemical absorbents [8].

High energy requirement for solvent regeneration, the high price of materials, high heat of absorption, high corrosion possibility, multiple side reactions, and emission of environmental pollutants are some disadvantages of chemical absorbents [8].

Amine and ammonia are some examples of chemical absorbents, but amine is the most used absorbent for CO_2 capture purposes. The following table 2.4 shows the properties and limitations of different types of amines [9].

Table 2.4: Desired solvent characteristics for the CO_2 capture process [9].

Amine	Chemical Structure	Advantage	Drawback
Primary amine	$H_2N\text{-}CH_2\text{-}CH_2\text{-}OH$ (*MEA*) $H_2N\text{-}CH_2\text{-}CH_2\text{-}O\text{-}CH_2\text{-}CH_2\text{-}OH$ (DGA)	• High absorption rate • Cheaper • Lower viscosity	• Lower absorption capacity • Higher heat capacity • It cannot be used to absorb COS and CS_2 mixed gas • Higher vapor pressure • Higher heat regeneration cost
Secondary amine	$HN\text{-}(CH_2\text{-}CH_2\text{-}OH)_2$ (*DEA*) $HN\text{-}(CH_2\text{-}C(OH)\text{-}CH_3)_2$ (DIPA)	• It can be used to capture COS and CS_2 gases • Higher loading • Lower heat capacity • Lower vapor pressure • Cheaper • Lower heat of reaction • Less corrosive than *MEA*	• Higher viscosity • A limited solubility in water
Tertiary amine	$N\text{-}(CH_2\text{-}CH_2\text{-}OH)_3$ (TEA) $CH_3\text{-}N\text{-}(CH_2\text{-}CH_2\text{-}OH)_2$ (*MDEA*)	• Higher loading • Lower heat capacity • Lower vapor pressure • Lower heat of reaction	• Lower absorption rate • More expensive • Higher viscosity
Steric hindrance	$HN\text{-}CH\text{-}(CH_3)_2\text{-}CH_2\text{-}OH$ (*AMP*)	• Higher loading • Higher absorption rate and higher loading • Good stripping property	• Higher heat capacity • More expensive • Higher viscosity
Piperazine	$C_4H_{10}N_2$ (*PZ*)	• Anti-oxidative • Anti-thermal degradation • Promote reaction rate	• Water and CO_2 absorption in air

Due to its lower cost and higher boiling point, monoethanolamine (MEA) has traditionally been used as a solvent for capturing CO_2. The MEA, diethanolamine (DEA), aminomethyl propanol (TEA), and methyl diethanolamine (MDEA) are some of the industrially important amines. It has been found that the use of mixed amines is more effective than the use of single amines in the absorption of acid gases. Therefore, to absorb CO_2, more efficient solvents have been developed to address the rapidly increasing energy demands [9]. In this study, monoethanolamine (MEA) is considered as the CO_2 absorbent.

2.4 Amine solution technology

An amine-based solution is currently the most advanced and cost-effective way because of the reversible reactions with CO_2. In this method, CO_2 is absorbed and captured in an aqueous amine solution, in which flue gas is passed. The rich amine, including absorbed CO_2 and leaving it at the bottom, is piped to another process column, called stripper, to be heated with steam. As a result, CO_2 is released from the amine solution. Figure 2.2 shows the schematic of an amine scrubbing unit [4].

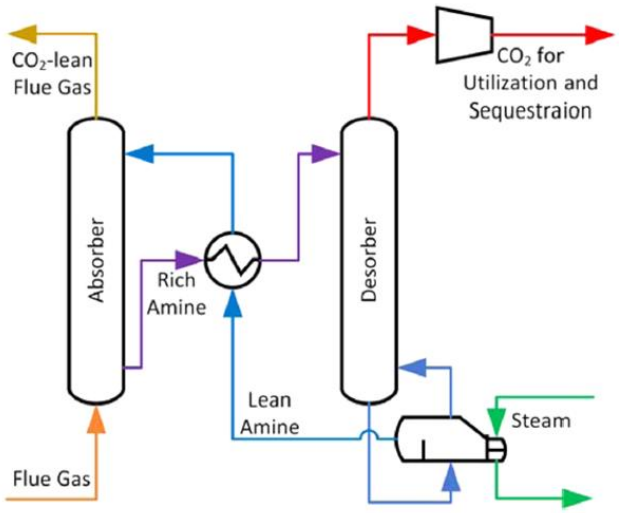

Figure 2.2: Schematic of amine scrubbing unit [4].

The most conventional amine for the CO_2 capture process is monoethanolamine (MEA) with the formula $H_2NC_2H_4OH$ or RNH_2, as it is considered in this study. Other amines that rapidly are used for CO_2 removal are the secondary alkanolamine, DEA (diethanolamine), and the tertiary amine, MDEA (methyl diethanolamine). The amines are usually 20-40 wt% solutions in water when are used as solvents [10].

The main advantage of using MEA is its low molecular weight, which gives the MEA high capacity even at low concentrations. Another advantage is the high alkalinity of primary amines. Moreover, MEA is considered a relatively cheap chemical compared with other amines used for CO_2 capture. It also has relatively less toxicity, and less environmental impact [10].

The main disadvantage of using MEA is the high-energy consumption needed for desorption, especially in higher absorption efficiencies. Moreover, MEA is degradable in high temperatures and reacts with oxygen and other components like sulfur oxides and nitrogen oxides when it is in contact with exhaust gas [10]. Another important issue is the CO_2 emitted during the production of MEA. When MEA is produced, CO_2 is emitted during the Haber-Bosch process. The evaluation of the overall balance of CO_2 emitted and captured is essential to determine the efficiency of the process [11].

Packed columns are often used for absorption and desorption processes. Various types of packing material can be used for this process. The packing material gives a large surface on which the solvent flows for the absorption or desorption of carbon dioxide [12].

It should be noted that there are also different alternatives for process optimization, for example, lean vapour compression (LVC), which can result in energy reductions in some cases. The lean amine from the stripper's bottom is flashed at a lower pressure than the stripper pressure and it is compressed and recycled to the stripper. The CO_2 loading (mole CO_2/mole MEA) in lean amine will decrease, thus reducing the required amine flowrate, or increasing the CO_2 removal efficiency in the absorber [13]. Another example is an absorber intercooling (AIC) in which, a portion of the semi-rich solvent is modified in the middle of the absorber by removing, cooling, and injecting, to reduce the temperature and increase solvent absorption capacity. AIC enhances the driving force of CO_2 transfer at the bottom of the column, which increases the solvent's absorption capacity resulting in a lower solvent circulation rate [14].

2.5 Chemistry of the absorption and desorption process

The carbon capture process happens through a set of reactions when there is contact between the CO_2 in the flue gas and the MEA solvent in the liquid phase. In general, CO_2 reacts with MEA and forms a mixture of carbamate and bicarbonate as the main reaction products during absorption. The following reactions describe how CO_2 can be absorbed into the mixture of MEA solution [15].

Reaction 2.1 and 2.2 describes the hydration reaction of aqueous CO_2 in water and the formation of bicarbonate and carbonate [15].

$$CO_2 + H_2O \leftrightarrow H^+ + HCO_3^- \tag{2.1}$$

$$CO_2 + H_2O \leftrightarrow 2H^+ + CO_3^{2-} \tag{2.2}$$

Reaction 2.3 describes the ionization of water.

$$H_2O \leftrightarrow H^+ + OH^- \tag{2.3}$$

Moreover, some bicarbonate can be formed according to reaction 2.4. The concentration of H_2CO_3 and thus this reaction is negligible at equilibrium condition compared to the concentration of CO_2.

$$H_2CO_3 \leftrightarrow H^+ + HCO_3^- \tag{2.4}$$

The absorption process of CO_2 into MEA solution can be described by reaction 2.5, where carbamate is formed.

$$HCO_3^- + RNH_2 \leftrightarrow RNHCOO^- + H_2O \tag{2.5}$$

It is also possible that CO_3^{2-} be hydrolyzed into HCO_3^- and react with MEA to form carbamate in a similar way as the reaction 2.6.

$$CO_3^{2-} + H^+ + RNH_2 \leftrightarrow RNHCOO^- + H_2O \tag{2.6}$$

CO_2 desorption from the CO_2-saturated MEA solution is a reverse process of absorption. Initially, some HCO_3^- is heated to release CO_2 as the reaction 2.7 and 2.8, and other HCO_3^- reacts with $MEAH^+$ to form carbamate as the reaction 2.9.

$$CO_3^{2-} + 2H^+ \xrightarrow{Heating} CO_2(g) + H_2O \tag{2.7}$$

$$HCO_3^- + 2H^+ \xrightarrow{Heating} CO_2(g) + H_2O \tag{2.8}$$

$$2HCO_3^- + RNH_3^+ \xrightarrow{Heating} RNHCOO^- + CO_2(g) + 2H_2O \tag{2.9}$$

Afterward, the carbamate is decomposed to MEA and CO_2 under thermolysis, to regenerate the solvent as the reaction 2.10.

$$RNHCOO^- + H^+ \xrightarrow{Heating} RNH_2 + CO_2(g) \tag{2.10}$$

Figure 2.3 illustrates the mechanism of CO_2 capture into the MEA solution.

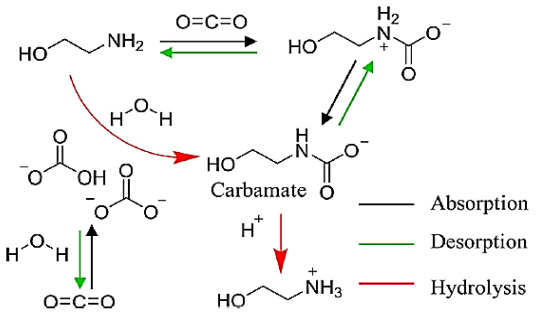

Figure 2.3: Mechanism of CO_2 capture into MEA solution [15].

2.6 Process description at TCM

Technology Centre Mongstad (TCM) is a highly flexible and well-instrumented generic amine plant, designed and constructed by Aker Solutions and Kværner, and it is aimed to accommodate a variety of technologies with capabilities of treating flue gas streams. The plant works generally with two different types of flue gas: Combined Heat and Power (CHP) and Refinery Residue Fluid Catalytic Cracker (RFCC). In general, CHP flue gas has a lower concentration of CO_2 in comparison with RFCC flue gas. Moreover, RFCC flue gas usually has a lower temperature (around 70°C) than CHP flue gas (around 140°C). The CHP flue gas can be further enriched with CO_2 from a CO_2 recycle line, and the RFCC flue gas can be diluted with air to reach a target CO_2 concentration [16]. Figure 2.4 shows the process flow diagram for CO_2 capture at TCM plant [17].

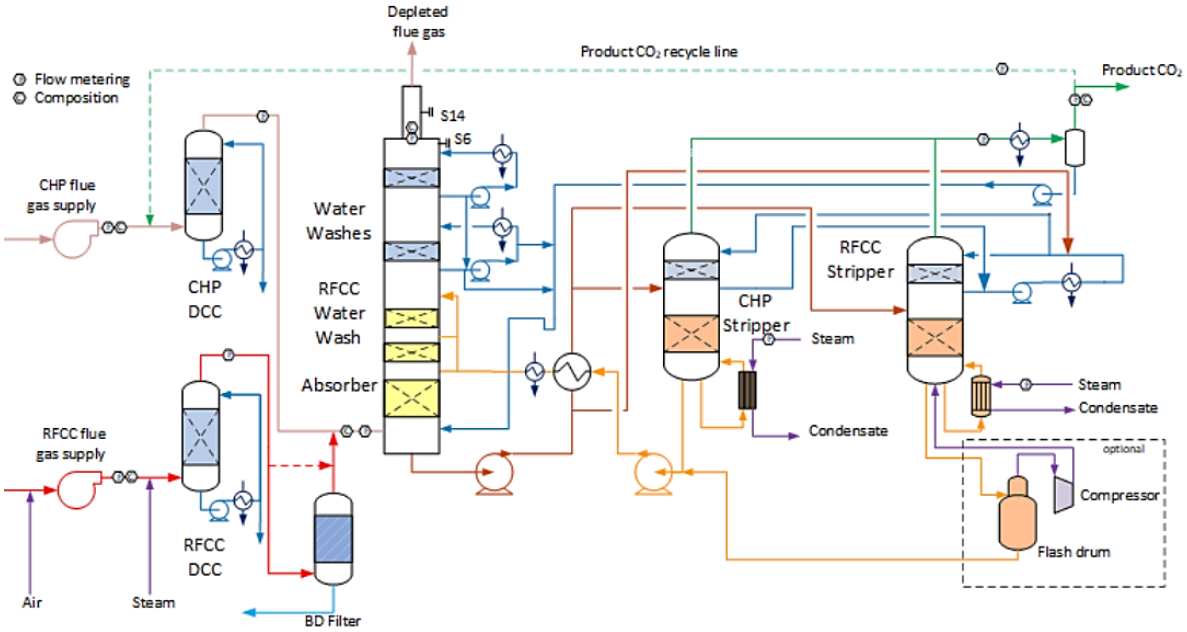

Figure 2.4: A process flow diagram of the TCM Amine plant with the illustration of the two different flue gas (CHP and RFCC) as well as the available strippers [17].

The major system at TCM includes [16]:

- Two induced draft (ID) blowers for both CHP and RFCC flue gas that sucks the flue gas out of the chimney to TCM by insulated pipes, to overcome the pressure drops and blow the flue gas through the plant with a lower output capacity of up to about 270 mbar and 70,000 Sm^3/h.

- Water spray system on the CHP flue gas duct to reduce the temperature of the gas before entering the direct-contact cooler system. Using that, the temperature will be decreased by around 50°C.

- CHP and RFCC direct-contact cooler (DCC) systems to quench and lower the temperature and saturate the incoming flue gas with a counter-current flow water to improve the efficiency of the absorption process and provide pre-scrubbing on the flue gas. It is noted that the temperature of the gas cannot be cooled down by more than 50°C with DCC, since it will cause a lot of pressure drop, which will lead to a significant heat duty. This is the main reason that water sprays are used before DCC at TCM plant.

- An absorber to remove CO_2 from the flue gas using MEA. The absorber has a rectangular polypropylene-lined concrete column with a cross-section area of 3.55*2 m and a total height of 62 m. The cross-sectional area is also corresponding to a diameter of 3 m in a circular cross-section.

- The lower regions of the tower, where the amine solution contacts the flue gas and consists of three sections of structured stainless-steel packing of 12 m, 6 m, and 6 m of height, respectively (total height is 24 m).

- Water-wash systems in the upper region of the absorber column, to scrub and clean the flue gas, particularly of any solvent carryover. The water-wash system consists of two sections of structured stainless-steel packing, both have a height of 3 m. The water-wash system is also used to maintain the water balance of the solvent by using heat exchangers to adjust the temperature of the circulating water.

- Liquid collector trays, and mesh mist eliminators that are located at various locations in the tower.

- A stack located at the top of the absorber, where the CO_2-depleted flue gas exits the absorber column through it.

- Striper columns to recover the captured CO_2 and return the lean MEA to the absorber. There are two independent stripper columns: CHP stripper with a 1.25 m diameter and a 30 m of height, and RFCC stripper with 2.2 m in diameter and also a 30 m of height. The rich MEA exits at the bottom of the absorber and is pumped to 1.6 m from the top of the strippers.

- A lean/rich plate heat exchanger in which, the rich MEA exiting the absorber recovers heat from the lean MEA exiting the stripper. During this transportation, the hot lean MEA releases energy to the rich MEA entering the desorber.

- An overhead condenser system that is connected to both stripper columns where the CO_2 and water leaving the strippers is cooled down to separate the water. The cooled and dried CO_2 is then released into the atmosphere.

- The upper region of the stripper column consists of a section of structured stainless-steel packing, with a height of 1.6 m, and the lower region of the stripper consists of structured stainless-steel packing with a height of 8 m.

- A CHP stripper reboiler, and an RFCC stripper reboiler that re-heats the lean MEA and put it back into the stripper to keep the strippers at the desired temperature.

- The RFCC stripper is also equipped with a Lean Vapour Compression (LVC) system, including a flash drum and a compressor. The hot lean amine exiting the stripper is throttled to a lower pressure and fed to the flash drum generating steam. In the flash drum, steam and lean amine solvent are separated. Steam from the flash drum is compressed in the compressor at the expense of electrical energy and is fed to the stripper bottom, which provides extra energy to regenerate rich amine and reduces the consumption of low-pressure steam. Lean amine solvent from the flash drum is pumped back to the absorber through the rich/lean heat exchanger [18].

- A heat exchanger as a cooler, which cools down the lean amine to the required feed temperature in the lean amine inlet [18].

- A cold rich-solvent bypass upstream before the lean-rich amine heat exchanger to the stripper top is introduced in a recent modification to the plant. This is intended to improve the energy performance of the plant. Using that, the separated water from the condenser will be sent to the lean/rich heat exchanger since it is only possible to send one stream to the top of the stripper at a time [17].

- An absorber intercooling (AIC) has been added to the plant in 2021 in which, a portion of the semi-rich solvent is modified in the middle of the absorber (12 m from the bottom of the absorber) by removing, cooling, and injecting, to reduce the temperature and increase solvent absorption capacity. It decreases the sensible heat required to raise the temperature of the solvent in the stripper column, thus reducing the regeneration energy [14].

2.7 Literature review

Relevant earlier work that has been done on the process of carbon capture is presented below.

- Lars Erik Øi (2007) simulated CO_2 removal by amine absorption from a gas-based power plant, using Aspen HYSYS, at USN. Lars showed that adjusting the Murphree Efficiency outside the simulation tool could be a practical approach to simulate CO_2 removal by Aspen HYSYS [19].

- Finn A. Tobiesen, Hallvard F. Svendsen, and Olav Juliussen from SINTEF (2007) developed a rate-based model of acid gas absorption and a simplified absorber model.

They validated the models against mass-transfer data obtained from a 3-month campaign in a laboratory pilot-plant absorber. It was found that the simplified model was satisfactory for lower CO_2 loading, whiles the rigorous model had a better fit for higher CO_2 loading [20].

- Luo et al., at NTNU (2009), used sixteen data sets from four different pilot plant studies and validated the data with simulations in four different simulation tools (Aspen Plus equilibrium-based, Aspen Plus rate-based, ProMax, ProTreat^{TM}, and CO_2SIM). They concluded that while the reboiler duties, concentration, and temperature profiles were less predictable, all the simulation tools were able to present reasonable predictions on the overall performance of the CO_2 absorption rate [21].

- Espen Hansen (2011) compared Aspen HYSYS, Aspen Plus, and ProMAX simulations of CO_2 capture with MEA in his master thesis at USN. He concluded that Aspen HYSYS and Aspen Plus give similar results, while the results from ProMAX deviated from the Aspen tools [22].

- Cousins (2011) analyzed process flow sheet modifications for energy-efficient CO_2 capture. His suggested modifications included split flow, rich bypass, vapour recompression, and inter cooling using rate-based simulation. Finding an optimum ratio of the rich-solvent bypass was also conducted by Cousins [23].

- Lars Erik Øi (2012) at USN, compared Aspen HYSYS and Aspen Plus (rate-based and equilibrium) simulation of CO_2 capture with MEA. The conclusion was that there were small deviations in the equilibrium-based model in Aspen HYSYS and Aspen Plus. Øi also found larger deviations between the equilibrium-based calculations and the rate-based calculations [24].

- Ying Zhang and Chau Chyun Chen (2013) at the University of Kaiserslautern, simulated 19 data sets of CO_2 absorption in MEA with rate-based and equilibrium-based models. Their result shows that the rate-based model yields reasonable predictions, while the equilibrium-based model fails to predict these key performance variables [25].

- Stian Holst Pedersen Kvam (2013) compared Aspen Plus (rate-based and equilibrium-based) and Aspen HYSYS (Kent-Eisenberg and Li-mather) simulations of CO_2 capture with MEA for his master thesis at USN. His main goal was to compare the energy consumption of a standard process, with vapour recompression and also with a vapour recompression with split stream [26].

- Kvam's work was similar to Even Solnes Birkelund (2013), who worked on his master's thesis at UIT. Birkelund used Aspen HYSYS and used Kent-Eisenberg as the thermodynamic model for the aqueous amine solution, and Peng-Robinson for the vapour phase for the simulation and compared a standard absorption process, a vapour recompression process, and a lean split with vapour recompression process. The configurations were evaluated due to the energy cost. The results showed that lean split vapour recompression and vapour recompression had the lowest, and the standard absorption process has a much higher energy cost [27].

- Lars Erik Øi and Stian Holst Pedersen Kvam (2014) at USN, used Aspen HYSYS and Aspen Plus and simulated different absorption and desorption configurations for 85% CO_2 removal from a natural gas combined cycle power plant. In Aspen Plus, both an equilibrium-based model including Murphree Efficiency, and a rate-based model were used. The results show that by changing the absorption process configuration from the standard process, all simulation models calculate the same trends in the reduction of equivalent heat consumption [28].

- Inga Strømmen Larsen (2014) simulated a rate-based Aspen Plus model and compared the results to experimental data from TCM for her master thesis at USN. Larsen found that the TCM model used in Aspen Plus was in general agreement with the experimental data. She also found temperature and loading profiles are similar to the experimental data by adjusting parameters [29].

- Espen Steinseth Hamborg et al (2014), published a paper with the results from the MEA testing at TCM during the 2013 test campaign. The paper shows the CO_2 removal efficiency, temperature measurement, and experimental data for the process [16].

- Solomon Aforkoghene Aromada and Lars Erik Øi (2015) at USN, studied on how reduction of energy consumption can be achieved by using alternative configurations. They simulated standard vapour recompression and vapour recompression with split stream in Aspen HYSYS, for 85% amine-based CO_2 removal. The results showed that it is possible to reduce energy consumption with both the vapour recompression and the vapour recompression combined with split-stream processes [30].

- Ye Zhu (2015) simulated an equilibrium model in Aspen HYSYS for his master thesis at USN, based on the data from TCM 2013 campaign published by Hamborg et al [16]. He adjusted the Murphree Efficiency to fit the CO_2 removal efficiency and temperature profile from the experimental results. Zhu found that a linear decrease in Murphree efficiency from top to bottom can give a good temperature prediction [31].

- Coarlie Desvignes (2015) worked on a master's thesis at Lyon CPE. He evaluated the performance of the TCM flowsheet model in Aspen Plus and compared it with the data obtained in the 2013 and 2014 test campaigns at TCM. Desvignes found that even though the Aspen Plus model for TCM performed well for 30 and 40wt% MEA, it cannot work well for higher solvent flow rates and flue gas temperatures [32].

- Kai Arne Sætre (2016) simulated 7 sets of experimental data from the amine-based CO_2 capture process at TCM, with Aspen HYSYS (Kent-Eisenberg and Li-Mather) and Aspen Plus (rate-based and equilibrium) for his master's thesis at USN. He found that it is possible to fit a rate-based model by adjusting the IAF and an equilibrium-based model by adjusting the E_M. Both Aspen HYSYS and Aspen Plus can give good results if there are only small changes in the parameters [33].

- Erik Sundbø (2017) for his master thesis at USN, simulated different absorber heights with Aspen HYSYS, varying between 5 and 15 m, and compared the cost for both a standard process and a vapour recompression configuration. He concluded that a

5-stage absorption column gives the lowest cost, while a vapour-recompression process with 15 stages is the most energy optimum case with the highest removal rate [34].

- Mohammad Rehan et al. (2017), studied the performance and energy savings of installing an intercooler in a CO_2 capture system. They used Aspen HYSYS to simulate the CO_2 capture model. The results showed improved CO_2 recovery performance and the potential for significant savings in MEA solvent loading and energy requirements, by installing an intercooler in the system [35].

- Erik Gjernes (2017) published the results from 30 wt% MEA performance testing at TCM. The main objective was to demonstrate and document the performance of the plant [36].

- Leila Faramarzi et al. (2017), published a paper with the results from the MEA testing at TCM during the 2015 test campaign. The paper shows CO_2 removal efficiency, temperature measurement, and experimental data for the process [37].

- Monica Garcia, Hanna K. Knuutila, and Sai Gu (2017) validated a simulation model of the desorption column built in Aspen Plus v8.6. They used four experimental pilot campaigns with 30wt% MEA. The results showed a good agreement between the experimental data and the simulated results [38].

- Ole Røsvik (2018) simulated the TCM data from the test campaign in 2013, published by Hamborg et al [16] in Aspen HYSYS and Aspen Plus (equilibrium and rate-based) for his master's thesis at USN. He found that both Aspen HYSYS and Aspen Plus will give good results if there are only small changes in the parameters [39].

- Lars Erik Øi, Kai Arne Sætre, and Espen Steinseth Hamborg (2018) at USN, compared 4 sets of experimental data from the amine-based CO_2 capture process at TCM, with different equilibrium-based models in Aspen HYSYS and Aspen Plus, and a rate-based model in Aspen Plus. They concluded that equilibrium and rate-based models perform equally well in fitting the performance data and in predicting the performance at different conditions [40].

- Muhammad Ismail Shah (2019) Presented the results of the advanced amine plant process configuration at TCM for 6 different cases of RFCC flue gas with 30 wt% MEA. The advanced configuration in addition to the conventional configuration consists of a Brownian diffusion filter, a three-stage water wash system, an online sampling system tolerating aerosol, and operational parameters. The result showed reduced SRD and aerosol-based amine emissions. Shah also suggested having a rich bypass of the solvent for further reduction of SRD [18].

- Meuleman (2019) discussed the results of CO_2 capture at TCM by using ION Engineering's advanced solvent on 8 different RFCC and 5 different cases of CHP flue gases from the adjacent Statoil refinery, with different CO_2 concentrations from 3.6% to 15% [41].

- Sofie Fagerheim (2019) used the stage efficiency profile developed by Zhu [31], to simulate and develop other profiles in Aspen HYSYS for her master's thesis at USN. Sofie concluded that the profiles can be fitted to different tests by using a multiplication factor named "Murphree efficiency factor". Five of the cases documented by Kai Arne Sætre [33] were used in her study. She also compared the result with rate-based model simulations using Aspen Plus [42].

- Fosbøl (2019) presented the process variables data from the lean vapour compressor campaign at TCM. He tested 16 cases with various parameters such as LVC pressure, solvent flow, inlet flue gas CO_2 concentration, and stripper pressure to create knowledge on the process performance of LCV on the CO_2 capture efficiency and energy profile of the TCM plant [43].

- Sumudu Karunarathne and Lars Erik Øi (2019) at USN compared the removal efficiency and physical properties of density and viscosity in a CO_2 absorption column in equilibrium-based and rate-based simulation in Aspen HYSYS and Aspen Plus. They fitted the experimental data from CO_2-rig located at USN, Norway, by adjusting the Murphree efficiency equal to 12% in all stages. Different flow rates were simulated in this study [44].

- Njål Sæter (2021) simulated the results of a pilot plant data from TCM for both high and low CO_2 exhaust gas inlet concentrations in both a rate-based model in Aspen Plus and an equilibrium-based model in Aspen HYSYS for his master's thesis at USN. In his work, the rate-based model was fitted by only changing the liquid hold-up factor, and in the equilibrium-based model, a Murphree efficiency was specified for 24 and 18 stages in the absorber column to fit the performance data and the temperature profile. An E_M-factor was used to fit other performance data in different scenarios [45].

- Hume (2021) presented the results from MEA testing at TCM with RFCC flue gas with a high concentration of CO_2 (13-14%). These data can provide a new baseline case for 30 wt% MEA solvent in higher concentration flue gas capture cases [46].

- Muhammad Ismail Shah (2021) conducted a cost reduction study for MEA-based CO_2 capture at TCM. During this campaign, the main focus was on thermal energy optimization at different flue gas flow rates through the absorber column and MEA emissions, with a target for reduced CAPEX and OPEX. New options such as rich-solvent bypass to stripper overhead were also conducted in his tests [17].

- Arshad (2023) at Khalifa University of Science and Technology studied techno-economic evaluations of advanced MEA-based CO_2 capture process configurations applied to a 750 MW Combined Cycle Gas Turbine (CCGT) power plant. Arshad validated and used a rigorous rate-based model in Aspen Plus including intercooling, rich solvent bypass, and lean vapour recompression, with a focus on energy and cost reductions [14].

2.8 Problem description

Background

Many MEA test campaigns have been performed at TCM during the last decade. Some of the results from TCM's open test campaigns have been published and used in this study and some of the other similar studies. However, there is new data that has not been published and will be used in this thesis for the first time.

The results from test campaigns at TCM were published by Hamborg (2014) [16], Faramarzi (2017) [37], Gjernes (2017) [36], Fosbøl (2019) [43], Meuleman (2019) [41], Hume (2021) [46], and Ismail Shah (2019 and 2021) [17], [18].

USN has produced several papers on amine-based CO_2 capture with different simulation tools, such as Aspen HYSYS and Aspen Plus. Performance data from the test campaigns at TCM have been used in these papers. In these studies, the rate-based model in Aspen Plus and the equilibrium-based model in both Aspen Plus and Aspen HYSYS have been used to simulate the plant and fit the performance data. Moreover, many studies tried to predict plant performance under changed conditions [19], [22], [24], [26], [28], [29], [31], [33], [34], [39], [40], [42], [45].

Some studies focused on the plant configuration modification and optimization of the energy and cost in the CO_2 capture process [17], [26], [28], [30], [34], [35], [44].

In general, there is still a potential in increasing the reliability of the results in the previous models and also in the operating condition at the plant.

Approach

In this thesis, a rate-based model in Aspen Plus v.12 is used to simulate the TCM plant, including intercooling, lean vapour compression, and rich solvent bypass. The heat exchangers, the reboilers, and the condenser are designed using Aspen Exchanger Design and Rating (Aspen EDR) v.12 as the real equipment in the plant. The accuracy of the model is tested by experimental data from previous test campaigns at TCM. Moreover, the plant limitations, the maximum operating capacity of the plant, the optimum operating condition by using maximum flow capacity, and the maximum achievable CO_2 removal efficiency are presented in this study.

Aim of Project

The project aims to contribute to achieving and verifying a rigorous rate-based model that gives reliable results in the CO_2 removal efficiency and other process parameters for the TCM plant operational data using MEA solvent from different test campaigns.

The second aim of the project is to investigate the operation limits and the maximum utilization capacity in different installed equipment of the TCM plant to be able to optimize the plant for high-capacity operations. Studying optimum operation conditions to achieve the maximum CO_2 removal efficiency by using maximum gas and amine flow rate and advanced configurations at TCM is another aim of the project.

3 Method

In this chapter, the simulation method, different simulation tools that have been used, necessary calculations, fluid properties in the simulation, model specification, and equipment specification for each piece of simulated equipment are presented.

3.1 Simulation methodology

The simulation tools used in this thesis and the required calculations together with the simulation and equipment specification of the TCM plant are discussed in this section.

3.1.1 Simulation tools

Several simulation tools can be used to simulate the amine-based CO_2 capture process and calculate the CO_2 removal efficiency such as Aspen HYSYS, Aspen Plus, Pro/II, ProTreat, and ProMax. In this thesis, a rate-based model in Aspen Plus v.12 is used. Rate-based models are based on rate expressions for chemical reactions, mass transfer, and heat transfer.

Heat exchanger design is an important part of this thesis to simulate an accurate model and predict the plant behavior properly. Heat exchangers, including reboilers and condensers, are designed in Aspen Exchanger Design and Rating (Aspen EDR) v.12 and the provided data is then imported to Aspen Plus.

3.1.2 Calculating composition of the lean amine

The lean amine in the reports is normally specified by the following parameters:

- Lean MEA concentration in water [wt%]
- Lean CO_2 loading (LL) [mol CO_2/mol MEA]
- Lean amine supply flow rate [kg/h]
- Lean amine supply temperature [°C]
- Lean amine density [kg/m^3]

The lean amine data in TCM reports includes LL and MEA concentration. However, to input these data in Aspen Plus, detailed compositions of the amine are required. By having the concentration and LL, the volume percentage of MEA, water, and CO_2 can be calculated using table 3.1 and the equation (3.1) to (3.3).

Table 3.1: Molecular weight of lean amine compositions

Lean amine composition	Molecular Weight	Unit
MEA	61.08	gr/mole
Water	18.0153	gr/mole
Carbon Dioxide	44	gr/mole

The volume percentage of MEA in the lean amine supply is calculated by the equation (3.1).

$$MEA\ vol\%\ in\ lean\ amine = \frac{\frac{MEA\ wt\%}{MWt\ MEA}}{\frac{MEA\ wt\%}{MWt\ MEA} + \frac{MEA\ wt\%}{MWt\ MEA} \cdot LL + \frac{1 - MEA\ wt\%}{MWt\ H_2O}} \quad (3.1)$$

MWt is an abbreviation for molecular weight. The volume percentage of CO_2 in the lean amine supply is calculated by the equation (3.2).

$$CO_2\ vol\%\ in\ lean\ amine = \frac{\frac{MEA\ wt\%}{MWt\ MEA} \cdot LL}{\frac{MEA\ wt\%}{MWt\ MEA} + \frac{MEA\ wt\%}{MWt\ MEA} \cdot LL + \frac{1 - MEA\ wt\%}{MWt\ H_2O}} \quad (3.2)$$

The volume percentage of water in the lean amine supply is calculated by the equation (3.3).

$$Water\ vol\%\ in\ lean\ amine = 1 - MEA\ vol\% - CO_2 vol\% \quad (3.3)$$

The volume percentage of MEA, CO_2, and water found above, can be used as lean amine supply specifications in Aspen Plus.

3.1.3 Calculating CO_2 removal efficiency

CO_2 removal efficiency can be found in four different ways as it is shown in table 3.2 [47].

Table 3.2: Different methods for calculating CO_2 removal efficiency.

Method 1	Method 2	Method 3	Method 4
$\frac{P}{S}$	$\frac{P}{P + D}$	$\frac{S - D}{S}$	$1 - \frac{O_{CO2}}{(1 - O_{CO2})} \frac{(1 - I_{CO2})}{I_{CO2}}$

S=Flue gas supply

D=Depleted flue gas

P=Product CO_2

O_{CO2}=Depleted flue gas CO_2 content, dry basis

I_{CO2}=Flue gas supply CO_2 content, dry basis

In this report, method 3 is used to calculate the CO_2 removal efficiency. This method only depends on the CO_2 flow in the flue gas supply and the depleted flue gas. The CO_2 flow from the stripper column is not included in this calculation and it will be shown as a separate parameter in the simulations. The uncertainty of this method was calculated as 2.8% in Hamborg (2014) [16].

3.1.4 Specific reboiler duty (SRD)

Specific reboiler duty (SRD) is an important parameter to measure the carbon capture process efficiency in energy consumption. SRD is defined as the amount of reboiler duty used in the stripper column for each kilogram of CO_2 that is released into the atmosphere, and it usually is presented with the unit of MJ/kgCO_2. Equation (3.4) shows the formula to calculate the SRD in a process.

$$SRD\ \left[\frac{MJ}{kg_{CO2}}\right] = \frac{Reboiler\ Duty\ \left[\frac{MJ}{hr}\right]}{CO_2\ released\ \left[\frac{kg_{CO2}}{hr}\right]} \tag{3.4}$$

3.1.5 Gas flow rate unit conversions

The inlet gas flow in the reports is given in Sm^3/hr. To convert the unit to kmol/hr, we need to use a coefficient as it is shown in the equation (3.5). This coefficient can be found by the ideal gas law formula in equation (3.6).

$$Gas\ flow\ rate\ \left[\frac{kmol}{hr}\right] = Gas\ flow\ rate\ \left[\frac{Sm^3}{hr}\right] \cdot \frac{1}{23.64}\left[\frac{kmol}{Sm^3}\right] \tag{3.5}$$

$$V_m = \frac{RT}{P} = \frac{8.314\left[\frac{kJ}{kmol \cdot k}\right] \cdot 288.15[K]}{101.325\ [kPa]} = 23.64\ \left[\frac{Sm^3}{kmol}\right] \tag{3.6}$$

The coefficient calculated in equation (3.6) is based on standard conditions chosen by TCM to be the temperature of 15°C and the pressure of 1 atm. Even though the input data to Aspen Plus can be in different units, there is a need to convert all the gas flow rates to kmol/hr. The reason is that the standard conditions can be different, and it can affect the simulation results.

The result from using equation (3.5) can deviate from measured data in some of the reports, where the inlet flue gas is given in both volume flow and molar flow. The reason might be due to uncertainties in the measured data at TCM. In this thesis, the calculated molar flow based on equation (3.5) is presented as the result.

3.1.6 Calculating deviation of the results

To be able to validate the simulation model, a comparison between the simulation results and the experimental data is necessary. This comparison is shown as a deviation, and it is calculated by equation (3.7). This equation is used in chapter 6.

$$Deviation\ [\%] = \frac{|Experimental\ data - Simulation\ result|}{Experimental\ data} \tag{3.7}$$

3.2 Simulation specification

3.2.1 Property method in the simulation tool

To start a rate-based simulation with Aspen Plus v.12, a local model example from Aspen library named "ENRTL-RK_Rate_Based_MEA_Model" was chosen. This file is categorized as a carbon capture process by using MEA with necessary defined properties, packages, and equation of states.

By using this file in Aspen Plus, Elec-NRTL thermodynamic package is chosen, including the Redlich-Kwong equation of state (RK) for the generation of gas properties. The property method chosen here is called NRTL-RK in Aspen Plus.

Further simulations in this thesis are based on this file and will start from scratch by regenerating the equipment and defining the streams.

3.2.2 Model specifications

The specifications of the rate-based model used in this thesis are constant in each simulation for the accuracy test and for the TCM plant in further sections. Table 3.3 shows the model specification used for the simulation.

Table 3.3: Specification of the model used for rate-based simulation

Specifications – Aspen Plus rate-based	
Calculation Type	Rate-based
Property method	ENRTL-RK
Henry comp ID	Global
Chemistry ID	MEA-CHEM
Valid phases	Vapor-Liquid

3.3 Equipment specification

Each piece of equipment is designed and simulated based on the real TCM plant, provided by the external partner of this thesis. Even though some minor changes might be considered for the accuracy test of the model with previous test campaigns such as absorber height and stages, model specification and reaction methods will be constant.

Different pieces of equipment in TCM plant were introduced in previous sections and this section will provide the simulation and performance details of each one of them.

3.3.1 Direct-contact cooler (DCC) and spray tower

Direct-contact cooler (DCC) for both CHP and RFCC flue gas is simulated in the same way. The purpose of using DCC is to cool down the flue gas and in Aspen Plus simulation, it is simulated as a RadFrac column. The specification of DCC is shown in table 3.4.

Table 3.4: Specification of DCC used in the rate-based simulation of TCM plant

Specification – DCC	
Calculation type	Rate-based
Pressure at stage one [bar]	1.03
Column pressure drop [bar]	0.03
Packing type	Flexipac, KOCH, Metal, 3x
Number of sections	1
Number of stages	6
Packing Height [m]	3.15
Diameter [m]	3
Flow model	Mixed
Interfacial area factor	1
Interfacial area method	Bravo et al., (1985)
Film liquid phase	Film reactions
Film vapor phase	Film reactions
Mass transfer coefficient method	Bravo et al., (1985)
Heat transfer coefficient method	Chilton and Colburn

It is noted that there are four flow models options in Aspen Plus for the bulk properties calculations [45]:

- Mixed: When the bulk properties for each phase are the same as the outlet conditions for each phase leaving the stage.
- Countercurrent: When the bulk properties are an average of the inlet and outlet properties for each phase.
- VPlug: Where the bulk properties are calculated by averaging the vapour and using outlet conditions for the liquid and outlet pressure.

- VPlugP: Which is the same as VPlug, but with average pressure instead of outlet pressure.

The water inlet to DCC is being recycled in a loop including a pump, a splitter, and a cooler to adjust the temperature and the flow rate coming back to DCC.

Since the temperature of CHP flue gas is relatively higher, a water spray is used to cool down the gas before entering DCC. In Aspen Plus, water spray is simulated as a flash column with no duty. The spray water flow rate should be adjusted in a way that almost no condensate water is coming out of the spray tower. It should be noted that there is no need to use a spray tower for RFCC flue gas.

The process flowsheet of the DCC and the spray tower configuration is shown in figure 3.1. The flowsheets in figures 3.1 to 3.7 are designed by Microsoft Visio.

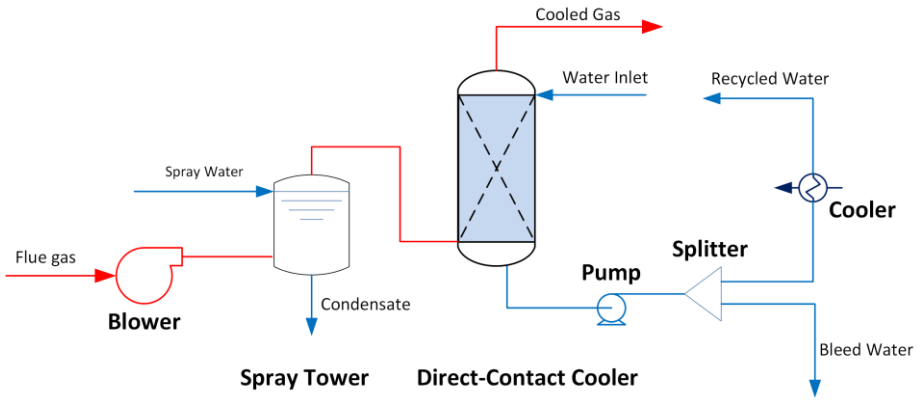

Figure 3.1: process flowsheet of DCC and spray tower configuration

3.3.2 Absorber

TCM plant has an absorber with a total height of 62 m, a packing height of 24 m, and a diameter of 3 m in the corresponding cross-sectional area to remove CO_2 from the flue gas by using MEA. Table 3.5 shows the specification of the absorber in the rate-based simulation.

Table 3.5: Specification of absorber used in the rate-based simulation of TCM plant

Specification – Absorber	
Reaction ID	MEA-STP
Pressure at stage one [bar]	1.01
Column pressure drop [bar]	0.02
Packing type	Flexipac, KOCH, Metal, 2x
Number of sections	3
Section 1	Packing height: 6 m Number of stages: 12
Section 2	Packing height: 6 m Number of stages: 12
Section 3	Packing height: 12 m Number of stages: 24
Total number of stages	48
Total packing Height [m]	24
Diameter [m]	3
Holdup	0.0001 for all stages
Holdup method	Bravo et al., (1992)
Flow model	VPlug
Interfacial area factor	1
Interfacial area method	Bravo et al., (1985)
Film liquid phase	Discretize film
Film vapor phase	Consider film
Mass transfer coefficient method	Bravo et al., (1985)
Heat transfer coefficient method	Chilton and Colburn

To test the accuracy of the simulated model, the interfacial area and holdup factor are not changed. However, the interfacial area and holdup method, and the mass and heat transfer

coefficient method are optimized to find out the most suitable conditions for TCM simulation in Aspen Plus. These parameters will remain constant in further simulations.

In 2021, an absorber intercooler (AIC) was added to the TCM plant, including a pump and a cooler. AIC is located at 12 m from the bottom of the absorber, and it will pump the semi-rich solvent from stage 24 to stage 25 while cooling it down to 30℃ in the simulation. The flow rate of the solvent being circulated in AIC should be approximately the total liquid flow in that stage, which can be seen in the absorber profile.

The process flowsheet of the absorber and AIC configuration is shown in figure 3.2.

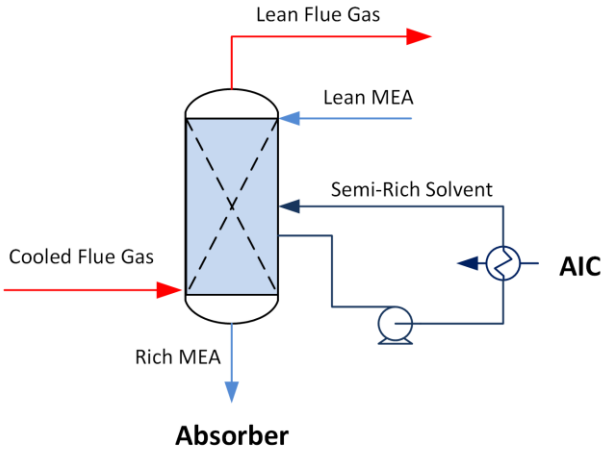

Figure 3.2: process flowsheet of absorber configuration

3.3.3 Water-wash systems

There are two water-wash systems at the top of the absorber column at the TCM plant to clean the flue gas of any solvent carryover. Two RadFrac columns in Aspen Plus were simulated for that. Table 3.6 shows the specification of two water-wash systems in the rate-based simulation.

Table 3.6: Specification of water-wash system used in the rate-based simulation of TCM plant

Specification – Water-Wash System	
Calculation type	Rate-based
Pressure at stage one [bar]	Column 1: 1.005 Column 2: 1
Column pressure drop [bar]	0.005 for both columns
Packing type	FlexipacHC, KOCH, Metal, 2YHC
Number of sections	1
Number of stages	6
Packing Height [m]	3
Diameter [m]	3
Flow model	Mixed
Interfacial area factor	1
Interfacial area method	Bravo et al., (1985)
Film liquid phase	Film reactions
Film vapor phase	Film reactions
Mass transfer coefficient method	Bravo et al., (1985)
Heat transfer coefficient method	Chilton and Colburn

Each of the columns has recycled water by using a pump, a splitter, and a cooler to adjust the water temperature and flow rate. The process flowsheet of water-wash systems is shown in figure 3.3.

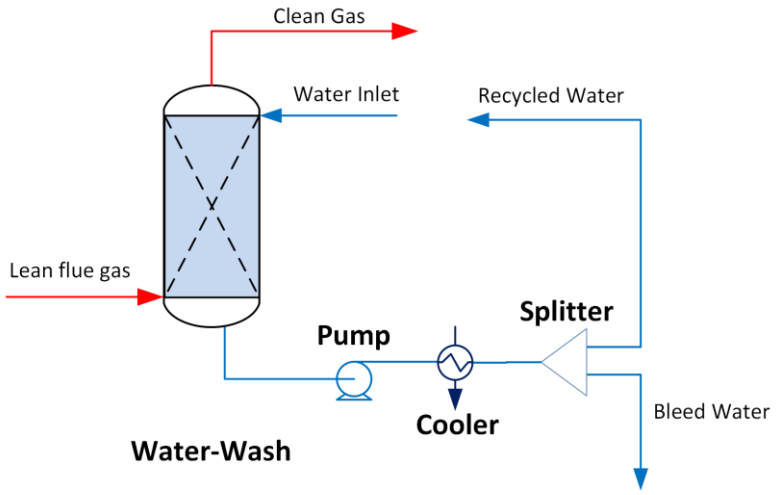

Figure 3.3: process flowsheet of each of the two water-wash systems configuration

3.3.4 Stripper Columns

There are two stripper columns at the TCM plant, named “CHP stripper” and “RFCC stripper”, to recover the captured CO_2 and return the lean MEA to the absorber. The specifications of these two strippers are shown in table 3.7.

Table 3.7: Specification of strippers used in the rate-based simulation of TCM plant

Specification – Strippers	
Pressure at stage one [bar]	1.85 for both strippers
Column pressure drop [bar]	0.1 for both strippers
Number of sections	2
Section 1	Packing height: 1.6 m Number of stages: 4
Section 2	Packing height: 8 m Number of stages: 16
Packing type	Section 1: FlexipacHC, KOCH, Metal, 2YHC Section 2: Flexipac, KOCH, Metal, 2x
Total number of stages	20
Total packing Height [m]	9.6
Diameter [m]	RFCC stripper: 2.2 CHP stripper: 1.25
Flow model	Mixed
Interfacial area factor	1
Interfacial area method	Bravo et al., (1985)
Film liquid phase	Film reactions
Film vapor phase	Film reactions
Mass transfer coefficient method	Bravo et al., (1985)
Heat transfer coefficient method	Chilton and Colburn

At the TCM plant, the rich amine is pumped to 1.6 m from the top of the strippers. This point is on stage 5 in our simulation, which is at the top of section 2. This configuration is the same for both CHP and RFCC strippers. Moreover, each stripper is equipped with a reboiler, which is defined internally in the simulation of the strippers.

There is also lean vapour compression (LVC) configuration at the RFCC stripper, including a flash drum and a compressor, to provide extra energy to regenerate rich amine and reduce the

consumption of low-pressure steam. The process flowsheet of the CHP stripper and RFCC stripper is shown in figure 3.4 and figure 3.5 respectively.

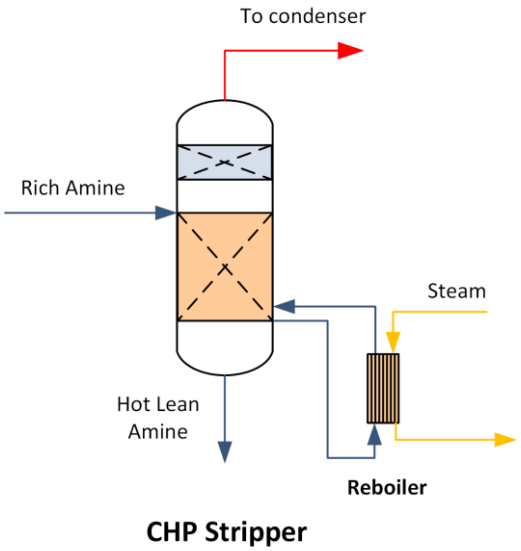

Figure 3.4: process flowsheet of the CHP stripper configuration

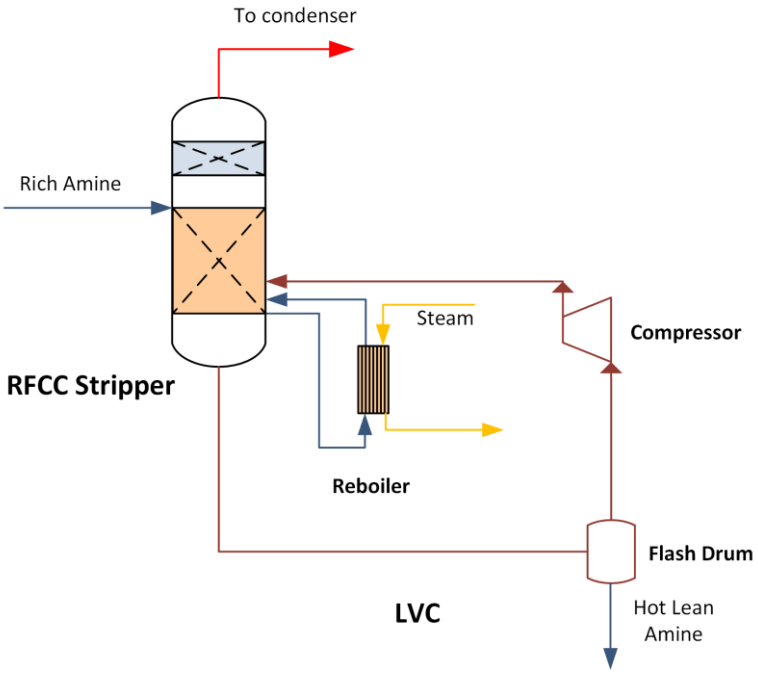

Figure 3.5: process flowsheet of the RFCC stripper configuration

3.3.5 Condenser

There is only one condenser at the TCM plant that is connected to both strippers. In simulation, the condenser is added externally and not in the stripper to be more similar to the real plant. This configuration includes a cooler, a pump, a flash drum to separate CO_2 and return the water

to the stripper, and a mixer to mix the gas coming out of the two strippers. The process flowsheet of the condenser is shown in figure 3.6.

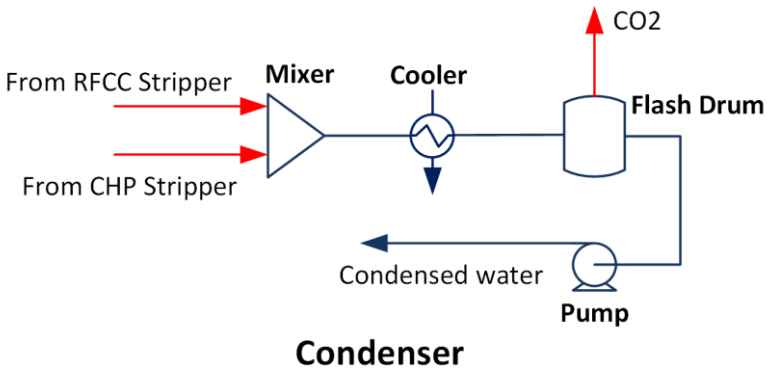

Figure 3.6: process flowsheet of the condenser configuration

3.3.6 Lean/rich heat exchanger

In the lean/rich heat exchanger, the rich MEA exiting the absorber recovers heat from the lean MEA exiting the stripper. A heat exchanger is simulated for it together with a rich and lean pump. Moreover, a cooler is used after the heat exchanger to reduce the lean amine temperature to the inlet MEA. The process flowsheet of the lean/rich heat exchanger is shown in figure 3.7.

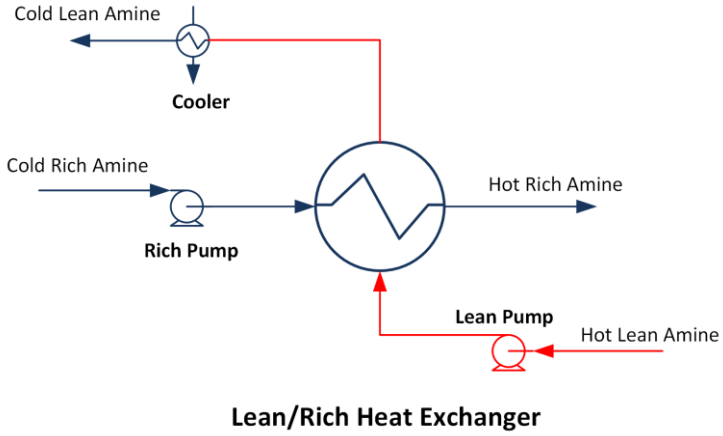

Figure 3.7: process flowsheet of the lean/rich heat exchanger configuration

The configuration of each piece of equipment is the basis of the simulation of the TCM plant in this thesis. Some changes might be considered in different configurations in the accuracy test and in TCM plant simulation, which will be discussed in chapters 4 and 5 respectively.

4 Model validation with previous test campaigns

To test the accuracy of the rate-based model simulated in Aspen Plus, the model is simulated with different scenarios performed by test campaigns at TCM in the last years. All scenarios were done by using the MEA amine solution. However, the weight percentage of MEA, amine lean loading, amine flow rate, flue gas properties and flow rate, and some configurations can be different from the real TCM plant, simulated in chapter 5.

This chapter provides performance data from the test campaigns and compares it with the results of the simulation implemented by those data. In each scenario, the gas and amine flow rate and the inlet lean loading are fixed by using experimental data. The results for other important simulation parameters, including CO_2 removal efficiency, stripper bottom and top temperature, outlet amine lean loading, required reboiler duty, and SRD were then observed and their deviation from the real data is calculated.

The adjustment of the outlet lean loading of the stripper can be done in two different ways: (1) outlet lean loading is increased by increasing the pressure drop in the stripper column. This can be changed if the pressure at the stripper is not fixed or is not mentioned in the scenario data. (2) outlet lean loading is decreased by increasing the reboiler duty of the stripper. In each simulation, adjusting the inlet and outlet lean loading is the priority.

4.1 CHP flue gas simulation

4.1.1 Scenario H14, Hamborg (2014)

Scenario H14 is data from the report published by Hamborg (2014). This report was produced during the test campaign at TCM in 2013 as a part of an independent verification protocol [16]. Moreover, this scenario has been used in several Master theses at USN earlier and the results are also previously verified by the simulation in earlier student works [31], [33], [39], [40], [42], [45].

The data from this scenario is attached in Appendix B. In this simulation, CHP flue gas is used in the simulation with only a CHP stripper. Figure 4.1 shows the flowsheet of the simulated plant based on scenario H14 in Aspen Plus.

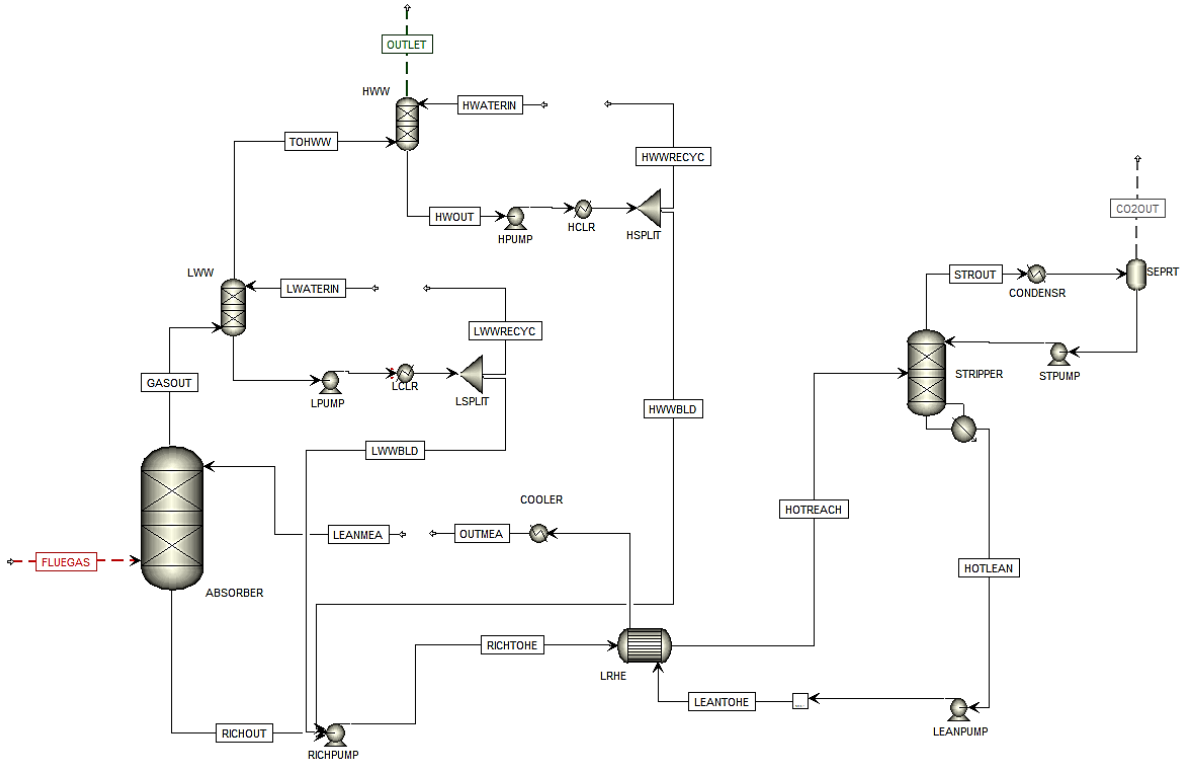

Figure 4.1: Simulation flowsheet of Scenario H14 in Aspen Plus

Table 4.1 shows the summary of the key parameters in scenario H14, compared with the results of the simulation.

Table 4.1: Experimental data for scenario H14 compared with the simulation results

Parameter	Experimental data	Simulation results	Unit
Lean amine loading	0.23	0.23	mol CO_2/mol MEA
Rich amine loading	0.48	0.49	mol CO_2/mol MEA
Reboiler duty	10.98 on average	11.5	GJ/hr
Stripper overhead temperature	99.8	98.2	℃
Produced CO_2 flow rate	2670	2897	kg/hr
Stripper Bottom temperature	122.3	122.1	℃
SRD	4.1 on average	3.77	MJ/kgCO_2
CO_2 removal efficiency	90	91	%

4.1.2 Scenario F17, Faramarzi (2017)

Scenario F17 is data from the report published by Faramarzi (2017). This report was produced during the 2015 test campaign at TCM as a part of an independent verification protocol [37]. Emission levels of MEA, NH_3, aldehydes, nitrosamines, and other compounds were also measured and were all below the permissible levels set by the Norwegian Environment Agency. Moreover, this scenario has been used in several Master theses at USN earlier and the results are also previously verified in earlier student works [42], [45].

The data from this scenario is attached in Appendix C. In this simulation, CHP flue gas is used in the simulation with only a CHP stripper. The flowsheet of the simulated plant based on scenario F17 in Aspen Plus is the same as scenario H14 shown in figure 4.1.

Table 4.2 shows the summary of the key parameters in scenario F17, compared with the results of the simulation.

Table 4.2: Experimental data for scenario F17 compared with the simulation results

Parameter	Experimental data	Simulation results	Unit
Lean amine loading	0.2	0.2	mol CO_2/mol MEA
Rich amine loading	0.48	0.49	mol CO_2/mol MEA
Reboiler duty	12 on average	13	GJ/hr
Stripper overhead Temperature	96.1	99.4	℃
Produced CO_2 flow rate	3325	3456	kg/hr
Stripper Bottom temperature	121.3	121.2	℃
SRD	3.62	3.75	MJ/kgCO_2
CO_2 removal efficiency	83.4	85.9	%

4.2 RFCC flue gas simulation

Several validation tests for the rate-based model in Aspen Plus have also been done on the RFCC flue gas by using the test campaigns' performance data. However, the data from the test campaigns using RFCC flue gas, are not as detailed as the results for the test campaigns using CHP flue gas.

4.2.1 Scenario S21, Hume (2021)

Scenario S21 is data from the report published by Hume (2021) during a test campaign at TCM in 2018 [46]. This scenario has not been used in the previous Master theses at USN before.

The data from this scenario is attached in Appendix D. In this simulation, RFCC flue gas is used in the simulation with only an 18 m of absorber packing height. Only an RFCC stripper with no LVC configuration has been used in this scenario. Figure 4.2 shows the flowsheet of the simulated plant based on scenario S21 in Aspen Plus, which is similar to the flowsheets for CHP flue gas.

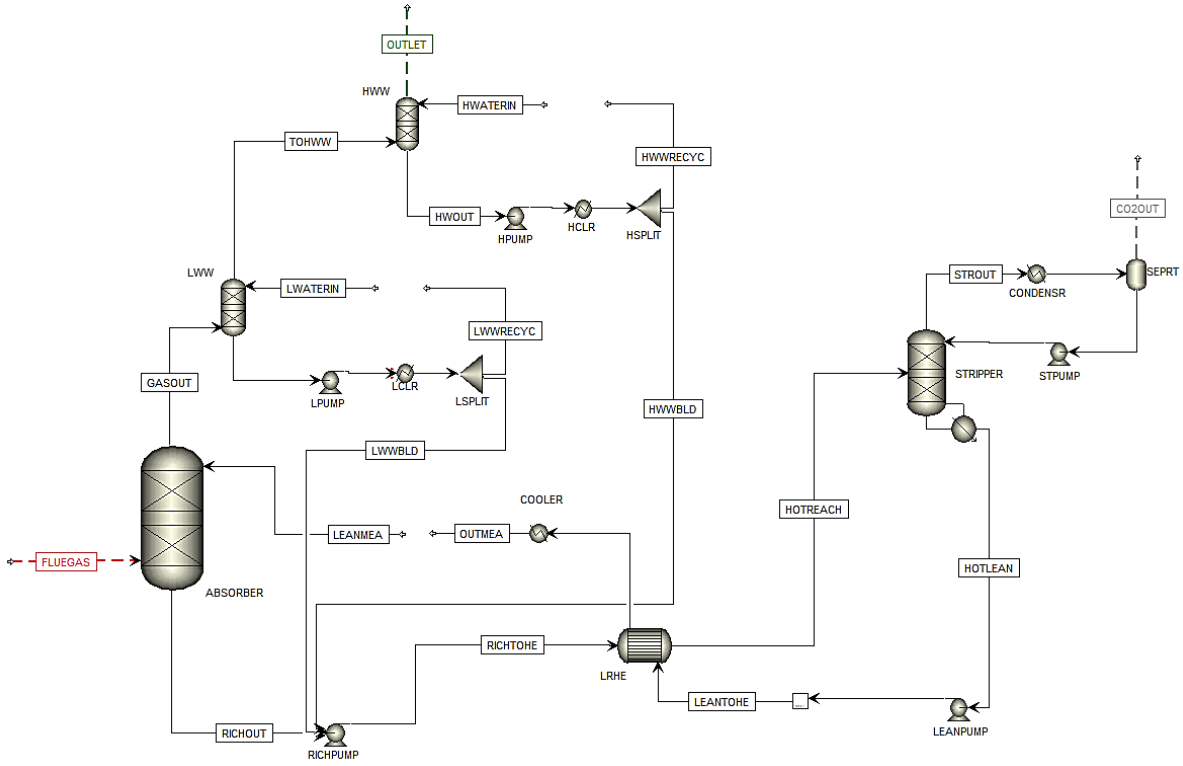

Figure 4.2: Simulation flowsheet of Scenario S21 in Aspen Plus

Table 4.3 shows the summary of the key parameters in scenario S21, compared with the results of the simulation.

Table 4.3: Experimental data for scenario S21 compared with the simulation results

Parameter	**Experimental data**	**Simulation results**	**Unit**
Lean amine loading	0.23	0.23	mol CO_2/mol MEA
Rich amine loading	0.48	0.5	mol CO_2/mol MEA
Reboiler duty	28.3 on average	28	GJ/hr
Produced CO_2 flow rate	8000	7443	kg/hr
Stripper Bottom temperature	121	120.9	°C
SRD	3.55	3.75	MJ/kgCO_2
CO_2 removal efficiency	91	88.62	%

4.2.2 Scenario M190 and M191, Meuleman (2019)

Scenarios M190 and M191 are data from the report published by Meuleman (2019) during the ION test campaign at TCM in 2016-2017 [41]. This test campaign has done 8 different tests on CHP and RFCC flue gases. Moreover, a relatively lower ratio of amine to gas flow rate, between 2.2 to 3 kg/Sm^3, is used in their process at TCM. This scenario has not been used in the previous Master theses at USN before. The data from this scenario is shown in appendix E.

In this study, only the first two test data on RFCC flue gas, named scenarios M190 and M191 respectively, were simulated. An absorber with an 18 m packing height and only an RFCC stripper with no LVC configuration have been used in this scenario. The flowsheet of the simulated plant based on the ION test campaign in Aspen Plus is the same as previous flowsheets for CHP and RFCC flue gas simulation, shown in figure 4.2.

Tables 4.4 and 4.5 show the summary of the key parameters in scenarios M190 and M191 respectively. As is shown in these tables, not much detail from the experimental data for the flue gas and the amine properties is provided in this paper. Since no amine lean loading and temperature have been specified in this paper, 0.2 molCO_2/molMEA and 37°C are considered in the simulation.

Table 4.4: Experimental data for scenario M190 compared with the simulation results

Parameter	**Experimental data**	**Simulation results**	**Unit**
Lean amine loading	Not provided	0.2	mol CO_2/mol MEA
Rich amine loading	Not provided	0.5	mol CO_2/mol MEA
Reboiler duty	Not provided	22.5	GJ/hr
Produced CO_2 flow rate	Not provided	6074	kg/hr
Stripper Bottom temperature	Not provided	121.9	°C
SRD	3.28	3.7	MJ/kgCO_2
CO_2 removal efficiency	89.2	75.12	%

Table 4.5: Experimental data for scenario M190 compared with the simulation results

Parameter	Experimental data	Simulation results	Unit
Lean amine loading	Not provided	0.2	mol CO_2/mol MEA
Rich amine loading	Not provided	0.5	mol CO_2/mol MEA
Reboiler duty	Not provided	23	GJ/hr
Produced CO_2 flow rate	Not provided	6217	kg/hr
Stripper Bottom temperature	Not provided	122	℃
SRD	3.36	3.7	MJ/kgCO_2
CO_2 removal efficiency	88.1	74.64	%

4.2.3 Scenario S6C, S6A, and S4, Ismail Shah (2019)

Scenarios S6C, S6A, and S4 are data from the report published by Ismail Shah (2019) during a test campaign at TCM in 2018 [18]. Ismail Shah used 6 different cases at the TCM plant, but only 3 of them are used in this study. These scenarios have not been used in the previous Master theses at USN before.

The data from this scenario is attached in Appendix F. RFCC flue gas is used in the simulation with only 18 m of absorber packing height. Only an RFCC stripper with no LVC configuration has been used. The inlet amine temperature is considered as 50℃ in this test campaign. The flowsheet of the simulated plant based on Ismail Shah (2019) test campaign in Aspen Plus is the same as previous flowsheets, shown in figure 4.2.

Tables 4.6, 4.7, and 4.8 show the summary of the key parameters in the scenario S6C, S6A, and S4 respectively, compared with the results of the simulation.

Table 4.6: Experimental data for scenario S6C compared with the simulation results

Parameter	Experimental data	Simulation results	Unit
Lean amine loading	0.16	0.16	mol CO_2/mol MEA
Rich amine loading	Not provided	0.5	mol CO_2/mol MEA
Reboiler duty	Not provided	27.8	GJ/hr
Produced CO_2 flow rate	Not provided	7217	kg/hr
Stripper Bottom temperature	121	122.8	℃
SRD	3.92	3.85	MJ/kgCO_2
CO_2 removal efficiency	88.3	87.5	%

Table 4.7: Experimental data for scenario S6A compared with the simulation results

Parameter	Experimental data	Simulation results	Unit
Lean amine loading	0.19	0.19	mol CO_2/mol MEA
Rich amine loading	Not provided	0.51	mol CO_2/mol MEA
Reboiler duty	Not provided	29	GJ/hr
Produced CO_2 flow rate	Not provided	7557	kg/hr
Stripper Bottom temperature	121	122.2	℃
SRD	3.92	3.83	MJ/kgCO_2
CO_2 removal efficiency	87.3	91.29	%

Table 4.8: Experimental data for scenario S4 compared with the simulation results

Parameter	Experimental data	Simulation results	Unit
Lean amine loading	0.273	0.273	mol CO_2/mol MEA
Rich amine loading	Not provided	0.5	mol CO_2/mol MEA
Reboiler duty	Not provided	30	GJ/hr
Produced CO_2 flow rate	Not provided	7515	kg/hr
Stripper Bottom temperature	121	119.4	℃
SRD	3.85	3.99	MJ/kgCO_2
CO_2 removal efficiency	85.9	88.36	%

4.3 LVC configuration simulation

Scenario F2A, F2B, F2C1, F2C2, F2C3, F2D1, F2D2, F2E, and F2F are data from the report published by Fosbøl (2019) during a test campaign at TCM [43]. Fosbøl used 16 different cases at the TCM plant, in which 7 cases were performed without LVC and 9 cases with LVC configuration. Only the 9 cases with LVC are used in this study. These scenarios have not been used in the previous Master theses at USN before.

The data from this scenario is attached in Appendix G. 18 m of absorber packing height and RFCC stripper with LVC configuration has been used in the simulation. The compressor work in this configuration is considered 75%. Figure 4.3 shows the flowsheet of the simulated plant based on Fosbøl (2019) test campaign in Aspen Plus.

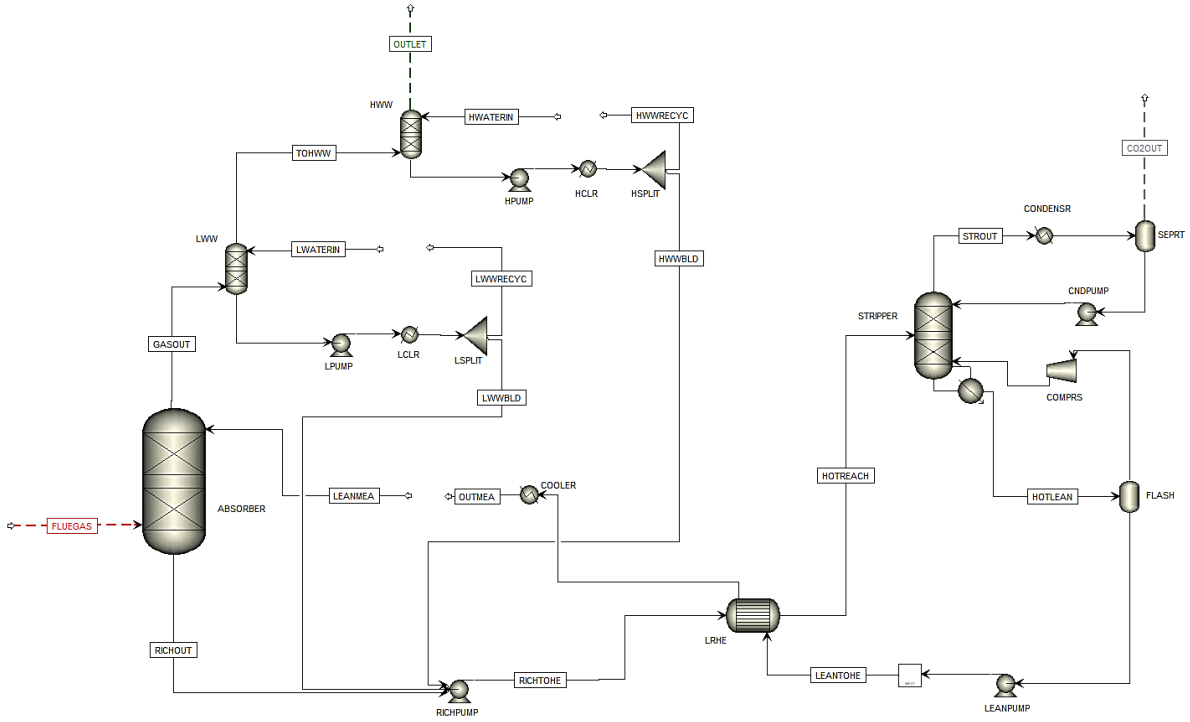

Figure 4.3: Simulation flowsheet of Fosbøl test campaign (2019) in Aspen Plus

Tables 4.9 to 4.17 show the summary of the key parameters in the scenario F2A, F2B, F2C1, F2C2, F2C3, F2D1, F2D2, F2E, and F2F respectively, compared with the results of the simulation.

Table 4.9: Experimental data for scenario F2A compared with the simulation results

Parameter	**Experimental data**	**Simulation results**	**Unit**
Lean amine loading	0.201	0.201	mol CO_2/mol MEA
Rich amine loading	0.543	0.504	mol CO_2/mol MEA
Reboiler duty	Not provided	21.3	GJ/hr
Produced CO_2 flow rate	7726	7336	kg/hr
Stripper Overhead temperature	88.8	90.4	℃
Stripper Bottom temperature	120.8	121.4	℃
Compressor Work	0.19	0.103	MJ/kgCO_2
SRD	2.84	2.78	MJ/kgCO_2
CO_2 removal efficiency	89.8	84.39	%

Table 4.10: Experimental data for scenario F2B compared with the simulation results

Parameter	**Experimental data**	**Simulation results**	**Unit**
Lean amine loading	0.266	0.266	mol CO_2/mol MEA
Rich amine loading	0.513	0.495	mol CO_2/mol MEA
Reboiler duty	Not provided	22.1	GJ/hr
Produced CO_2 flow rate	7473	7534	kg/hr
Stripper Overhead temperature	88.7	90	℃
Stripper Bottom temperature	118.6	118.4	℃
Compressor Work	0.19	0.124	MJ/kgCO_2
SRD	2.9	2.81	MJ/kgCO_2
CO_2 removal efficiency	89.4	88.09	%

Table 4.11: Experimental data for scenario F2C1 compared with the simulation results

Parameter	**Experimental data**	**Simulation results**	**Unit**
Lean amine loading	0.284	0.284	mol CO_2/mol MEA
Rich amine loading	0.493	0.475	mol CO_2/mol MEA
Reboiler duty	Not provided	23.5	GJ/hr
Produced CO_2 flow rate	7290	7596	kg/hr
Stripper Overhead temperature	89.1	90.9	℃
Stripper Bottom temperature	117.1	117.3	℃
Compressor Work	0.19	0.139	MJ/kgCO_2
SRD	3.04	2.96	MJ/kgCO_2
CO_2 removal efficiency	87.4	88.66	%

Table 4.12: Experimental data for scenario F2C2 compared with the simulation results

Parameter	**Experimental data**	**Simulation results**	**Unit**
Lean amine loading	0.28	0.28	mol CO_2/mol MEA
Rich amine loading	0.488	0.473	mol CO_2/mol MEA
Reboiler duty	Not provided	25.6	GJ/hr
Produced CO_2 flow rate	7419	7657	kg/hr
Stripper Overhead temperature	91.1	93.3	℃
Stripper Bottom temperature	117.5	117.3	℃
Compressor Work	0.14	0.082	MJ/kgCO_2
SRD	3.29	3.2	MJ/kgCO_2
CO_2 removal efficiency	88.4	89.49	%

Table 4.13: Experimental data for scenario F2C3 compared with the simulation results

Parameter	**Experimental data**	**Simulation results**	**Unit**
Lean amine loading	0.285	0.285	mol CO_2/mol MEA
Rich amine loading	0.483	0.477	mol CO_2/mol MEA
Reboiler duty	Not provided	24.5	GJ/hr
Produced CO_2 flow rate	7539	7604	kg/hr
Stripper Overhead temperature	88.5	90.1	℃
Stripper Bottom temperature	117.6	117	℃
Compressor Work	0.21	0.161	MJ/kgCO_2
SRD	3	2.82	MJ/kgCO_2
CO_2 removal efficiency	89.5	88.26	%

Table 4.14: Experimental data for scenario F2D1 compared with the simulation results

Parameter	**Experimental data**	**Simulation results**	**Unit**
Lean amine loading	0.318	0.318	mol CO_2/mol MEA
Rich amine loading	0.493	0.49	mol CO_2/mol MEA
Reboiler duty	Not provided	20.5	GJ/hr
Produced CO_2 flow rate	6627	6807	kg/hr
Stripper Overhead temperature	87.2	89.1	℃
Stripper Bottom temperature	115	114.3	℃
Compressor Work	0.21	0.134	MJ/kgCO_2
SRD	3.03	2.89	MJ/kgCO_2
CO_2 removal efficiency	79.2	78.4	%

Table 4.15: Experimental data for scenario F2D2 compared with the simulation results

Parameter	**Experimental data**	**Simulation results**	**Unit**
Lean amine loading	0.318	0.318	mol CO_2/mol MEA
Rich amine loading	0.501	0.488	mol CO_2/mol MEA
Reboiler duty	Not provided	22.2	GJ/hr
Produced CO_2 flow rate	6627	6761	kg/hr
Stripper Overhead temperature	89.3	91.3	℃
Stripper Bottom temperature	115.2	114.6	℃
Compressor Work	0.14	0.077	MJ/kgCO_2
SRD	3.23	3.15	MJ/kgCO_2
CO_2 removal efficiency	80.5	78.96	%

Table 4.16: Experimental data for scenario F2E compared with the simulation results

Parameter	**Experimental data**	**Simulation results**	**Unit**
Lean amine loading	0.288	0.288	mol CO_2/mol MEA
Rich amine loading	0.496	0.476	mol CO_2/mol MEA
Reboiler duty	Not provided	26.3	GJ/hr
Produced CO_2 flow rate	7409	7463	kg/hr
Stripper Overhead temperature	89.2	90.5	℃
Stripper Bottom temperature	115.7	115.1	℃
Compressor Work	0.15	0.107	MJ/kgCO_2
SRD	3.2	3.06	MJ/kgCO_2
CO_2 removal efficiency	89.6	87.69	%

Table 4.17: Experimental data for scenario F2F compared with the simulation results

Parameter	Experimental data	Simulation results	Unit
Lean amine loading	0.301	0.301	mol CO_2/mol MEA
Rich amine loading	0.467	0.456	mol CO_2/mol MEA
Reboiler duty	Not provided	19.5	GJ/hr
Produced CO_2 flow rate	6111	6151	kg/hr
Stripper Overhead temperature	90.8	92.3	℃
Stripper Bottom temperature	116.7	115.7	℃
Compressor Work	0.24	0.158	MJ/kgCO_2
SRD	3.26	3.04	MJ/kgCO_2
CO_2 removal efficiency	89.4	88.01	%

4.4 Rich bypass configuration simulation

Scenarios Shah1, Shah2, Shah3, Shah4, and Shah5 are data from the report published by Ismail Shah (2021) during a test campaign at TCM [17]. Shah used 6 different cases at the TCM plant and in 5 of them he used cold rich-solvent bypass to stripper overhead. Only the 5 cases with rich solvent bypass configuration are used in this study. Moreover, the MEA data from test campaigns in 2017 and 2018 (MEA-1 to MEA-5) were used in this campaign. These scenarios have not been used in the previous Master theses at USN before.

The data from this scenario is attached in Appendix H. Both 24 m and 18 m of absorber packing height, together with both CHP and RFCC stripper with no LVC configuration have been used in the simulation. A cold rich-solvent bypass of 20% to the top of the stripper is considered in all cases. It is noted that since other than the hot rich amine, only one stream can be fed to the stripper at the TCM plant, the condensed stream out of the condenser will be sent back to the rich pump and not to the stripper again. Figure 4.4 shows the flowsheet of the simulated plant based on Ismail Shah (2021) test campaign in Aspen Plus.

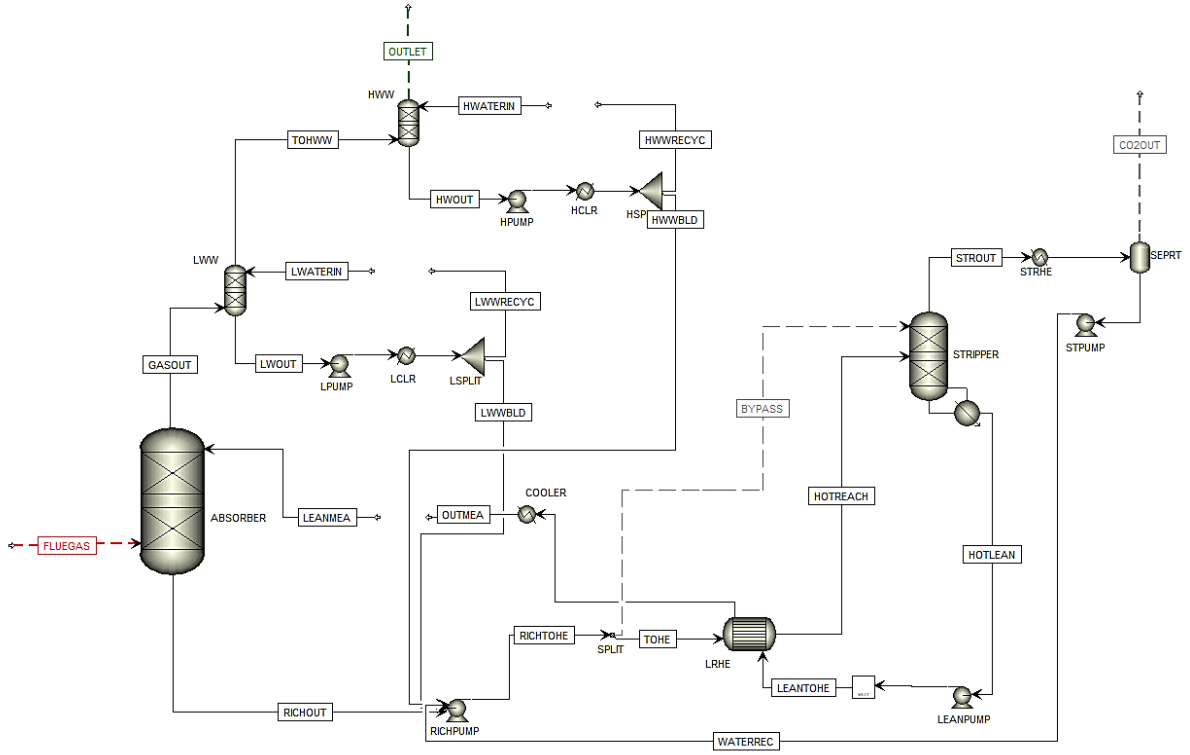

Figure 4.4: Simulation flowsheet of Ismail Shah test campaign (2021) in Aspen Plus

Tables 4.18 to 4.22 show the summary of the key parameters in the Shah1, Shah2, Shah3, Shah4, and Shah5 respectively, compared with the results of the simulation.

Table 4.18: Experimental data for scenario Shah1 compared with the simulation results

Parameter	**Experimental data**	**Simulation results**	**Unit**
Lean amine loading	0.24	0.24	mol CO_2/mol MEA
Rich amine loading	Not provided	0.49	mol CO_2/mol MEA
Reboiler duty	Not provided	13.1	GJ/hr
Produced CO_2 flow rate	Not provided	3427	kg/hr
Stripper Bottom temperature	121.4	121.9	°C
SRD	3.6	3.82	MJ/kgCO_2
CO_2 removal efficiency	91	92.49	%

Table 4.19: Experimental data for scenario Shah2 compared with the simulation results

Parameter	Experimental data	Simulation results	Unit
Lean amine loading	0.24	0.24	mol CO_2/mol MEA
Rich amine loading	Not provided	0.49	mol CO_2/mol MEA
Reboiler duty	Not provided	12.8	GJ/hr
Produced CO_2 flow rate	Not provided	3292	kg/hr
Stripper Bottom temperature	121.4	121.8	℃
SRD	3.6	3.88	MJ/kgCO_2
CO_2 removal efficiency	91	93.26	%

Table 4.20: Experimental data for scenario Shah3 compared with the simulation results

Parameter	Experimental data	Simulation results	Unit
Lean amine loading	0.21	0.21	mol CO_2/mol MEA
Rich amine loading	Not provided	0.49	mol CO_2/mol MEA
Reboiler duty	Not provided	18.5	GJ/hr
Produced CO_2 flow rate	Not provided	4751	kg/hr
Stripper Bottom temperature	122.5	122.6	℃
SRD	3.7	3.89	MJ/kgCO_2
CO_2 removal efficiency	97	96.07	%

Table 4.21: Experimental data for scenario Shah4 compared with the simulation results

Parameter	Experimental data	Simulation results	Unit
Lean amine loading	0.21	0.21	mol CO_2/mol MEA
Rich amine loading	Not provided	0.48	mol CO_2/mol MEA
Reboiler duty	Not provided	18.5	GJ/hr
Produced CO_2 flow rate	Not provided	4678	kg/hr
Stripper Bottom temperature	122.5	122.6	℃
SRD	3.7	3.95	MJ/kgCO_2
CO_2 removal efficiency	97	95.9	%

Table 4.22: Experimental data for scenario Shah5 compared with the simulation results

Parameter	Experimental data	Simulation results	Unit
Lean amine loading	0.26	0.26	mol CO_2/mol MEA
Rich amine loading	Not provided	0.48	mol CO_2/mol MEA
Reboiler duty	Not provided	15.9	GJ/hr
Produced CO_2 flow rate	Not provided	4033	kg/hr
Stripper Bottom temperature	121	121.1	℃
SRD	3.8	3.94	MJ/kgCO_2
CO_2 removal efficiency	90	88.75	%

5 TCM plant simulation

In previous chapters, a rate-based model in Aspen Plus has been simulated. The simulation verification with different flue gas and amine composition, different flow rates, and different plant configurations, including the LVC and the rich solvent bypass configuration, has been performed.

This chapter presents the extended verified rate-based model in Aspen Plus to simulate the TCM plant with a more detailed heat exchanger simulation. The limitations for each piece of installed equipment at the plant are discussed and obtained by the simulation. Moreover, a modification of the model to the maximum capacity of the plant and an optimization of the operating condition and energy consumption for maximum CO_2 removal efficiency are also presented in this chapter.

5.1 Designing the real heat exchangers with Aspen EDR

To simulate and find the limitations of the real plant with all the equipment, a more detailed simulation is needed. All the heat exchangers in the Aspen Plus rate-based simulation are designed with Aspen Exchanger Design and Rating (Aspen EDR) v.12 in this chapter.

In previous chapters, heat exchangers were simulated either in “design” mode in Aspen Plus or as a simple cooler with defined outlet temperature and pressure drop. Aspen EDR can simulate different types of heat exchangers based on real manufacturer data and calculate the outlet temperature and pressure of both cold and hot streams.

To change each of the coolers and heat exchangers in Aspen Plus to a real version, specific heat exchangers with the real manufacturer data and dimensions are defined in Aspen EDR with the imported process data from the previous Aspen Plus simulation. The process data should also include fouling resistance, estimated and allowable pressure drop in each stream. The result of the EDR simulation will present thermal, hydraulic, and mechanical results, and an API sheet including the outlet process data, vapour and liquid properties, and the heat exchanger configuration. The EDR file then can be used as an input for Aspen Plus after changing the heat exchangers from “design” to “simulation” mode.

The heat exchangers at the TCM plant that must be replaced with the real model include a DCC cooler, water-wash cooler, AIC cooler, lean/rich heat exchanger, lean cooler, condenser, and RFCC and CHP reboiler. It is noted that the reboilers used in the strippers are designed internally and not by Aspen EDR. However, the simulation results and the limitations of the reboilers will be checked constantly by defining a pseudo stream in the strippers, which is described in section 5.3.4.

5.2 Simulation modifications

Different configurations have been discussed and validated in the previous chapter. The necessary specifications in the simulation and the modification of the simulated plant are presented in this section. Different modifications and configurations discussed here will be considered in all the further simulations on the TCM plant.

5.2.1 Process flowsheet of the TCM plant

Figure 5.1 shows the simulation flowsheet of the TCM plant simulated in Aspen Plus, which is shown in two separate parts: one for the DCC and the spray tower, and one for other parts of the plant, including absorber, strippers, etc. The total flowsheet of the plant is also shown in appendix I.

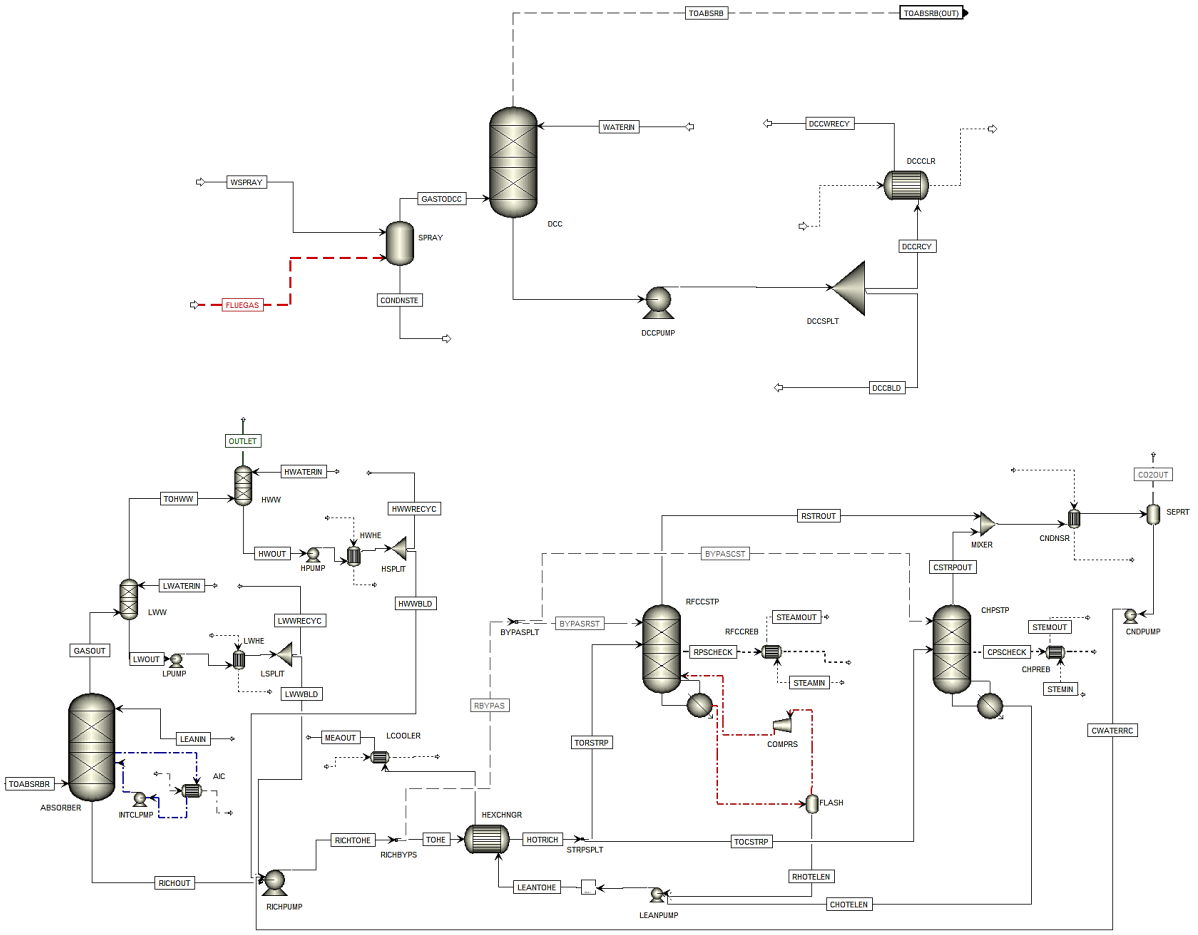

Figure 5.1:Simulation flowsheet of the TCM plant in Aspen Plus

As shown in figure 5.1, advanced configurations at the TCM plant are used in the rate-based model simulation. A spray tower and DCC column are used to cool down the flue gas before entering the absorber. On top of the absorber column, the water-wash system is simulated in two separate columns. An absorber intercooler (AIC) is also implemented in this simulation, which is marked by a blue dotted line.

RFCC and CHP strippers are simulated in two separate columns. LVC configuration is also implemented in the RFCC stripper and is marked with a red dotted line. A condenser, a lean/rich heat exchanger, a lean cooler, and lean and rich pumps are also implemented in the model.

A cold rich-solvent bypass separator is marked with “RICHBYPS” before the lean/rich heat exchanger and sends the bypass flow to the strippers. The separator marked with “BYPASPLT” splits the bypass flow between RFCC and CHP strippers. The separator marked with “STRPSPLT” splits the hot-rich amine flow between RFCC and CHP stripper. In general, the split fraction for “BYPASPLT” and “STRPSPLT” is the same amount.

5.2.2 Scenario MHP

Scenario MHP is used for the simulation of the TCM plant in this study. This is a Mongstad refinery flue gas from a gas-fired heat plant. This plant was working as a CHP plant previously, but now the combustion energy is only used for heating without power production. The CO_2 concentration of the gas is 10%. Table 5.1 shows the characteristics of scenario MHP used at the TCM plant.

Table 5.1: The characteristics of scenario MHP used for the TCM simulation

Parameter	Value	Unit
Temperature	145	°C
Pressure	1.05	bar
Carbon Dioxide percentage	10	vol %
Water percentage	21	vol %
Nitrogen percentage	67.5	vol %
Oxygen percentage	1.5	vol %

5.2.3 Parameters to be fixed

The main purpose of the TCM simulation model is to find the maximum plant operation capacity. As a result, the CO_2 removal efficiency is fixed at 90% by adjusting the lean amine flow rate, and the gas flow rate is changed until the equipment limits at the plant are found. Amine lean loading is also fixed as 0.2 molCO_2/molMEA in the simulations. The results of other important parameters such as reboiler duty, SRD, and stripper bottom and top temperature are observed and compared in the next sections.

5.2.4 Amine lean loading adjustment

To maintain the same lean loading in the hot lean solvent out of the stripper bottom and lean solvent to absorber inlet, design specifications have been used in Aspen Plus for the strippers in every simulation with different configurations. Since the pressure at the stripper column is fixed in the TCM plant simulation, lean loading adjustment can only be done by changing the reboiler duty in the strippers. Increasing the reboiler duty will reduce the lean loading out of the stripper and vice versa.

5.2.5 Stream transfer

In some sections of the plant, water is being recycled in a loop and being used as the water inlet again such as water-wash systems and DCC column, as it is shown in figure 5.1. The properties of the inlet water and the water being recycled, including the temperature, pressure, and flow rate, should be the same. A tool called “stream transfer” is used in Aspen Plus to adjust the stream properties in a loop for each of the water-wash and DCC columns.

5.2.6 Cold rich-solvent bypass

A cold rich-solvent bypass before the lean/rich amine heat exchanger to the stripper top is implemented at the TCM plant and has been considered in the modified simulation of the plant in this study. A default value of 20% for the bypass fraction has been considered. However, this amount can be modified based on the plant and stripper capacity, as there was a previous study on it [17].

5.2.7 Intercooler specification

An absorber intercooler is implemented in the plant simulation and will be considered in all the simulations on the plant. The rich solvent from stage 24 is cooled down and pumped to stage 25 and the flow rate of the solvent being circulated is defined as around the same amount as the total liquid flow in stage 24.

5.2.8 Temperature adjustment of the outlet gas

The temperature of the gas going out of the top of the water-wash system should be the same as the temperature of the gas going to the absorber to maintain the water balance in the plant. The reason is that temperature differences will create condensed water in the plant and can affect the calculations. In all TCM plant simulations, these temperatures should remain close, and it is done by adjusting the water inlet flow rate of the heat exchangers in the water-wash loops.

5.2.9 Other considerations

- It is necessary to avoid flooding in the absorber and DCC column. As a result, in each simulation, the absorber hydraulic plot is monitored so the flooding percentage (the chance of approaching the flood) is not more than 70%. This amount is set by TCM as the warning limit for flooding.
- In an inaccurate simulation, the absorber stages temperature can be shown as negative values. It is important to always check if all the temperatures in the absorber stages are positive.
- Lean and rich amine pumps should have an outlet pressure of 7 bar. The reason is to avoid flashing in the plant.
- The outlet MEA of the lean cooler has the same temperature as the inlet MEA to the absorber. However, there is a pressure difference and a small difference in the flow rate of these two streams. This matter is not solved in the simulations here, since it will cause simulation problems, but at the TCM plant, it can be solved by using elevations before sending the lean amine from the lean cooler to the absorber.
- The pressure in all columns (absorber, water-wash, and strippers) should be less than the inlet streams entering the column.
- In addition to the rich-solvent bypass, a stripper separator is also implemented in the plant to be able to decide how much of the solvent should be directed to CHP or RFCC stripper. There is the same amount of splitting percentage for the bypass flow to the strippers and the rich amine flow to the strippers, but it is not the same as the rich-solvent bypass fraction.

5.3 The limitations of TCM plant

There are many limitations and bottlenecks at the TCM plant that can affect the operation by the maximum capacity. The most important limitations that must be considered in the simulations are found and listed below. Scenario MHP with only RFCC stripper is used in the simulations to find the limits for the absorber and DCC column. RFCC stripper is larger compared to CHP stripper and it can process larger solvent amounts, and this is the reason that this stripper is used in the simulation.

5.3.1 DCC column

The chance of approaching flooding must be less than 70% in the DCC column at all sections. To find the maximum capacity of DCC column at the TCM plant, the inlet flue gas flow rate is increased to the maximum possible amount while being in the flooding limit. Table 5.2 shows the DCC column limits at the TCM plant using scenario MHP.

Table 5.2: DCC column limits at TCM plant by operating in the maximum flow capacity with scenario MHP

Parameter	Value	Unit
Maximum gas flow rate to the DCC column	78845 3335	Sm^3/hr kmol/hr
Maximum flooding approach in all stages	69.99	%

The maximum capacity of the DCC column is 78845 Sm^3/hr. However, This limit in this study is presented as 78500 Sm^3/hr.

5.3.2 Absorber column

The chance of approaching flooding must also be less than 70% in the absorber column at all sections. The maximum possible inlet gas flow rate to the absorber while being in the flooding limit is found by the simulation. Table 5.3 shows the absorber column limits at the TCM plant using scenario MHP.

Table 5.3: Absorber column limits at TCM plant by operating in the maximum flow capacity with scenario MHP

Parameter	Value	Unit
Maximum inlet flue gas flow rate to absorber	52157 2206	Sm^3/hr kmol/hr
Maximum flooding approach in all stages	69.99	%
Lean amine loading	0.2	mol CO_2/mol MEA
Rich amine loading	0.499	mol CO_2/mol MEA
Lean amine flow rate	178500	kg/hr
CO_2 removal efficiency	90	%

Although the simulation result shows a maximum capacity of 52157 Sm^3/hr, this limit is presented as 52000 Sm^3/hr in this study.

5.3.3 Reboiler duty

There are limitations in the reboiler duty in RFCC and CHP strippers at the TCM plant. The maximum possible reboiler duty for the RFCC stripper is 8.4 MW and for the CHP stripper is 3.4 MW. New modifications should be considered in case of a higher need for reboiler duty in each stripper.

5.3.4 Real capacity of the reboilers

Even though the reboiler duty is within the defined limits of TCM, there is a possibility that the real reboilers at the TCM plant cannot operate properly at a very high flow rate. As a result, there is a need for checking the performance of the real reboilers at specific flow rates in each simulation.

A pseudo stream is added at stage 19 of each stripper with the real CHP and RFCC reboiler, designed in Aspen EDR to check the performance of the real reboilers. The flow rate of the pseudo stream should be the same as the total liquid flow at stage 19, observed in the stripper profile. The real reboiler duty is constantly checked in each simulation, and it must not be less than the defined reboiler duty in the stripper to be able to convey the required heat. The pseudo stream and the simulated reboilers are shown in figure 5.1 with black dotted lines.

5.3.5 The capacity of the heat exchangers

Designing the real heat exchangers in Aspen EDR provides the possibility to check whether they can operate at the given flow rates or not. The Aspen Plus simulation will not show the results if the heat exchangers cannot convey the given flows.

5.3.6 Lean amine flow rate

The lean amine flow rate entering the absorber column cannot exceed the maximum limit. This is due to the maximum possible amine velocity and is found by equation (5.1). The amine density is considered 1050 kg/m^3, the pipe diameter is 0.2 m, and the maximum velocity of the amine is 2 m/s. At the TCM plant, there is a maximum allowable lean amine flow rate of 230 ton/hr.

$$Max\ amine\ flow\ rate\ \left[\frac{kg}{hr}\right] = v_{Max}\left[\frac{m}{s}\right] \cdot \rho_{Amine}\left[\frac{kg}{m^3}\right] \cdot A_{Pipe}[m^2] \cdot 3600\left[\frac{s}{hr}\right] \quad (5.1)$$

$$Max\ amine\ flow\ rate = 2 \cdot 1050 \cdot \pi \cdot {0.2^2}/{4} \cdot 3600 = 237504\ \left[\frac{kg}{hr}\right]$$

5.4 Plant optimization for maximum gas flow rate

In the previous section, scenario MHP with only an RFCC stripper, LVC configuration, and a default bypass fraction value of 20% was used with the maximum possible flue gas to the absorber column. Moreover, the maximum allowable reboiler duty of 8.4 MW was used in the stripper. The lean amine loading of the lean cooler outlet in this configuration was 0.229 molCO_2/molMEA, which is higher than 0.2 molCO_2/molMEA in the inlet lean amine. As a result, the RFCC stripper alone cannot handle the total solvent and achieve the required stripping efficiency and lean loading. In this section, different configurations with scenario MHP are simulated to adjust the lean loading.

5.4.1 Cold rich-solvent bypass fraction optimization

The amount of cold rich-solvent bypass fraction can affect the required reboiler duty and lean loading. As a result, an optimization study is performed on the same configuration used in the previous section, and the bypass fraction is changed between 0 to 30%. Table 5.4 and figure 5.2 show the optimization result of the rich-solvent bypass fraction.

Table 5.4: Cold rich-solvent bypass fraction optimization result using only RFCC stripper

Rich-solvent bypass fraction [%]	Lean loading [mol CO_2/mol MEA]
0	0.237
10	0.227
12	0.225
15	0.224
18	0.226
20	0.229
25	0.239
30	0.255

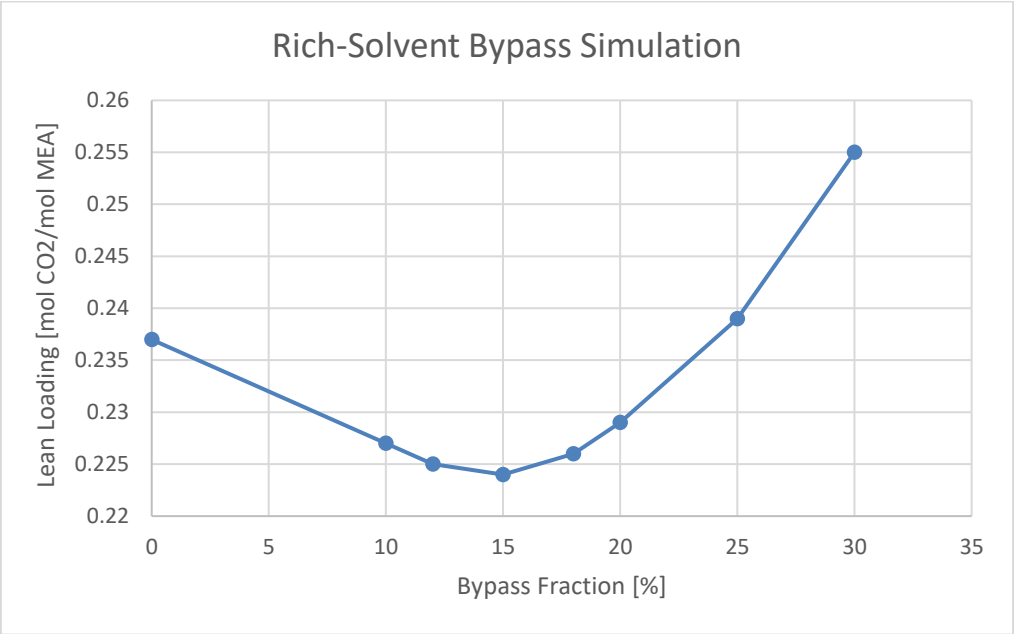

Figure 5.2: Cold rich-solvent bypass fraction optimization using only RFCC stripper

A bypass fraction of 15% shows the minimum lean loading with 0.224 molCO_2/molMEA out of the lean cooler. Further modifications must be made to adjust the stripping efficiency and the lean loading.

5.4.2 Reboiler duty adjustment

The lean amine loading outlet from the lean cooler can be reduced by increasing the reboiler duty in the stripper. In this simulation, only an RFCC stripper was used and with the maximum possible reboiler duty of 8.4 MW and adjusting the cold rich-solvent bypass to 15%, there is still a need of reducing the returned amine lean loading.

The amine lean loading can reach 0.2 molCO_2/molMEA by increasing the reboiler duty to the amount of 9.12 MW, which will give an SRD of 2.95 MJ/kgCO_2. This means at the TCM plant, we need an additional 0.72 MW to be able to adjust the inlet and outlet lean loading. Increasing the reboiler duty to more than 8.4 MW in the RFCC stripper cannot be practical at TCM, but it gives an insight into what is needed to operate with the maximum flow capacity at the plant.

5.4.3 Using both CHP and RFCC stripper

To operate within the practical conditions of the TCM plant, the maximum reboiler duty of the RFCC stripper cannot be more than 8.4 MW. As a result, a new modification of the simulation is performed to use both CHP and RFCC strippers at the same time with the maximum flow capacity.

In this simulation, the cold rich-solvent bypass has remained at 15%, but the split fraction to the strippers and the reboiler duty of the strippers are adjusted to have the necessary splitting efficiency and a same outlet lean loading from both strippers and the outlet lean loading from the lean cooler as the inlet lean loading. Table 5.5 shows the modified parameters used in RFCC and CHP strippers to adjust the lean loading.

Table 5.5: Modified parameters of RFCC and CHP strippers to adjust the lean loading

Parameter	Value	Unit
Rich-solvent bypass fraction	15	%
RFCC stripper flow fraction	91.35	%
CHP stripper flow fraction	8.65	%
Outlet lean loading from RFCC stripper	0.2	mol CO_2/mol MEA
Outlet lean loading from CHP stripper	0.2	mol CO_2/mol MEA
Outlet lean loading from lean cooler	0.2	mol CO_2/mol MEA
RFCC stripper reboiler duty	8,16	MW
CHP stripper reboiler duty	1,1	MW
Total reboiler duty	9,16	MW
Total SRD	3.0	MJ/kg CO_2
Rich amine loading	0.498	mol CO_2/mol MEA

This configuration allows us to use the maximum gas flow capacity while operating at the practical limits of the TCM plant.

5.5 Plant optimization for maximum CO_2 removal efficiency

TCM plant limitations to operate with the maximum gas flow capacity were found in the previous section and the operation was modified considering the practical limitations. This section presents the maximum achievable CO_2 removal efficiency at TCM by operating at the maximum plant capacity.

The CO_2 removal efficiency is not fixed at 90% in this section, but the gas flow rate is fixed at the maximum operating limit for the absorber and the amine flow rate is fixed at the maximum flow limit.

5.5.1 Maximum achievable CO_2 removal efficiency

To find the maximum achievable CO_2 removal efficiency at the TCM plant by using the maximum allowable flue gas flow rate, the amine flow rate needs to be increased. The

maximum inlet amine flow rate is set to 230 ton/hr as mentioned before and will be used in this simulation.

A similar approach for the results of the lean loading is considered in this simulation in which the outlet lean loading from both strippers must be the same as the outlet lean loading from the lean cooler and in the inlet amine solution. This amount is considered as 0.2 molCO_2/molMEA.

Using the maximum allowable gas and amine flow rate will give a CO_2 removal efficiency of 98% at the TCM plant. Table 5.6 shows the simulation parameters using the maximum capacity of the plant.

Table 5.6: Simulation parameters of the TCM plant to achieve maximum CO_2 removal efficiency

Parameter	**Value**	**Unit**
Inlet amine flow rate	230	ton/hr
Rich-solvent bypass fraction	15	%
RFCC stripper flow fraction	84.9	%
CHP stripper flow fraction	15.1	%
Outlet lean loading from RFCC stripper	0.2	mol CO_2/mol MEA
Outlet lean loading from CHP stripper	0.201	mol CO_2/mol MEA
Outlet lean loading from lean cooler	0.2	mol CO_2/mol MEA
Produced CO_2 flow rate	10485	kg/hr
RFCC stripper reboiler duty	8.4	MW
CHP stripper reboiler duty	2.22	MW
Total reboiler duty	10.62	MW
Total SRD	3.645	MJ/kg CO_2
Rich amine loading	0.417	mol CO_2/mol MEA
CO_2 removal efficiency	98	%

5.5.2 Cold rich-bypass optimization using maximum capacity

As mentioned before, changing the rich amine flow rate to each of the strippers can affect the required reboiler duty. As a result, a new optimization on cold rich-solvent bypass using the maximum amine and gas flow rate at the TCM plant is performed. In this optimization, the flow fraction for strippers remains constant as in the previous simulation and the cold-rich bypass fraction is changed between 15 to 22%. Table 5.7 shows the optimization result of the cold rich-solvent bypass fraction in this configuration.

Table 5.7: Rich-solvent bypass fraction optimization result using maximum plant capacity

Parameter	**Value**	**Value**	**Value**	**Value**	**Value**	**Value**	**Value**	**Value**
Rich-solvent bypass fraction [%]	15	16	17	18	19	20	21	22
RFCC stripper lean loading [mol CO_2/ mol MEA]	0.200	0.1995	0.1993	0.1991	0.1991	0.1992	0.1994	0.1996
CHP stripper lean loading [mol CO_2/ mol MEA]	0.201	0.2007	0.2004	0.2003	0.2002	0.2004	0.2004	0.2007
Lean cooler outlet lean loading [mol CO_2/ mol MEA]	0.200	0.1997	0.1994	0.1993	0.1993	0.1994	0.1995	0.1998
Produced CO_2 flow rate [kg/hr]	10485	10499	10509	10515	10518	10515	10507	10493
Total SRD [MJ/kg CO_2]	3.6450	3.6412	3.6379	3.6358	3.6349	3.6359	3.6384	3.6433

A minimum outlet amine lean loading, a minimum SRD, and a maximum produced CO_2 flow rate are observed by using 19% of the rich solvent in bypass flow. These trends are shown in figures 5.3 to 5.5. This means that the total reboiler duty used in the strippers can also be decreased. By adjusting the lean loading to 0.2 molCO_2/molMEA, the reboiler duty for CHP and RFCC stripper is 8.4 and 2.17 MW respectively. The total reboiler duty and SRD will therefore be 10.57 MW and 3.63 MJ/kg CO_2, which is less than using 15% of the bypass fraction.

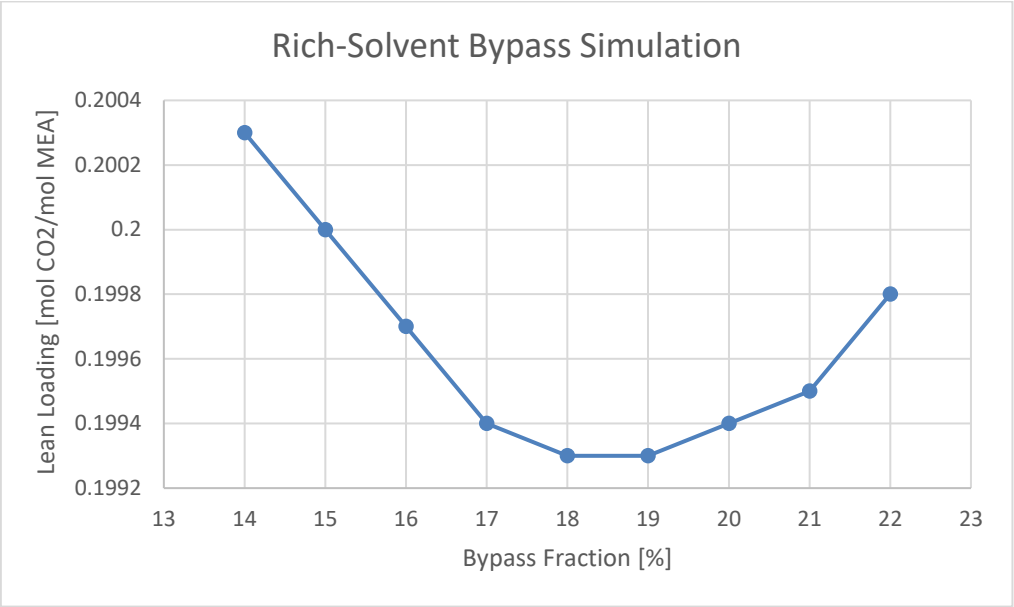

Figure 5.3: Cold rich-solvent bypass fraction optimization considering lean loading using maximum capacity

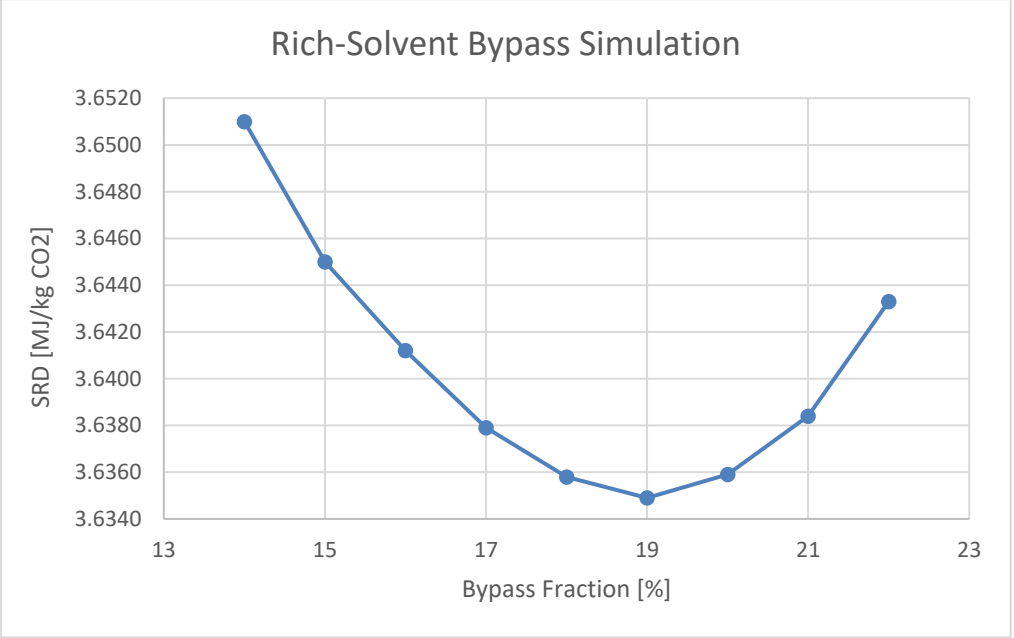

Figure 5.4: Cold rich-solvent bypass fraction optimization considering SRD using maximum capacity

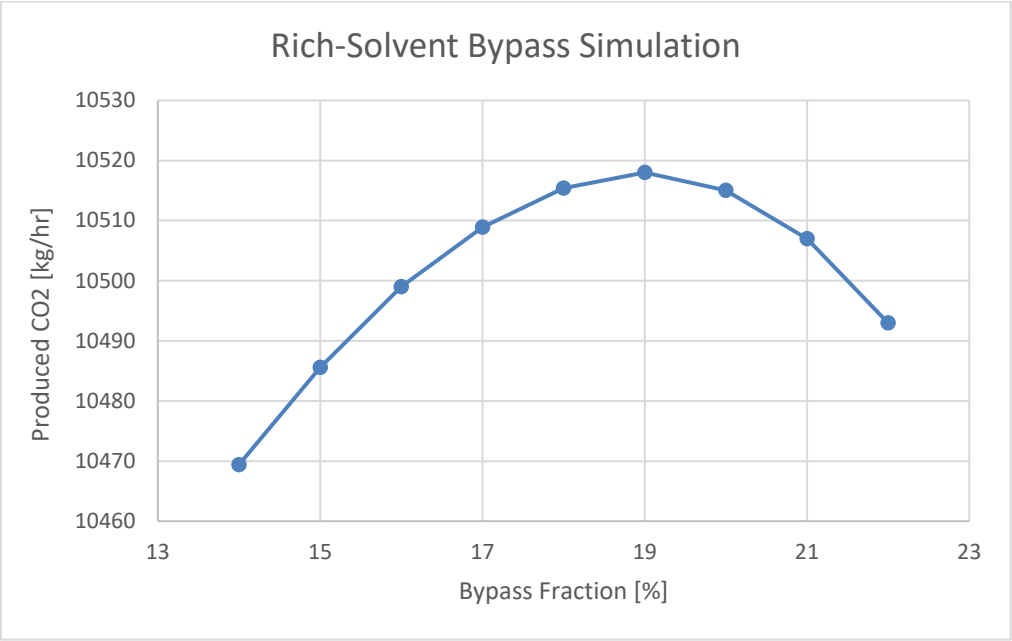

Figure 5.5: Cold rich-solvent bypass fraction optimization considering produced CO_2 using maximum capacity

5.5.3 Send the condensed water to CHP stripper

In the last simulation of this study, another configuration is tested to check the possibility of reducing energy consumption in the reboilers. In previous configurations and since only one stream can be fed to each stripper other than the hot-rich solvent, the condensed water out of the condenser was sent back to the rich pump and not to the strippers. In this configuration, all the cold rich-solvent bypass is sent to the RFCC stripper while the cold rich bypass fraction has remained at 19%. As a result, it is possible to send the condensed water to the CHP stripper. Figure 5.6 and table 5.8 show the simulation flowsheet and parameters of this configuration in Aspen Plus.

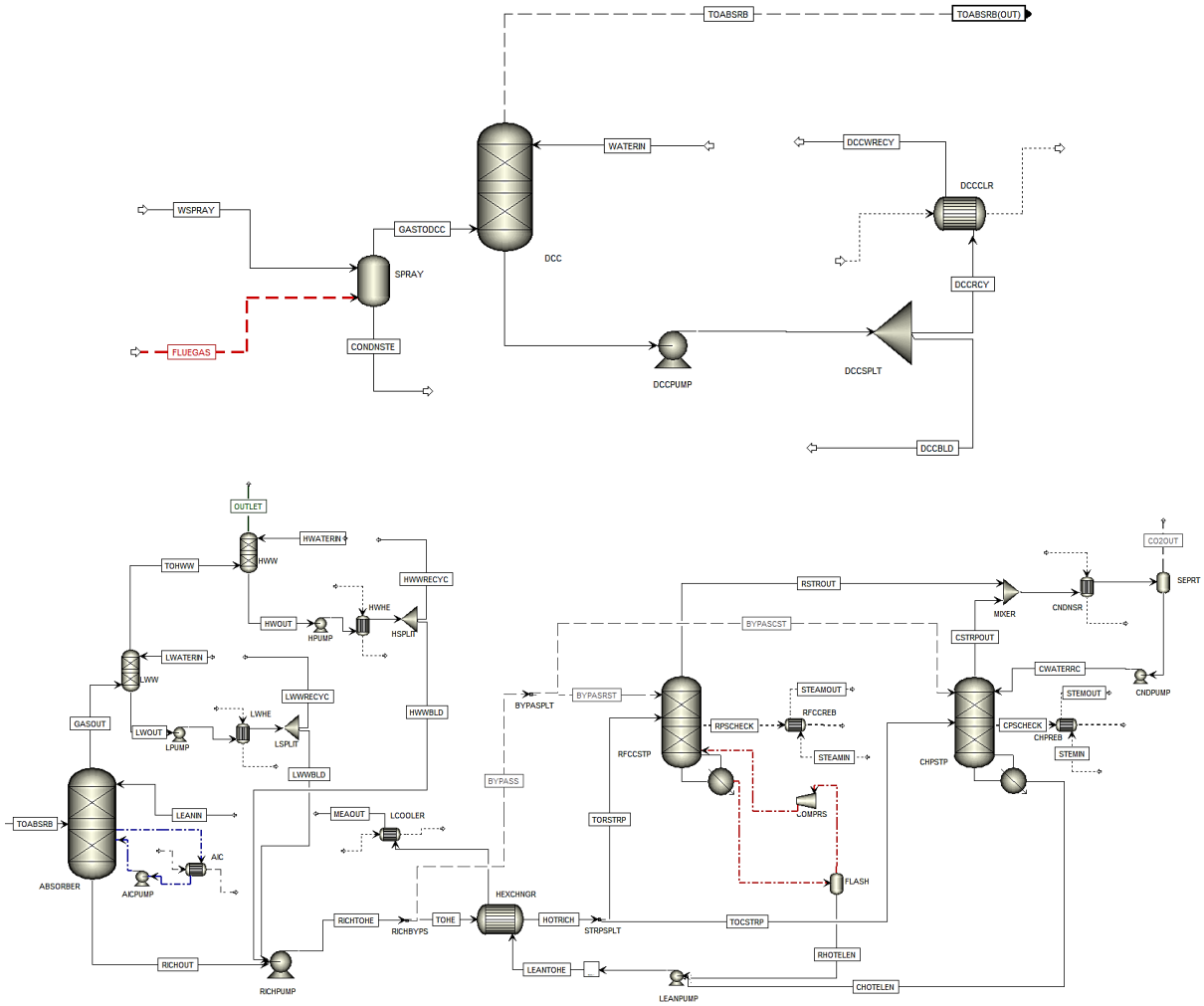

Figure 5.6: Simulation flowsheet to send the condensed water to CHP stripper

Table 5.8: Simulation parameters of sending the condensed water to CHP stripper

Parameter	**Value**	**Unit**
Inlet amine flow rate	230	ton/hr
Rich-solvent bypass fraction	0.18	%
RFCC stripper flow fraction	100	%
CHP stripper flow fraction	0	%
Outlet lean loading from RFCC stripper	0.2	mol CO_2/mol MEA
Outlet lean loading from CHP stripper	0.201	mol CO_2/mol MEA
Outlet lean loading from lean cooler	0.2	mol CO_2/mol MEA
Produced CO_2 flow rate	10843	kg/hr
RFCC stripper reboiler duty	8,4	MW
CHP stripper reboiler duty	2,26	MW
Total reboiler duty	10,66	MW
Total SRD	3.65	MJ/kg CO_2
Rich amine loading	0.417	mol CO_2/mol MEA

6 Results and discussion

The rate-based simulation of the real TCM plant in Aspen Plus together with the extended model to maximum flow capacity, optimized configuration for maximum CO_2 removal efficiency, and the TCM limits were presented in the previous chapter.

This chapter presents the results of the model validation results for different configurations, a summary of the TCM plant operating limits and modifications, and a discussion about the model accuracy, plant optimization, and energy consumption. Recommended future works are also mentioned in the last section of the chapter.

6.1 Model validation results

6.1.1 CHP flue gas results

The rate-based model with defined parameters and properties has been simulated for the CHP flue gas at the TCM plant. The results show less than a 4% deviation in CO_2 removal efficiency, rich loading, and stripper overhead and bottom temperature. There is 3.6-8.5% derivation in the reboiler duty, produced CO_2 flow rate, and SRD. Figure 6.1 shows the deviation between the experimental data and the simulation results for the important parameters in the validation of the model for CHP flue gas.

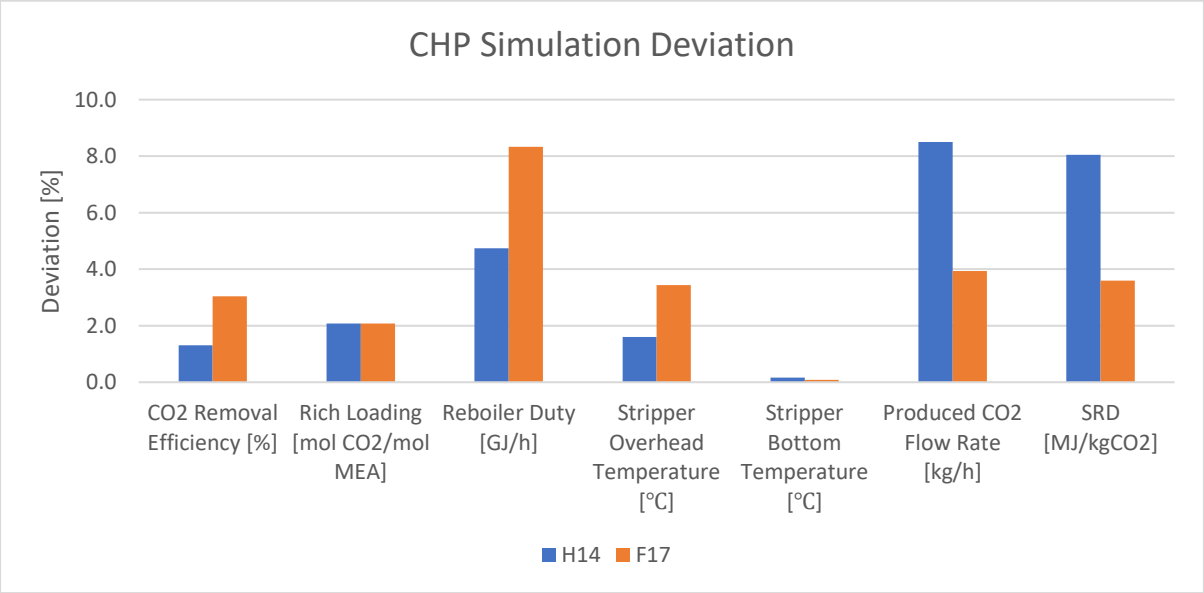

Figure 6.1: Deviation between the experimental data and the simulation results for CHP flue gas

6.1.2 RFCC flue gas validation results

The rate-based model with defined parameters and properties has been simulated for the RFCC flue gas at the TCM plant. However, not many details in the experimental data are available in these test campaigns' reports. The results show a relatively large deviation for scenarios M190 and M191 in both SRD, which is 10.1-12.8%, and CO_2 capture efficiency, which is 15.3-15.8%. In comparison with these scenarios, there is more consistency in the deviation of

scenarios S21, S6C, S6A, and S4. The results show less than a 2% deviation in stripper bottom temperature and less than a 6% deviation in SRD. There is also less than a 5% derivation in CO_2 capture efficiency for these scenarios. Figure 6.2 shows the deviation between the experimental data and the simulation results for the important parameters in the validation of the model for RFCC flue gas.

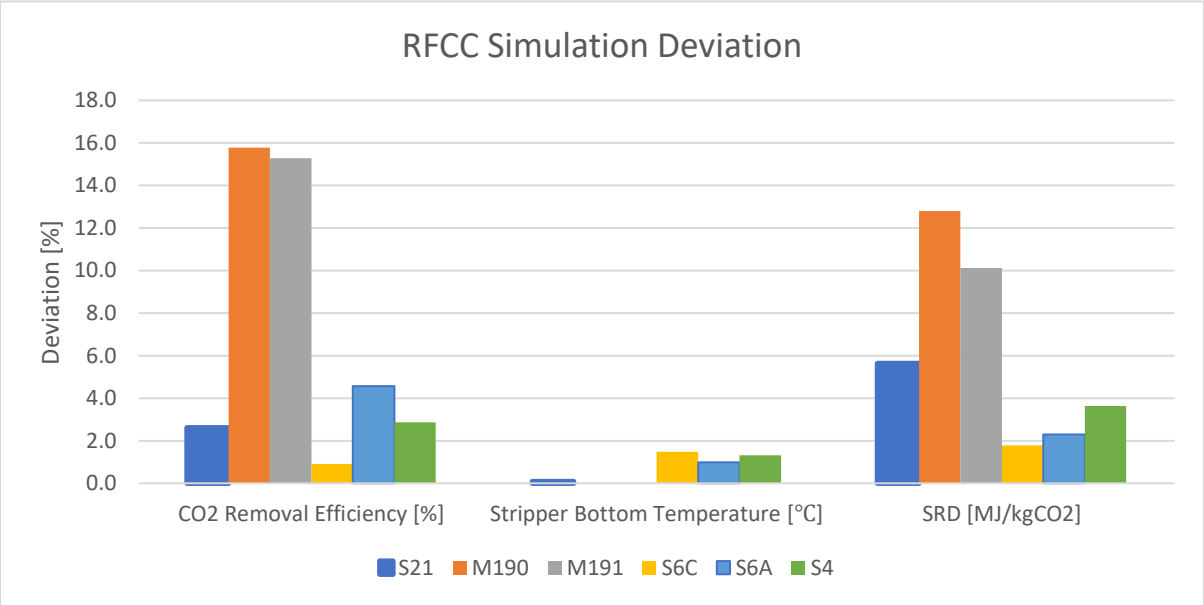

Figure 6.2: Deviation between the experimental data and the simulation results for RFCC flue gas

6.1.3 LVC configuration validation results

The rate-based model with defined parameters and properties has been simulated to test the LVC configuration at the TCM plant. The results show less than a 2.5% deviation in the stripper overhead temperature and less than 1% in the stripper bottom temperature. The produced CO_2 flow rate and the SRD have 0.7-5% and 2.1-6.7% deviation respectively. Except for scenario F2A with a CO_2 removal efficiency deviation of 6% and rich loading deviation of 7.2%, other scenarios have 1-2.1% and 0.6-4% deviation in these parameters respectively. Figure 6.3 shows the deviation between the experimental data and the simulation results for the important parameters in the validation of the LVC configuration.

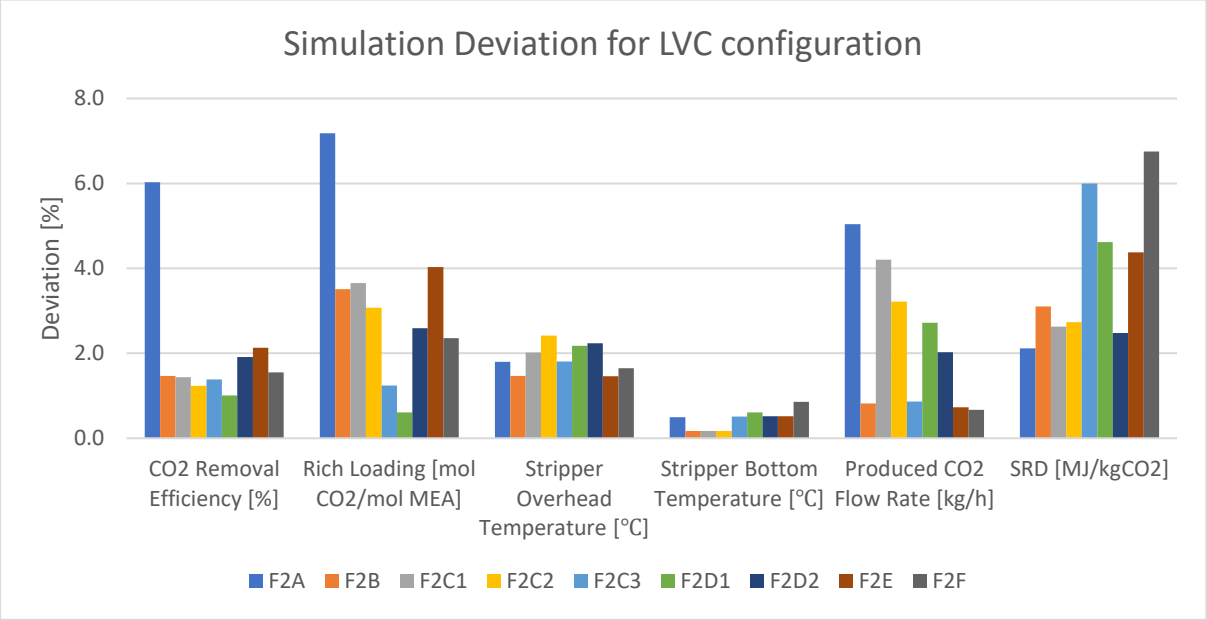

Figure 6.3: Deviation between the experimental data and the simulation results for LVC Configuration

Moreover, there is a relatively higher deviation observed in compressor work for LVC configuration with a 23.3-45.8% deviation. Figure 6.4 shows the deviation between the experimental data and the simulation results for the compressor work in the validation of the LVC configuration.

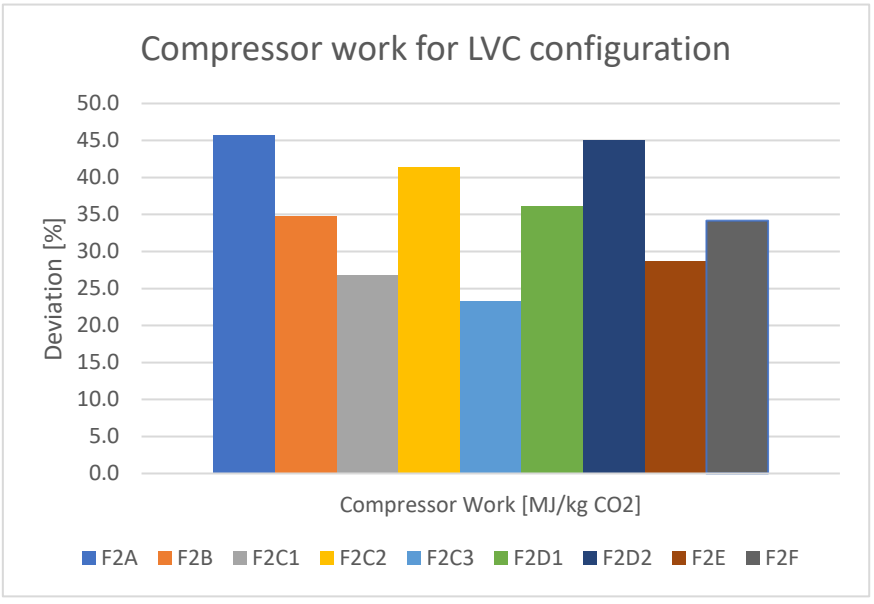

Figure 6.4: Compressor work deviation for LVC configuration

6.1.4 Cold rich-solvent bypass configuration validation results

The rate-based model with defined parameters and properties has been simulated to test the cold rich-solvent bypass configuration at the TCM plant. The results show less than a 2.5% deviation in the CO_2 removal efficiency and less than 0.5% in the stripper bottom temperature. There is a derivation of 3.7-7.8% in SRD value. No more experimental results were presented

to compare the other simulation parameters. Figure 6.5 shows the deviation between the experimental data and the simulation results for the important parameters in the validation of the cold rich-solvent bypass configuration.

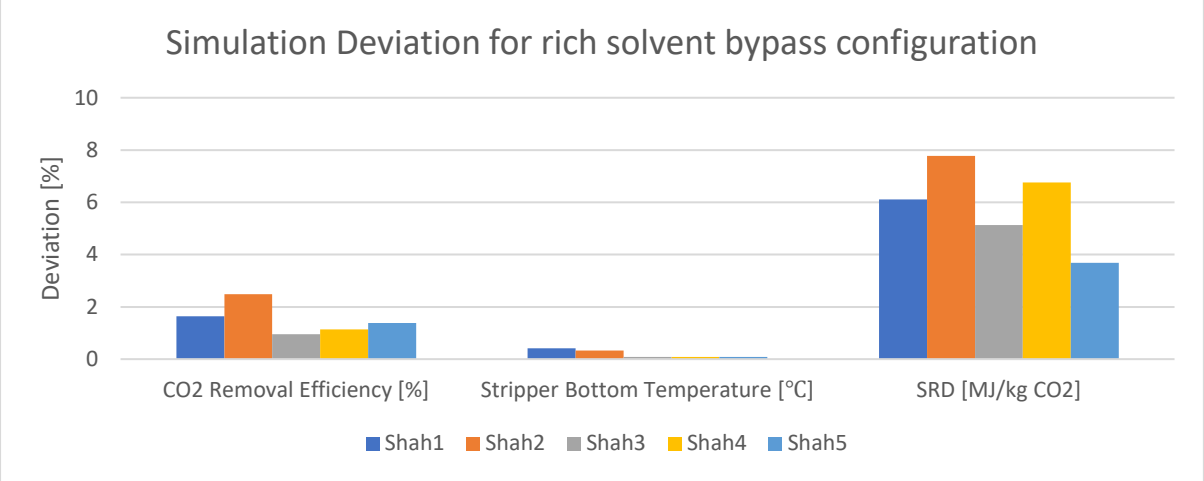

Figure 6.5: Deviation between the experimental data and the simulation results for cold rich-bypass configuration

6.2 TCM plant simulation results

6.2.1 Plant limitations

The verified Aspen Plus rate-based model is used for the simulation of the TCM plant to find the operation limits by using scenario MHP with only the RFCC stripper. RFCC stripper has more capacity than CHP stripper due to a larger cross-section area and that is the reason to use this stripper in this configuration. The gas flow has been changed to find the maximum plant capacity, but the amine flow rate is specified so the CO_2 removal efficiency in the plant is 90%. The maximum allowable flooding approach in DCC and absorber column is considered as 70%. A cold rich-solvent bypass default fraction of 20% is also used in the simulation. Table 6.1 shows the summary of the most important plant limitations found by the simulation model or provided by the supervisors. In addition to this table, the real capacities of the heat exchangers and the reboilers are also checked in the simulation.

Table 6.1: Results of the TCM plant limitations and specifications

Parameter	Value	Unit
Maximum lean amine flow rate	230000	kg/hr
Lean amine loading	0.2	mol CO_2/mol MEA
Maximum allowable inlet flue gas flow rate to DCC	78500	Sm^3/hr
Maximum allowable inlet flue gas flow rate to absorber	52000	Sm^3/hr
Maximum RFCC reboiler duty	8.4	MW
Maximum CHP reboiler duty	3.4	MW
Specified CO_2 removal efficiency	90	%
Maximum allowable flooding approach	70	%

6.2.2 Plant optimization to maximum flow capacity

To adjust the inlet and outlet amine lean loading from the lean cooler and the strippers, different configurations with scenario MHP have been simulated. Since the plant is operating by the maximum RFCC reboiler duty, an optimization on the cold rich-solvent bypass fraction is performed to adjust the stripper efficiency and optimize the operating condition at the TCM plant. The result shows that a fraction of 15% gives the minimum outlet lean loading of 0.224 molCO_2/molMEA.

To reduce the amine lean loading to 0.2 molCO_2/molMEA, there is an additional need for 0.72 MW in the RFCC reboiler. Since using both strippers is practical at the TCM plant, sending a fraction of the bypass flow to the CHP stripper can provide the additional reboiler duty needed in the plant while operating within the energy consumption limits. This new plant modification considering the practical limitations is done by sending 91.35% of the cold rich bypass flow to RFCC and the rest to the CHP stripper. The result shows 8.16 MW and 1.1 MW energy used in RFCC and CHP stripper respectively, which gives the total reviler duty and SRD of 9.16 MW and 3.0 MJ/kgCO_2 in the plant respectively. The rich amine loading is also 0.498 molCO_2/mol MEA in this simulation.

6.2.3 Maximum achievable CO_2 removal efficiency

A configuration is simulated to find the maximum achievable CO_2 removal efficiency by using the maximum flue gas and lean amine flow rate considering the plant operating limits. Moreover, since the amine flow rate is changed, an optimization of the cold rich-solvent bypass is performed again. The optimized simulation result shows that by using 19% of the cold rich-

solvent bypass and sending 84.9% of the cold rich bypass flow to RFCC and the rest to the CHP stripper, the inlet and outlet lean loading is the same (0.2 mol CO_2/mol MEA) and the reboiler duty in RFCC and CHP stripper will be 8.4 and 2.17 MW respectively. This gives the total reboiler duty and SRD of 10.57 MW and 3.63 MJ/kgCO_2 in the plant. This configuration will give the maximum achievable CO_2 removal efficiency of 98% in the plant. The rich amine loading is also 0.417 molCO_2/molMEA in this simulation.

Furthermore, another configuration is tested by sending the condensed water to CHP stripper instead of the rich pump while all the rich amine is sent to the RFCC stripper. Sending no bypass flow to the CHP stripper provides this opportunity since it is only possible to send one stream to each stripper other than the hot-rich solvent. In this case, the total reboiler duty and SRD in the plant are 10.66 MW and 3.65 MJ/kgCO_2 respectively.

6.3 Discussion

6.3.1 Model accuracy

Aspen Plus rate-based model used in this study has been tested with many different scenarios, using different configurations and inlet flue gases. The study aimed to check whether the model can show a reliable deviation between the experimental data from different test campaigns and the simulation results. As a result, no change has been made in the rate-based model parameters, such as the interfacial area or the liquid holdup factor. The only modification was to change the interfacial area, holdup, and mass and heat transfer method to gain the best possible results. To adjust the model for more accurate simulation results or to predict the plant performance by changing parameters, more optimizations should be done on the simulation model for each scenario. This has been done previously on some of the scenarios used in this study by the master students at USN [31], [33], [39], [40], [42], [45].

The results obtained from the model verification with different scenarios show that the model can provide more reliable data with more detailed input parameters for both flue gas and inlet lean amine to the absorber. A small change in the inlet parameters can deviate the results from the experimental data, such as lean amine flow rate, gas compositions, amine lean loading, and inlet temperatures and pressures.

For example, there is more detailed information for the test campaigns on CHP flue gas (scenarios H14 and F17) than RFCC flue gas (scenarios S21, M190, M191, S6C, S6A, and S4). The deviation for scenarios H14 and F17 is less than 8.5%, while the deviation for scenarios M190 and M191 can also be 16%, in a lack of information about amine lean loading and temperature. As expected, the simulated rate-based model with more detailed input data will generate more reliable results.

The same behavior can be observed in the scenarios using different configurations at TCM. For example, the test campaign for the scenarios Shah1, Shah2, Shah3, Shah4, and Shah5, using cold rich-solvent bypass provides good details for input parameters and the results show 0.1-7.8% deviation.

However, there might be other parameters affecting the deviation in the results as it is observed in the simulation of the scenarios F2A to F2F in which, LVC configuration is used. Even though this test campaign has provided very detailed information and the deviation is less than 4% in most of the parameters in these scenarios, the deviation for some of the parameters can be relatively high. Scenario F2A shows the most deviation in CO_2 removal efficiency, rich amine

loading, and produced CO_2 with 6%, 7.2%, and 5% respectively. The reason might be that the amine flow rate in this scenario is much less than the others used in this test campaign, and it seems that the rate-based model is very sensitive to this parameter, as it is less deviation in other scenarios with higher amine flow rates.

Furthermore, the input practical parameters of the plant equipment can affect the deviation, as it is a relatively high deviation in the compressor work for this test campaign. The compressor efficiency is assumed as 75% in the simulation, which can be different from the real efficiency. This can highly affect the compressor work, the produced CO_2 flow rate, and SRD, and increase the deviation as it is observed in the simulation result. Further optimization is needed to adjust this parameter.

An inconsistency seen in the model validation result is that in scenarios F2B, F2C3, F2D1, F2D2, F2E, and F2F a higher result in the produced CO_2 flow rate is observed than the experimental data. This is while the CO_2 removal efficiency is less than in the test campaigns. One reason might be the sensibility of produced CO_2 to reboiler duty and compressor work, which need further optimization. Another reason might be in the data measurement at the test campaign. As it is shown in Appendix G, the standard deviation of these parameters is between 29 to 49 and much higher than other measured parameters. As a result, some inconsistency in some of the scenarios for this sensible parameter can be seen.

6.3.2 Cold rich-solvent bypass optimization

The main purpose of having a cold rich-solvent bypass is to split the solvent stream from the bottom of the absorber column into two streams: (1) unheated stream entering the top of the stripper column; (2) heated stream entering the middle of the stripper column. In the standard process, vapour released from the hot rich stream passes directly through the condenser and provides no benefit. However, with a rich-solvent bypass, the released vapour passes up the stripper column and pre-strips the cold rich solvent entering the top of the stripper. This can enhance the cooling and heating duties inside the stripper, thus reducing the reflux from the condenser and minimizing energy losses.

Moreover, having a rich-solvent bypass allows greater flashing of the CO_2 from the hot rich solvent stream and allows further release of CO_2 in the upper stages of the stripper, which is a result of the pre-stripping of the cold rich solvent stream. This can be seen in the increased CO_2 flow rate in scenarios Shah1 to Shah5 in comparison with the other scenarios without bypass configuration. In scenario Shah5, the CO_2 flow rate is 4084 kg/hr in comparison with scenarios H14 and F17 with approximately the same flue gas flow rate and CO_2 concentration with the CO_2 flow rate of 2899 kg/hr and 3461 kg/hr respectively.

In this study, the cold rich-solvent bypass fraction was varied to find the minimum lean amine loading out of the stripper and a closer amount to the inlet lean loading. A minimum in lean loading and thus the reboiler duty and SRD was found by 15% split fraction by only using RFCC stripper and 19% split fraction by only using both strippers and maximum amine flow rate.

To understand why the minimum in the reboiler duty and the amine lean loading occurs, we need to consider the energy provided by the reboiler. In addition to reversing the CO_2 absorption reaction and increasing the amine temperature, the heat provided by the reboiler will generate steam in the column. The steam will lower the CO_2 operating partial pressure below that of the equilibrium partial pressure and thus stripping occurs. With more flow as the split stream, a lower flow rate goes through the lean/rich heat exchanger. It means the hot rich

amine will have a higher temperature and thus a higher vapour fraction, which leads to more steam generated for the pre-stripping process. The additional steam can have no benefit for the cold stream at the top of the stripper. As a result, a minimum in the reboiler duty should occur when a balance happens between the vapour generated in the reboiler and the energy needed by the cold rich solvent for the pre-stripping process.

The split fraction can be different in each simulation with different solvent flow rates and reboiler duties. This is the reason why optimization has also been done for the maximum amine flow at the TCM plant with two strippers as well. Moreover, two different types of strippers are used in the plant and since only one stripper is equipped with LVC configuration, the split fraction is a different amount than using only an RFCC stripper. However, in optimization of the cold-rich bypass, there is always a tendency to send as much as possible to the RFCC stripper since the LVC configuration will reduce the energy consumption in comparison with the CHP stripper with no LVC.

6.3.3 Energy optimization

In addition to presenting the plant capacity and limitations, some modifications have been made for the energy optimization of the TCM plant. This includes AIC to increase the solvent's absorption capacity by decreasing the temperature and the required sensible heat in the stripper, LVC to compress and send back the lean amine to the stripper, producing additional stripping steam, and reducing the required regeneration energy, and rich-solvent bypass to minimize the energy loses in the stripper and condenser.

This study presented the optimum operation conditions of each configuration that can reduce the energy consumption in the plant. These conditions were presented based on the practical limitations of the heat exchangers, reboiler duties, absorber and DCC column, and lean amine flow rate.

The minimum reboiler duty and thus the minimum SRD is affected by many parameters. The total reboiler duty and SRD required to adjust the lean loading by using only the RFCC stripper were 9.12 MW and 2.95 MJ/kgCO_2 respectively, which is not practical to use at the TCM plant. As a result, a modification using both CHP and RFCC stripper was introduced, and the total reboiler duty and SRD in the plant increased to 9.16 MW and 3.0 MJ/kgCO_2. The reason for this increase in energy consumption is that no LVC configuration is used in the CHP stripper and with the same fluid flow, more reboiler duty is needed in this stripper to adjust the lean loading. In this configuration, 8.65% of the flow is sent to the CHP stripper instead of the RFCC stripper with LCV and as a result, it has affected the total reboiler duty needed in the plant.

By using the maximum plant capacity in amine flow and flue gas flow rate, the energy consumption of the plant is also increased. Using the same cold rich-solvent bypass fraction shows the total reboiler duty and SRD of 10.62 MW and 3.64 MJ/kgCO_2 respectively. By using 19% as the bypass fraction, lower SRD and reboiler duty together with higher CO_2 production is observed. The reason is that with a good balance between the vapour generated in the reboiler and the energy needed by the cold rich solvent, the more pre-stripping process happens, resulting in more CO_2 production. Without changing the energy consumption in the stripper, lower SRD is observed. The new reboiler duty and SRD after adjusting the reboiler duties in this configuration are 10.57 MW and 3.63 MJ/kgCO_2.

A similar trend is observed to achieve the maximum CO_2 removal efficiency. The total reboiler duty and SRD needed in the plant by using the maximum amine flow rate after sending the

condensed water to CHP stripper increased to 10.66 MW and 3.65 MJ/kgCO_2 respectively. The reason is that the condensed water enters the CHP stripper without LVC configuration and afterward is sent to the lean/rich heat exchanger. In this way, the stream will not be sent back to the rich-solvent bypass going through the RFCC stripper, and this causes an increase in the total required reboiler duty, even though all the bypass stream is entering the RFCC stripper.

6.4 Future work

Simulation of the TCM plant and finding different limitations and capacities has much more potential to work on in the future. This study presented some and not all aspects of the plant optimization process simulation. Some recommendations for future work on the TCM plant are presented below.

- The same procedure for this study can be done on RFCC flue gas or other future scenarios provided by TCM supervisors. Finding the plant capacity and maximum achievable CO_2 removal efficiency can also be done by using other operating scenarios.

- The simulation can be expanded by using the maximum heat exchanger area in the plant. There are physical possibilities at TCM to use multiple or bigger heat exchangers in each piece of equipment of the plant and the operating capacities can vary in a new heat exchanger configuration.

- As is seen in sections 5.3 and 5.4, the rich amine loading exiting the absorber column is different in the results of the maximum gas flow rate (0.498 mol CO_2/mol MEA) and maximum amine flow rate (0.417 mol CO_2/mol MEA) configurations. A change in the inlet amine lean loading will vary the rich amine loading, and an optimization is required to keep the rich amine loading over 0.45 [mol CO_2/mol MEA] and operate on the recommended practical conditions.

- The compressor efficiency in LVC configuration is considered as 75% in this simulation, which can be different from the real operating efficiency. A modification of the compressor efficiency can adjust the result to the experimental data.

- The stripper pressure in this study was considered as a constant amount between 1.85 and 1.95 bar. Using a high-pressure stripper is another possibility at the TCM plant. A thorough study of different stripper pressures and their effect on lean loading can be done for future work.

- Condenser is an important part of the plant and can affect many results of the simulation. Adjusting the cold-water inlet and condenser duty can be a suggestion for the optimization of gas and amine composition, flow rate, and temperature.

7 Conclusion

A variety of methods have been studied for CO_2 capture from exhaust gas and industrial waste in the last decades. One mature method is to absorb CO_2 in an aqueous amine-based solution. To be able to improve this method, an accurate simulation tool is required. Aspen Plus and Aspen HYSYS are common tools used in this process.

In this thesis, the CO_2 capture process at Technology Centre Mongstad (TCM) by using an MEA solution has been simulated using a rate-based model in Aspen Plus. The main purpose of this study was to develop a rigorous model for the TCM plant with modified configurations that generates reliable simulation results to be able to find the operating limits and maximum utilization capacity for each piece of installed equipment at TCM and the optimum operation condition to achieve the maximum CO_2 removal efficiency.

Many test campaigns have been performed at TCM and some of which have published reports during the last decades. Several studies have been done based on these reports at USN. The rate-based model accuracy was tested using different scenarios based on the reports from test campaigns and the simulation results of different configurations were presented. No change has been made in the interfacial area and the liquid holdup factor, and the only modification was to change the interfacial area, holdup, and mass and heat transfer method. Specific simulation modifications were performed based on each test campaign for equipment and the simulation model.

The model verification was performed with different scenarios and configurations and the deviation between the experimental data and the simulation results for the process parameters were compared. This has been done in general with four main configurations including CHP flue gas, RFCC flue gas, LVC configuration, and cold rich-solvent bypass. CO_2 removal efficiency is usually the most important parameter to be compared between the experimental and the simulation results. The deviation of the CO_2 removal efficiency is less than 3% in all scenarios by using CHP flue gas, less than 2.5% in rich-solvent bypass, and less than 6% in LVC configuration. Except for one test campaign result with near 16% deviation, less than 5% deviation is observed in the scenarios with RFCC flue gas.

In general, there is more consistency between the experimental and simulation data with more detailed input parameters for flue gas and lean amine. However, some other parameters can affect the results even though detailed data has been provided. More deviation is observed by using a relatively low amine flow rate. Moreover, accurate practical parameters are required in the simulation such as the compressor efficiency, as it can affect many output parameters, such as compressor work, SRD, and produced CO_2 flow rate.

The verified rate-based model was used to simulate the TCM plant by using scenario MHP and including AIC, LVC, RFCC and CHP strippers, and modified configurations to find the operating limits. Aspen Exchanger Design (EDR) has also been used to design real heat exchangers at the plant. To avoid flooding, the maximum gas flow rate to DCC and absorber column cannot be more than 78500 Sm^3/hr and 52000 Sm^3/hr respectively. In addition, there is a maximum allowable reboiler duty of 8.4 MW for RFCC reboiler and 3.4 MW for CHP reboiler.

The plant was then optimized for using the maximum flow in the absorber column and only using the RFCC stripper since it has more capacity than the CHP stripper. A cold rich-solvent bypass fraction of 15% shows less lean loading from the stripper. To adjust the lean loading to

the inlet amine and operate within the practical limits, using both strippers is necessary. The results of the modified configuration show that a total reboiler duty of 9.16 MW and a total SRD of 3.0 MJ/kgCO_2 are needed in the plant in this case.

A maximum allowable amine flow rate of 230 ton/hr was used to find the maximum achievable CO_2 efficiency of the plant in the next case. The results show that a CO_2 removal efficiency of 98% can be achieved with a cold rich-solvent bypass fraction of 19%, total reboiler duty of 10.57 MW, and total SRD of 3.63 MJ/kgCO_2 as the optimum operating condition in this case.

To check the possibility of reducing energy consumption in the plant, the condensed water out of the condenser was sent back to the CHP stripper instead of the rich pump and all the rich-solvent bypass was sent to the RFCC stripper, while the bypass fraction remained at 19%. The total reboiler duty and SRD, in this case, are 10.66 MW and 3.65 MJ/kgCO_2 respectively, which shows more energy consumption than the previous configuration.

The results from this study show that the carbon capture process at TCM and the energy consumption at the plant can be optimized for using the maximum plant capacity and considering the operation limits with a rigorous rate-based model. However, further study on different flue gases and scenarios, heat exchanger capacities, rich amine loading, LVC parameter, and stripper pressure is required to achieve a more detailed result.

References

[1] "Technology Centre Mongstad | Test centre for CO2 capture." https://tcmda.com/about-tcm/ (accessed May 03, 2023).

[2] B. Li, Y. Duan, D. Luebke, and B. Morreale, "Advances in CO2 capture technology: A patent review," *Applied Energy*, vol. 102, pp. 1439–1447, Feb. 2013, doi: 10.1016/j.apenergy.2012.09.009.

[3] IPCC, I. P. on C. Change, and I. P. on C. C. W. G. III, *Carbon Dioxide Capture and Storage: Special Report of the Intergovernmental Panel on Climate Change*. Cambridge University Press, 2005.

[4] "Amine-Based CO2 Capture Technology Development from the Beginning of 2013—A Review | ACS Applied Materials & Interfaces." https://pubs.acs.org/doi/full/10.1021/am507465f?casa_token=e73KtduxneEAAAAA%3AQDIGROcBCEc4fOLpieWg-werIE_cQKA2H9UliKlsAZ07tHLsiAR5g3NoL4lzyRkw6A_R7-La954iirKK6A (accessed Sep. 12, 2022).

[5] chrisodgen, "CO2 affects human health at lower levels than previously thought," *AirQualityNews*, Jul. 10, 2019. https://airqualitynews.com/2019/07/10/co2-affects-human-health-at-lower-levels-than-previously-thought/ (accessed Sep. 12, 2022).

[6] N. G. C. Change, "Carbon Dioxide Concentration | NASA Global Climate Change," *Climate Change: Vital Signs of the Planet*. https://climate.nasa.gov/vital-signs/carbon-dioxide (accessed Jan. 30, 2023).

[7] P. M. Mathias, S. Reddy, A. Smith, and K. Afshar, "A Guide to Evaluate Solvents and Processes for Post-Combustion CO2 Capture," *Energy Procedia*, vol. 37, pp. 1863–1870, Jan. 2013, doi: 10.1016/j.egypro.2013.06.066.

[8] T. N. Borhani and M. Wang, "Role of solvents in CO2 capture processes : the review of selection and design methods," *Renewable and Sustainable Energy Reviews*, vol. 114, Oct. 2019, Accessed: Sep. 14, 2022. [Online]. Available: https://eprints.whiterose.ac.uk/151055/

[9] P.-C. Chen, H.-H. Cho, J.-H. Jhuang, and C.-H. Ku, "Selection of Mixed Amines in the CO2 Capture Process," *C*, vol. 7, no. 1, Art. no. 1, Mar. 2021, doi: 10.3390/c7010025.

[10] L. E. Øi, "Removal of CO2 from exhaust gas," p. 165.

[11] P. Luis, "Use of monoethanolamine (MEA) for CO2 capture in a global scenario: Consequences and alternatives," *Desalination*, vol. 380, Aug. 2015, doi: 10.1016/j.desal.2015.08.004.

[12] U. S. P. Arachchige and M. C. Melaaen, "Selection of packing materials for gas absorption," 2012, Accessed: Jan. 30, 2023. [Online]. Available: https://openarchive.usn.no/usn-xmlui/handle/11250/2438548

[13] S. A. Aromada and L. E. Øi, "Energy and Economic Analysis of Improved Absorption Configurations for CO2 Capture," *Energy Procedia*, vol. 114, pp. 1342–1351, Jul. 2017, doi: 10.1016/j.egypro.2017.03.1900.

[14] N. Arshad and A. Alhajaj, “Process synthesis for amine-based CO2 capture from combined cycle gas turbine power plant,” *Energy*, vol. 274, p. 127391, Jul. 2023, doi: 10.1016/j.energy.2023.127391.

[15] B. Lv, B. Guo, Z. Zhou, and G. Jing, “Mechanisms of CO2 Capture into Monoethanolamine Solution with Different CO2 Loading during the Absorption/Desorption Processes,” *Environ. Sci. Technol.*, vol. 49, no. 17, pp. 10728–10735, Sep. 2015, doi: 10.1021/acs.est.5b02356.

[16] M. Chhaganlal, B. Fostås, and E. Hamborg, “Results from MEA testing at the CO2 Technology Centre Mongstad. Part II: Verification of baseline results,” *Energy Procedia*, Jan. 2014, Accessed: Jan. 31, 2023. [Online]. Available: https://www.academia.edu/31946794/Results_from_MEA_testing_at_the_CO2_Technology_Centre_Mongstad_Part_II_Verification_of_baseline_results

[17] M. I. Shah, E. Silva, E. Gjernes, and K. I. Åsen, “Cost Reduction Study for MEA based CCGT Post-Combustion CO_2 Capture at Technology Center Mongstad.” Rochester, NY, Apr. 06, 2021. doi: 10.2139/ssrn.3821061.

[18] M. I. Shah, G. Lombardo, B. Fostås, C. Benquet, A. Kolstad Morken, and T. de Cazenove, “CO2 Capture from RFCC Flue Gas with 30w% MEA at Technology Centre Mongstad, Process Optimization and Performance Comparison.” Rochester, NY, Apr. 16, 2019. doi: 10.2139/ssrn.3366149.

[19] L. E. Øi, “Aspen HYSYS Simulation of CO2 Removal by Amine Absorption from a Gas Based Power Plant,” p. 9.

[20] “Experimental Validation of a Rigorous Absorber Model for CO2 Postcombustion Capture,” *SINTEF*. https://www.sintef.no/en/publications/publication/371103/ (accessed Feb. 06, 2023).

[21] X. Luo *et al.*, “Comparison and validation of simulation codes against sixteen sets of data from four different pilot plants,” *Energy Procedia*, vol. 1, no. 1, pp. 1249–1256, Feb. 2009, doi: 10.1016/j.egypro.2009.01.164.

[22] E. Hansen, “Comparison of Process simulation programs for CO2 removal,” Faculty of Technology, Telemark University College, Porsgrunn, 2011.

[23] A. Cousins, L. T. Wardhaugh, and P. H. M. Feron, “Preliminary analysis of process flow sheet modifications for energy efficient CO2 capture from flue gases using chemical absorption,” *Chemical Engineering Research and Design*, vol. 89, no. 8, pp. 1237–1251, Aug. 2011, doi: 10.1016/j.cherd.2011.02.008.

[24] L. Erikøi, “Comparison of Aspen HYSYS and Aspen Plus simulation of CO2 Absorption into MEA from Atmospheric Gas,” *Energy Procedia*, vol. 23, 2012, Accessed: Feb. 06, 2023. [Online]. Available: https://cyberleninka.org/article/n/383641

[25] Y. Zhang and C.-C. Chen, “Modeling CO2 Absorption and Desorption by Aqueous Monoethanolamine Solution with Aspen Rate-based Model,” *Energy Procedia*, vol. 37, pp. 1584–1596, Jan. 2013, doi: 10.1016/j.egypro.2013.06.034.

[26] S. H. P. Kvam, “Vapor recompression in absorption and desorption process for CO2 capture,” Master thesis, Høgskolen i Telemark, 2013. Accessed: Feb. 06, 2023. [Online]. Available: https://openarchive.usn.no/usn-xmlui/handle/11250/2439010

[27] E. S. Birkelund, “CO2 Absorption and Desorption Simulation with Aspen HYSYS,” Master thesis, Universitetet i Tromsø, 2013. Accessed: Feb. 06, 2023. [Online]. Available: https://munin.uit.no/handle/10037/8159

[28] L. E. Øi and S. H. P. Kvam, “Comparison of Energy Consumption for Different CO2 Absorption Configurations Using Different Simulation Tools,” *Energy Procedia*, vol. 63, pp. 1186–1195, 2014, doi: 10.1016/j.egypro.2014.11.128.

[29] I. S. Larsen, “Simulation and validation of CO2 mass transfer processes in aqueous MES solution with Aspen Plus at CO2 Technology Centre Mongstad,” Master thesis, Faculty of Technology, Telemark University College, 2014.

[30] L. E. Øi and S. A. Aromada, “Simulation of improved absorption configurations for CO2 capture,” Nov. 2015, doi: 10.3384/ecp1511921.

[31] Y. Zhu, “Simulation of CO2 capture at Mongstad using Aspen HYSYS,” Master thesis, Porsgrunn : Faculty of Technology, Telemark University College, 2015.

[32] C. Desvignes, “Simulation of Post-combustion CO2 capture process with amines at CO2 Technology Centre Mongstad,” Master thesis, Lyon CPE, 2015.

[33] K. A. Sætre, “Evaluation of process simulation tools at TCM,” Master thesis, Porsgrunn : Faculty of Technology, University College of Southeastern Norway, 2016.

[34] E. Sundbø, “Partial CO2 capture simulation and cost estimation,” Master thesis, Høgskolen i Sørøst-Norge, 2017. Accessed: Feb. 06, 2023. [Online]. Available: https://openarchive.usn.no/usn-xmlui/handle/11250/2484667

[35] M. Rehan, N. Rahmanian, X. Hyatt, S. P. Peletiri, and A.-S. Nizami, “Energy Savings in CO 2 Capture System through Intercooling Mechanism,” *Energy Procedia*, vol. 142, p. 3683, 2017.

[36] E. Gjernes *et al.*, “Results from 30 wt% MEA Performance Testing at the CO2 Technology Centre Mongstad,” *Energy Procedia*, vol. 114, pp. 1146–1157, Jul. 2017, doi: 10.1016/j.egypro.2017.03.1276.

[37] L. Faramarzi *et al.*, “Results from MEA Testing at the CO2 Technology Centre Mongstad: Verification of Baseline Results in 2015,” *Energy Procedia*, vol. 114, pp. 1128–1145, Jul. 2017, doi: 10.1016/j.egypro.2017.03.1271.

[38] M. Garcia, H. K. Knuutila, and S. Gu, “ASPEN PLUS simulation model for CO2 removal with MEA: Validation of desorption model with experimental data,” *Journal of Environmental Chemical Engineering*, vol. 5, no. 5, pp. 4693–4701, Oct. 2017, doi: 10.1016/j.jece.2017.08.024.

[39] O. Røsvik, “Process simulation of CO2 capture at Mongstad,” Master thesis, Porsgrunn : Faculty of Technology, University College of Southeastern Norway, 2018.

[40] L. Øi, K. A. Sætre, and E. Hamborg, “Comparison of simulation tools to fit and predict performance data of CO2 absorption into monoethanol amine at CO2 Technology Centre Mongstad (TCM),” Nov. 2018, pp. 230–235. doi: 10.3384/ecp18153230.

[41] E. Meuleman *et al.*, “ION 6-Month Campaign at TCM with its Low-Aqueous Capture Solvent Removing CO2 from Natural Gas Fired and Residue Fluid Catalytic Cracker Flue Gases.” Rochester, NY, Apr. 14, 2019. doi: 10.2139/ssrn.3366392.

[42] S. Fagerheim, “Process simulation of CO2 absorption at TCM Mongstad,” Master thesis, University of South-Eastern Norway, 2019. Accessed: Jan. 30, 2023. [Online]. Available: https://openarchive.usn.no/usn-xmlui/handle/11250/2644680

[43] P. Loldrup Fosbøl *et al.*, “Results of the fourth Technology Centre Mongstad campaign: LVC testing,” *International Journal of Greenhouse Gas Control*, vol. 89, pp. 52–64, Oct. 2019, doi: 10.1016/j.ijggc.2019.06.025.

[44] S. S. Karunarathne and L. E. Øi, *Aspen Hysys and Aspen Plus Simulations for Amine Based Absorption Process Compared to Results from Experiments in CO2-RIG*. SINTEF Academic Press, 2019. Accessed: Feb. 06, 2023. [Online]. Available: https://sintef.brage.unit.no/sintef-xmlui/handle/11250/2637962

[45] N. Sæter, “Process simulation of CO2 absorption data fitted to performance efficiency at TCM Mongstad,” Master thesis, Faculty of Technology, Natural sciences, and Maritime Science, University of South-Eastern Norway, Porsgrunn, 2021.

[46] S. Hume *et al.*, “Results From MEA Testing at the CO_2 Technology Centre Mongstad. Verification of Residual Fluid Catalytic Cracker (RFCC) Baseline Results.” Rochester, NY, Apr. 06, 2021. doi: 10.2139/ssrn.3821037.

[47] D. Thimsen *et al.*, “Results from MEA testing at the CO2 Technology Centre Mongstad. Part I: Post-Combustion CO2 capture testing methodology,” *Energy Procedia*, vol. 63, pp. 5938–5958, Jan. 2014, doi: 10.1016/j.egypro.2014.11.630.

List of figures

List of tables

Appendices

Appendix A – Task description

Appendix B – TCM data for scenario H14

Appendix C – TCM data for scenario F17

Appendix D – TCM data for scenario S21

Appendix E – TCM data for scenario M190 and M191

Appendix F – TCM data for scenarios S6C, S6A, and S4

Appendix G – TCM data for scenarios F2A to F2F

Appendix H – TCM data for scenarios Shah1 to Shah5

Appendix I – Simulation flowsheet of TCM plant

Appendix A – Task description

FMH606 Master's Thesis

Title: Optimum conditions and maximum capacity at the amine-based CO_2 capture plant at TCM Mongstad

USN supervisor: Lars Erik Øi, Cosupervisor: Koteswara Rao Putta, TCM

External partner: CO_2 Technology Centre Mongstad (TCM)

Task background:
Technology Centre Mongstad (TCM) is the world's largest facility for testing and improving CO_2 capture. To be able to predict process behaviour it is necessary to have good and robust simulation models. There have been performed several projects at Telemark University College/ University of South-Eastern Norway on process simulation of amine-based CO_2 capture processes. Most of the simulations have been performed with the program Aspen HYSYS, but the process has also been simulated using Aspen Plus. In several Master Thesis projects from 2014 to 2022, both programs have been used to simulate the monoethanol amine (MEA) based CO_2 capture process at TCM. These projects have mainly been limited to the absorption column. The models at USN have not included the stripping part, intercooling or lean vapour compression.

Task description:
The aim of the project is to develop simulation models for amine-based CO_2 capture.

1. A literature search on performance data of CO_2 capture using aqueous MEA as solvent with emphasis on data from TCM.
2. Develop Aspen HYSYS and/or Aspen Plus simulation models for the MEA based CO_2 capture process at TCM also including the stripping column, intercooling and lean vapour recompression.
3. Extend the models to maximum gas flow capacity and optimize the conditions for maximum capture rate.
4. Evaluate the limits for the TCM plant and limits for the simulation models.

Student category: Reserved for Shahin Kermani

The task is suitable for online students (not present at the campus): Yes (but it must be possible to run the Aspen HYSYS and Aspen Plus programs)
Practical arrangements:

The work will be carried out mainly in Porsgrunn or from home. The aim is to base the work on open available data, so that the thesis can be open. In case confidential information from TCM Mongstad is utilized, this information must however be treated confidentially.

Supervision:

As a general rule, the student is entitled to 15-20 hours of supervision. This includes necessary time for the supervisor to prepare for supervision meetings (reading material to be discussed, etc).

Signatures:

Supervisor (date and signature):

Student (write clearly in all capitalized letters):

Student (date and signature):

Appendix B – TCM data for scenario H14

Espen S. Hamborg et al. / Energy Procedia 63 (2014) 5994 – 6011

Table 8. Typical amine plant process information during Base-Case testing

Process parameter	Units	Value
Operating capacity	%	80
CHP flue gas supply rate	Sm^3/hr	46970
CHP flue gas supply temperature	°C	25.0
CHP flue gas supply pressure	barg	0.063
CHP flue gas supply CO_2 concentration (wet)	vol%	3.7
CHP flue gas supply O_2 concentration (wet)	vol%	13.6
Depleted flue gas temperature	°C	24.7
Lean MEA concentration	wt%	30
Lean CO_2 loading	mol CO_2 / mol MEA	0.23
Lean amine supply flow rate	kg/hr	54900
Lean amine supply temperature	°C	36.5
Lean amine density	kg/m^3	1067
Active absorber packing height	m	24
Temperature, upper absorber packing – 6	°C	45.4
Temperature, upper absorber packing – 5	°C	51.1
Temperature, upper absorber packing – 4	°C	51.2
Temperature, upper absorber packing – 3	°C	50.3
Temperature, upper absorber packing – 2	°C	49.6
Temperature, upper absorber packing – 1	°C	48.5
Temperature, middle absorber packing – 6	°C	46.7
Temperature, middle absorber packing – 5	°C	45.2
Temperature, middle absorber packing – 4	°C	43.5
Temperature, middle absorber packing – 3	°C	41.7
Temperature, middle absorber packing – 2	°C	40.6
Temperature, middle absorber packing – 1	°C	39.0
Temperature, lower absorber packing – 12	°C	38.4
Temperature, lower absorber packing – 11	°C	39.1
Temperature, lower absorber packing – 10	°C	35.0
Temperature, lower absorber packing – 9	°C	33.7
Temperature, lower absorber packing – 8	°C	32.2
Temperature, lower absorber packing – 7	°C	30.4
Temperature, lower absorber packing – 6	°C	29.8
Temperature, lower absorber packing – 5	°C	29.3
Temperature, lower absorber packing – 4	°C	28.1
Temperature, lower absorber packing – 3	°C	28.4
Temperature, lower absorber packing – 2	°C	27.6
Temperature, lower absorber packing – 1	°C	27.2

Rich solution return temperature	°C	27.7
Temperature above upper absorber packing	°C	38.1
Wash water 1 supply flow rate	kg/hr	55000
Wash water 1 inlet temperature	°C	28.4
Wash water 1 withdrawal temperature	°C	43.9
Temperature above Wash Water 1	°C	36.2
Wash water 2 supply flow rate	kg/hr	62000
Wash water 2 inlet temperature	°C	23.5
Wash water 2 withdrawal temperature	°C	35.0
Temperature above Wash Water 2	°C	24.7
Rich CO_2 loading	mol CO_2 / mol MEA	0.48
Rich solution supply flow rate	kg/hr	57200
Rich solution supply temperature	°C	108.6
Lean solution return temperature	°C	119.1
Rich amine density	kg/m^3	1114
Reboiler steam flow rate	kg/hr	4800
Reboiler steam temperature	°C	169
Reboiler steam pressure	barg	4.42
Reboiler condensate temperature	°C	118.8
Reboiler condensate pressure	barg	4.11
Stripper overhead pressure	barg	0.90
Stripper overhead temperature	°C	99.8
Stripper overhead reflux flow rate	kg/hr	1370
Stripper overhead reflux temperature	°C	23.3
Stripper sump temperature	°C	119.3
Reboiler solution temperature	°C	122.3
Lean vapour compressor system	-	off
Product CO_2 flow rate	kg/hr	2670
Product CO_2 discharge temperature	°C	17.7
Product CO_2 discharge pressure	barg	0.023

Appendix C – TCM data for scenario F17

Leila Faramarzi et al. / Energy Procedia 114 (2017) 1128 – 1145

Table 12. Averaged process data for the test period C3–4 of baseline testing in September 2015.

Operating capacity	%	100
CHP flue gas supply rate	Sm^3/h	59 430
CHP flue gas supply temperature	°C	29.8
CHP flue gas supply pressure	barg	0.01
CHP flue gas supply CO_2 concentration (dry)	vol%	3.7
CHP flue gas supply O_2 concentration (wet)	vol%	14.6
CHP flue gas supply water content	vol%	3.7
Depleted flue gas temperature	°C	30.4
Lean MEA concentration (CO_2 free)	wt%	31
Lean MEA concentration (incl CO_2)	wt%	30
Lean CO_2 loading	mol CO_2/mol MEA	0.20
Lean amine supply flow rate	kg/h	57 434
Lean amine supply temperature	°C	37.0
Lean amine density	kg/m^3	1 073
Rich solution return temperature	°C	33.2
Temperature above upper absorber packing	°C	39.7
Wash water 1 (lower) supply flow rate	kg/h	55 005
Wash water 1 inlet temperature	°C	30.4
Wash water 1 withdrawal temperature	°C	44.9
Temperature above Wash Water 1	°C	38.0
Wash water 2 (upper) supply flow rate	kg/h	54 997
Wash water 2 inlet temperature	°C	30.4
Wash water 2 withdrawal temperature	°C	37.3
Temperature above Wash Water 2	°C	30.4

Rich CO_2 loading	mol CO_2/mol MEA	0.48
Rich solution supply flow rate	kg/h	60 775
Rich solution supply temperature	°C	110.7
Lean solution return temperature	°C	121.3
Rich amine density	kg/m^3	1 125
Reboiler steam flow rate	kg/h	5 398
Reboiler steam temperature	°C	156
Reboiler steam pressure	barg	2.04
Reboiler condensate temperature	°C	132.8
Reboiler condensate pressure	barg	1.96
Stripper overhead pressure	barg	0.91
Stripper overhead temperature	°C	96.1
Stripper overhead reflux flow rate	kg/h	1 227
Stripper overhead reflux temperature	°C	17.64
Stripper sump temperature	°C	121.0
Reboiler solution temperature	°C	125.1
Lean vapour compressor system	-	off
Product CO_2 flow rate	kg/h	3 325
Product CO_2 discharge temperature	°C	17.9
Product CO_2 discharge pressure	barg	0.017
Product CO_2 water content	vol%	1.3
Active absorber packing height	m	24
Temperature, upper absorber packing – 6	°C	47.4
Temperature, upper absorber packing – 5	°C	51.7
Temperature, upper absorber packing – 4	°C	51.6
Temperature, upper absorber packing – 3	°C	50.5
Temperature, upper absorber packing – 2	°C	49.9
Temperature, upper absorber packing – 1	°C	48.9
Temperature, middle absorber packing – 6	°C	47.2
Temperature, middle absorber packing – 5	°C	46.0
Temperature, middle absorber packing – 4	°C	44.4
Temperature, middle absorber packing – 3	°C	43.1
Temperature, middle absorber packing – 2	°C	42.2
Temperature, middle absorber packing – 1	°C	40.9
Temperature, lower absorber packing – 12	°C	40.6
Temperature, lower absorber packing – 11	°C	41.6
Temperature, lower absorber packing – 10	°C	37.4
Temperature, lower absorber packing – 9	°C	37.1

Temperature, lower absorber packing – 8	°C	35.9
Temperature, lower absorber packing – 7	°C	34.3
Temperature, lower absorber packing – 6	°C	34.1
Temperature, lower absorber packing – 5	°C	33.8
Temperature, lower absorber packing – 4	°C	32.9
Temperature, lower absorber packing – 3	°C	33.2
Temperature, lower absorber packing – 2	°C	32.5
Temperature, lower absorber packing – 1	°C	32.4
Stripping section packing height	m	8
Temperature, stripper packing – 7	°C	102.7
Temperature, stripper packing – 6	°C	103.1
Temperature, stripper packing – 5	°C	104.5
Temperature, stripper packing – 4	°C	107.7
Temperature, stripper packing – 3	°C	112.1
Temperature, stripper packing – 2	°C	114.7
Temperature, stripper packing – 1	°C	119.4

Appendix D – TCM data for scenario S21

GHGT-15 Scott Hume

Table 6. Stripper reboiler thermal energy consumption

Test period	Reboiler steam flow rate kg/hr	Reboiler duty MJ/hr	Using the product CO_2 flow (P)[i]		Using CO_2 removed (S – D)	
			Product CO_2 Flow kg/hr	Specific Thermal Use GJ/t CO_2	Product CO_2 Flow kg/hr	Specific Thermal Use GJ/t CO_2
C5-1	12,343	28,173	8142	3.46	7849	3.59
C5-2	12,459	28,343	8138	3.48	7843	3.61
C5-3	12,436	28,315	8159	3.47	7863	3.60
C5-4	12,463	28,376	8072	3.52	7824	3.63
C5-5	12,457	28,380	8070	3.52	7827	3.63
C5-6	12,369	28,365	8085	3.51	7835	3.62
C5-7	12,630	28,678	8078	3.55	7865	3.65
C5-8	12,585	28,592	8088	3.54	7902	3.62
C5-9	12,641	28,771	8133	3.54	7984	3.60
C5-10	12,571	28,593	8093	3.53	7962	3.59
C5-11	12,583	28,636	8069	3.55	7988	3.58
C5-12	12,397	28,427	8093	3.51	7984	3.56
C5-13	11,592	26,529	7724	3.43	7548	3.51

i The wet CO_2 flow is obtained by using the FTIR measured moisture content of the product CO_2

Table 11. Results of RFCC baseline testing in 2018

Baseline year	**2018**		
Packing height (m)	18	Lean loading	0.23
Flue gas flow (Sm^3/h)	35 000	Rich loading	0.48
Flue gas supply temperature (°C)	31.0	Stripper bottom temperature (°C)	121.0
Flue gas supply pressure (bar)	0.02	CO_2 capture (%)	91
Lean amine flow (kg/h)	133 000	SRD (MJ/kg CO_2)	3.55

Appendix E – TCM data for scenarios M190 and M191

List of KPIs for inclusion in the RFCC campaign									
KPI	**Units**	**Base-0**	**Base-1**	**Base-2**	**Low SRD**	**Conc-1**	**EPRI-1**	**EPRI-2**	**EPRI-3**
Sample Date		Mar 1, 2017	Mar 4-6, 2017	Mar 14-16, 2018	Mar 11, 2017	Mar 28, 2017	Apr 18, 2017	Apr 19, 2017	Apr 20, 2017
CO2 in Flue Gas	%vol	12.4	12.6	12.5	12.6	14.5	12.4	12.5	12.6
L/G	kg/Sm3	2.73	2.75	2.78	2.99	4.07	2.23	2.23	2.21
Specific Reboiler Duty	MJ/kg CO_2	3.28	3.36	3.31	3.25	3.39	3.36	3.37	3.38
CO2 Capture Efficiency	%	89.2%	88.1%	85.8%	91.1%	85.4%	89.5%	89.0%	88.8%
CO2 Product Purity	%vol	97.1%	98.1%	98.7%	99.2%	99.2%	99.5%	99.5%	99.0%
Emissions to atm	Ratio to MEA	No data for MEA operation under similar conditions are available for comparison at time of publication							

Appendix F – TCM data for scenarios S6C, S6A, and S4

Parameter	UoM	Range
Number of test cases		10
Absorber Packing height	m	18
Flue gas flow into absorber	Sm^3/h (w)	35,000
Flue gas composition:		
CO_2	mole%	13.1-13.5
H_2O	mole%	4.0 – 4.2
O_2	mole%	12.2 – 13.5
Flue gas inlet temperature	°C	29 – 30
Conc. of MEA in lean solvent (CO_2 loaded)	wt%	28-30.2
Lean solvent flow rate	kg/h	100,000 – 165,000
Lean solvent temperature	°C	50 to 55
Liquid to Gas ratio	kg/Sm^3	2.8-4.6
Stripper bottom temperature	°C	119.5 – 122.6
CO_2 capture rate	%	86-89
Stripper pressure	barg	0.95-0.96

Case ID	Flue gas flow rate (Sm^3/h)	Lean amine flow rate (kg/h)	Lean amine loading(mol CO_2/mol MEA)	CO_2 Capture rate (%)*	SRD (GJ/ton CO_2)*
2C-CHP-6C Recy	33,908	99,670	0.160	88.3%	3.92
2C-CHP-6A Recy	33,900	114,873	0.19	87.3%	3.70
2C-CHP-5C Recy	33,934	116,455	0.204	87.3%	3.67
2C-CHP-8A Recy	33,918	120,360	0.199	87.4%	3.67
2C-CHP-3 Recy	33,699	136,867	0.251	88.1%	3.71
2C-CHP-4 Recy	33,874	160,821	0.273	85.9%	3.85

*Tabulated Capture rate and SRD is based on Meth 1.

Appendix G – TCM data for scenarios F2A to F2F

Table 1
Overview of process variables for the 16 cases, 1A to 2F.

Description	Unit		Case 1A-1	Case 1B	Case 1C	Case 1A-2	Case 1D	Case 1E	Case 1F	Case 2A	Case 2B	Case 2C-1	Case 2C-2	Case 2C-3	Case 2D-1	Case 2D-2	Case 2E	Case 2F
CHP Flue gas flow rate into absorber	Sm^3/h	mean	34985	34983	34996	34997	34985	34984	34995	34996	34986	34988	34989	34995	35001	34991	34996	34991
		stdev	60	45	50	61	63	60	63	63	60	61	42	53	65	47	60	47
CO_2 concentration into absorber	vol%, dry	mean	13.5	13.7	13.6	13.5	13.7	13.5	11.0	13.9	13.7	13.7	13.7	13.8	13.9	13.7	13.6	11.2
		stdev	0.04	0.06	0.04	0.05	0.03	0.09	0.02	0.03	0.04	0.03	0.04	0.03	0.02	0.03	0.04	0.04
Flue gas temperature into absorber	°C	mean	30.2	30.1	30.0	30.0	30.1	30.0	30.0	30.1	30	30.1	29.9	30.0	29.9	30	30	30.0
		stdev	0.25	0.04	0.04	0.04	0.05	0.04	0.05	0.04	0.04	0.04	0.04	0.04	0.03	0.06	0.04	0.05
Flue gas inlet pressure	barg	mean	0.017	0.017	0.018	0.017	0.018	0.018	0.018	0.017	0.017	0.018	0.018	0.018	0.018	0.019	0.018	0.018
		stdev	6E-05	2E-04	5E-05	3E-04	2E-04	2E-04	7E-18	36E-04	2E-04	7E-18	1E-04	7E-05	3E-05	2E-04	2E-05	1E-17
Lean solvent temperature	°C	mean	54	54.0	54.0	52.5	54.0	54.0	54.0	50.8	54.00	54.0	54.0	54.0	54.0	54.0	54.0	54.0
		stdev	0.23	0.10	0.02	0.4	0.02	0.07	0.02	0.09	0.17	0.1	0.02	0.04	0.03	0.04	0.02	0.03
Lean solvent density	kg/m^3	mean	1047	1058	1060	1047	1069	1061	1064	1048	1059	1065	1063	1062	1070	1069	1063	1065
		stdev	0.80	0.70	0.26	0.46	0.79	0.32	0.48	0.10	0.19	0.19	0.42	0.09	0.18	0.14	0.15	0.15
Lean solvent flow rate	t/h	mean	120.1	160.7	200.5	120.5	200.6	200.1	201.3	120.2	165.6	200.9	200.8	200.6	201.7	201.7	200.9	202.1
		stdev	0.2	0.2	0.2	0.1	0.5	0.7	0.2	0.3	0.3	1.2	0.3	0.5	0.3	0.3	0.3	0.4
Flue gas temperature out of absorber	°C	mean	31.4	30.7	30.7	34.0	31.4	32.1	31.6	31.6	31.4	30.8	31.5	31.4	32.3	33.7	30.9	31.6
		stdev	0.12	0.06	0.06	0.36	0.12	0.09	0.03	0.14	0.09	0.1	0.15	0.03	0.15	0.14	0.06	0.04
CO_2 out of the absorber	vol%, wet	mean	1.5	1.7	1.5	1.6	3.1	1.5	1.2	1.6	1.6	1.9	1.7	1.6	3.1	2.9	1.5	1.3
		stdev	0.06	0.08	0.02	0.09	0.03	0.04	0.02	0.06	0.04	0.03	0.08	0.01	0.02	0.04	0.03	0.02
Rich amine T out from absorber	°C	mean	43.4	47.6	51.3	43	49.8	51.2	51.7	43.2	48.1	51	50.9	51.4	49.6	49.7	51.4	51.8
		stdev	0.14	0.23	0.04	0.48	0.11	0.09	0.03	0.1	0.06	0.09	0.09	0.04	0.04	0.04	0.05	0.05
Rich amine flow going to the HE	t/h	mean	127.3	168.0	208.0	128.0	207.5	207.5	207.5	128.0	173.0	208.0	208.0	208.0	208.0	208.0	208.0	208.0
		stdev	0.5	0.02	0.3	0.05	0.04	0.06	0.04	0.04	0.03	0.04	0.04	0.03	0.04	0.03	0.03	0.02
Rich amine density to HE	kg/m^3	mean	1107	1100	1093	1104	1098	1094	1090	1107	1100	1097	1096	1095	1100	1099	1096	1092
		stdev	1.1	0.77	0.33	0.92	0.60	0.41	0.42	0.13	0.17	0.21	0.29	0.09	0.18	0.17	0.21	0.25
Rich amine out from HE	°C	mean	109.3	108.9	108.3	110.3	106.6	106.8	108.1	95.1	93.9	93.3	96.1	92.1	91.9	94.8	93.1	93.2
		stdev	0.14	0.08	0.06	0.33	0.09	0.1	0.06	0.07	0.06	0.13	0.05	0.05	0.06	0.05	0.04	0.06
Lean amine to HE	°C	mean	120.6	119.1	118.3	120.4	116.7	116.5	117.8	103.2	101.8	101	104.3	99.5	99.8	103.1	100.8	100.7
		stdev	0.03	0.03	0.02	0.04	0.03	0.05	0.03	0.02	0.05	0.06	0.03	0.03	0.05	0.03	0.02	0.05
Lean amine to sea water cooler	°C	mean	51.9	57.3	60.9	52.5	59.3	60.6	61.2	50.8	55.4	58.3	58.6	58.5	56.9	57.4	58.6	59.0
		stdev	0.13	0.19	0.06	0.37	0.08	0.13	0.05	0.09	0.06	0.13	0.08	0.04	0.06	0.07	0.05	0.05
P in stripper bottom	barg	mean	0.98	0.98	0.98	0.98	0.98	0.84	0.98	0.98	0.98	0.98	0.98	0.98	0.98	0.98	0.84	0.98
		stdev	0.001	0.002	0.001	0.001	0.001	0.002	0.001	0.001	0.001	0.002	0.001	0.001	0.001	0.001	0.001	0.001
Temperature in stripper bottom	°C	mean	120.9	119.4	118.5	120.9	116.9	116.7	118.2	120.8	118.6	117.1	117.5	117.6	115	115.2	115.7	116.7
		stdev	0.03	0.03	0.02	0.02	0.05	0.04	0.03	0.01	0.04	0.05	0.11	0.02	0.05	0.05	0.05	0.05
Top stripper outlet temperature	°C	mean	96.9	97.5	98.7	98.1	96.7	97.2	99.9	88.8	88.7	89.1	91.1	88.5	87.2	89.3	89.2	90.8
		stdev	0.12	0.15	0.05	0.11	0.07	0.11	0.07	0.09	0.05	0.08	0.11	0.04	0.08	0.16	0.06	0.08
Top stripper outlet pressure	barg	mean	0.94	0.95	0.95	0.95	0.94	0.80	0.95	0.94	0.95	0.94	0.95	0.95	0.95	0.95	0.80	0.95
		stdev	0.001	0.002	0.002	0.001	0.001	0.002	0.001	0.002	0.001	0.001	0.001	0.001	0.001	0.001	0.001	0.001

(continued on next page)

Table 1 (*continued*)

Description	Unit		Case 1A-1	Case 1B	Case 1C	Case 1A-2	Case 1D	Case 1E	Case 1F	Case 2A	Case 2B	Case 2C-1	Case 2C-2	Case 2C-3	Case 2D-1	Case 2D-2	Case 2E	Case 2F
Top stripper outlet flow	kg/h	mean	8623	8655	8971	8842	7474	9511	7543	7357	7084	6979	7431	7159	5935	6404	7728	5997
		stdev	40	77	35	55	26	66	41	36	33	49	64	34	52	32	40	43
CO_2 Outlet overhead system pressure	barg	mean	0.90	0.90	0.90	0.90	0.90	0.75	0.90	0.90	0.90	0.90	0.90	0.90	0.90	0.90	0.75	0.90
			0.0008	0.0008	0.0004	0.0009	0.0003	0.002	0.0007	0.001	0.0005	0.001	0.0008	0.0007	0.0003	0.0006	0.0009	0.0004
Temperature out of reboiler (HE)	°C	mean	123.3	122.7	122.5	123	119.7	118.4	120.1	122.6	121.8	119.6	119.6	119.8	118.4	118.5	117.5	119.3
		stdev	0.09	0.04	0.03	0.03	0.11	0.05	0.02	0.02	0.03	0.04	0.05	0.02	0.03	0.02	0.02	0.03
Pressure out of reboiler (HE)	barg	mean	0.95	0.96	0.96	0.96	0.96	0.83	0.97	0.95	0.96	0.97	0.98	0.97	0.97	0.97	0.83	0.97
		stdev	0.001	0.002	0.002	0.001	0.002	0.002	0.001	0.001	0.001	0.001	0.001	0.001	0.0004	0.001	0.001	0.001
Temperature into reboiler (HE)	°C	mean	120.8	119.1	118.2	120.6	116.7	116.6	117.9	120.5	118.3	116.8	117.2	117.4	114.7	114.9	115.5	116.5
		stdev	0.05	0.03	0.02	0.04	0.04	0.05	0.04	0.02	0.06	0.05	0.12	0.03	0.04	0.04	0.04	0.05
Pressure into reboiler (HE)	barg	mean	1.1	1.2	1.2	1.2	1.2	1.1	1.2	1.2	1.2	1.2	1.2	1.2	1.2	1.2	1.1	1.2
		stdev	0.001	0.002	0.002	0.001	0.004	0.002	0.001	0.001	0.002	0.002	0.001	0.001	0.001	0.001	0.001	0.001
Temperature of steam into reboiler	°C	mean	160.2	157.2	166.7	157.1	159.1	168.5	162.1	158.8	159.2	159.9	154.5	157.6	156.9	155.6	155.4	158
		stdev	3.3	1.1	0.32	0.31	1.1	0.60	0.46	0.17	1.2	0.15	0.23	0.09	0.10	0.32	0.6	0.8
Pressure of steam into reboiler	barg	mean	2.8	2.8	2.9	2.7	2.3	2.5	2.4	2.3	2.3	2.1	2.3	2.2	1.9	2.0	2.0	2.0
		stdev	0.01	0.01	0.01	0.01	0.01	0.02	0.01	0.01	0.01	0.01	0.01	0.01	0.004	0.01	0.01	0.01
Flow of steam into reboiler	kg/h	mean	12088	12629	13282	12141	11527	12628	11649	9652	9770	9960	11011	10147	9089	9723	10656	8898
		stdev	204	98	40	66	58	53	42	41	47	49	97	50	34	38	65	48
Temperature of steam upstream	°C	mean	156.7	150.6	168.2	153.0	159.3	170.4	163.2	160.8	161.1	161.8	154.5	159.4	159.3	157.6	156.6	160.4
		stdev	7.5	4.2	0.4	1.2	1.7	0.6	0.5	0.2	1.4	0.2	0.7	0.2	0.1	0.4	0.9	0.8
Reboiler outlet temperatue, steam	°C	mean	122.7	120.9	119.8	122.0	117.9	117.3	118.8	122.5	120.5	118.1	118.1	118.5	116	116.1	116.2	117.6
		stdev	0.07	0.04	0.04	0.06	0.11	0.07	0.02	0.01	0.12	0.05	0.08	0.02	0.06	0.04	0.04	0.06
Reboiler outlet pressure, steam	barg	mean	2.8	2.8	2.9	2.7	2.3	2.5	2.4	2.3	2.3	2.1	2.2	2.2	1.9	2.0	2.0	2.0
		stdev	0.009	0.01	0.01	0.01	0.01	0.02	0.007	0.007	0.007	0.008	0.013	0.007	0.004	0.006	0.008	0.008
Condenser bottom flow	kg/h	mean	2878	2977	3254	3123	2484	3415	2893	1746	1689	1708	1999	1706	1413	1619	1991	1600
		stdev	34	39	17	36	16	21	23	20	15	19	31	20	7	13	19	14
Condenser bottom temperature	°C	mean	16.7	16	16.4	16.1	16.4	16.3	15.7	16.7	16.7	16.4	16.4	16.1	16.7	16.3	16.7	15.7
		stdev	0.06	0.13	0.03	0.09	0.17	0.12	0.1	0.07	0.07	0.05	0.06	0.02	0.08	0.37	0.02	0.06
Condenser outlet temperature, hot side	°C	mean	17.5	17.0	17.5	17.0	17.4	17.3	17.5	16.8	17.5	16.9	17.5	16.7	17.6	17.3	17.5	16.5
		stdev	0.13	0.14	0.06	0.13	0.2	0.18	0.11	0.11	0.1	0.13	0.12	0.08	0.08	0.3	0.09	0.09
Flow of seawater to condenser inlet	kg/h	mean	92278	98716	104193	105040	81885	128612	90363	55781	47816	49786	54966	51890	34865	40070	59047	43988
		stdev	852	117	617	106	508	610	554	57	484	49	731	41	391	487	450	544
Temperature of seawater to condenser inlet	°C	mean	7.7	7.6	7.6	7.7	8.6	8.4	8.4	7.7	7.7	7.7	7.7	7.6	7.7	7.7	7.8	8.0
		stdev	0.02	0.006	0.02	0.01	0.17	0.11	0.02	0.008	0.03	0.05	0.01	0.02	0.01	0.02	0.07	0.06
Temperature of seawater to condenser outlet	°C	mean	28.3	27.4	28.0	27.2	28.4	25.7	29	28.7	31.0	30.1	30.3	29.1	33.6	32.5	29.6	31.2
		stdev	0.22	0.21	0.07	0.18	0.22	0.21	0.17	0.19	0.18	0.18	0.23	0.13	0.17	0.67	0.18	0.23
Flow of CO_2 out of condenser drum	kg/h	mean	7553	7468	7404	7443	6589	7408	6038	7726	7473	7290	7419	7539	6627	6627	7409	6114
		stdev	21	33	26	47	23	48	27	33	29	47	49	35	26	23	33	45

P. Fosbøl et al. / Data in brief 26 (2019) 104483

P. Fosbøl et al. / Data in brief 26 (2019) 104483

Amine flash vessel pressure	barg	mean	1.0	1.0	1.0	1.0	1.0	0.87	1.0	0.046	0.046	0.047	0.20	−0.0061	0.043	0.19	0.046	0.044
		stdev	0.001	0.001	0.001	0.003	0.002	0.001	0.001	0.001	0.002	0.002	0.001	0.001	0.001	0.001	0.001	0.002
Flash vessel inlet temperature	°C	mean	112.0	110.3	108.5	111	107	108.8	108	101.7	100.8	100.3	103.8	99	99.1	102.6	100.3	100.1
		stdev	0.07	0.09	0.06	0.68	0.12	0.06	0.16	0.03	0.05	0.06	0.03	0.03	0.05	0.03	0.03	0.05
Lean amine temperature to antisurge HE	°C	mean	120.8	119.2	118.4	120.5	116.8	116.6	117.9	102.3	101.4	100.8	104.1	99.4	99.5	102.9	100.7	100.5
		stdev	0.05	0.03	0.03	0.03	0.03	0.05	0.04	0.02	0.04	0.05	0.04	0.02	0.05	0.03	0.02	0.05
Lean amine flow to flash vessel	t/h	mean	114.9	152.6	190.3	116.0	188.5	189.6	190.6	117.7	160.4	193.4	193.2	194.6	192.6	191.7	193.5	194.6
		stdev	0.5	0.3	0.3	0.6	1.0	0.4	0.3	0.4	0.5	0.8	0.7	0.5	0.4	0.7	0.8	0.8
Inlet pressure to compressor	barg	mean	0.95	0.95	0.94	0.95	0.94	0.80	0.94	−0.066	−0.069	−0.060	0.091	−0.13	−0.077	0.089	−0.061	−0.072
		stdev	0.005	0.0006	0.0009	0.004	0.001	0.002	0.001	0.001	0.002	0.002	0.001	0.001	0.001	0.002	0.001	0.001
Inlet temperature to compressor	°C	mean	35.6	45.4	44.5	42.7	60.0	42.3	62.5	100.4	99.5	98.9	102.8	97.3	97.6	101.6	99.0	98.6
		stdev	0.74	0.52	0.60	10.2	0.25	5.8	0.73	0.02	0.04	0.05	0.03	0.02	0.05	0.04	0.03	0.05
Outlet pressure from compressor	barg	mean	0.92	0.87	0.86	0.88	0.88	0.70	0.87	1.04	1.05	1.06	1.00	1.04	0.99	0.97	0.87	1.01
		stdev	0.01	0.009	0.005	0.005	0.004	0.004	0.002	0.003	0.009	0.003	0.001	0.002	0.002	0.004	0.002	0.006
Outlet temperature from compressor	°C	mean	25.0	20.9	17.8	18.9	29.3	22.0	41.3	192.2	190.7	188.9	171.9	197.5	188.8	170.7	178.3	189.4
		stdev	0.86	0.17	0.16	1.0	0.33	1.0	3.0	0.06	0.15	0.28	0.18	0.07	0.06	0.2	0.09	0.43
Lean loading[a]	mol/mol		0.215	0.265	0.290	-[b]	0.318	0.273	0.292	0.201	0.266	0.284	0.280	0.285	0.318	0.318	0.288	0.301
Rich loading[a]	mol/mol		0.483	0.524	0.507	-[b]	0.507	0.486	0.467	0.543	0.513	0.493	0.488	0.483	0.493	0.501	0.496	0.467
CO_2 capture	%	mean	90.1	88.9	89.7	88.9	78.7	89.8	89.5	89.8	89.4	87.4	88.4	89.5	79.2	80.5	89.6	89.4
		stdev	0.4	0.5	0.1	0.6	0.2	0.3	0.2	0.2	0.3	0.2	0.5	0.1	0.1	0.02	0.2	0.2
Q^{c}_{SRD}	MJ/kg CO_2	mean	3.60	3.77	4.00	3.66	3.90	3.83	4.34	2.79	2.90	3.04	3.29	3.00	3.03	3.23	3.20	3.26
		stdev	0.06	0.04	0.02	0.04	0.03	0.04	0.02	0.02	0.02	0.02	0.02	0.02	0.02	0.02	0.03	0.02
Q^{d}_{LVC}	GJ electric/ton CO_2	mean	0.000	0.000	0.000	0.000	0.000	0.000	0.000	0.19	0.19	0.19	0.14	0.21	0.21	0.14	0.15	0.24
		stdev	0.000	0.000	0.000	0.000	0.000	0.000	0.000	0.008	0.001	0.001	0.001	0.001	0.001	0.002	0.001	0.001
Antisurge cooler inlet cold side temp	°C	mean	121	119	118	121	117	117	118	102	101	101	104	99	99	103	101	101
		stdev	0.05	0.03	0.03	0.03	0.03	0.05	0.04	0.02	0.04	0.05	0.04	0.02	0.05	0.03	0.02	0.05
Antisurge cooler outlet cold side temp	°C	mean	120.6	119.1	118.3	120.4	116.7	116.5	117.8	103.2	101.8	101	104.3	99.5	99.8	103.1	100.8	100.7
		stdev	0.03	0.03	0.02	0.04	0.03	0.05	0.03	0.02	0.05	0.06	0.03	0.03	0.05	0.03	0.02	0.05
Antisurge cooler outlet cold side flow	t/h	mean	117.6	161.7	201.52	122.7	199.4	200.6	201.4	120.8	164.3	198.1	198.9	198.1	197.8	198.3	198.5	199.1
		stdev	0.26	0.26	0.27	0.13	0.69	0.76	0.36	0.38	0.35	0.11	0.33	0.56	0.3	0.32	0.32	0.36
Seawater flow to antisurge	kg/h	mean	33294	33118	33329	33189	33173	32818	33242	33243	33308	33253	33362	33301	33350	33399	33331	33468
		stdev	72	32	418	251	173	158	161	167	64	191	152	201	155	156	212	154
Temp. of seawater out of antisurge	°C	mean	7.8	7.7	7.6	7.7	8.6	8.4	8.4	8.9	8.7	8.8	8.8	8.4	8.3	8.6	8.7	9.0
		stdev	0.09	0.03	0.03	0.05	0.15	0.09	0.02	0.01	0.05	0.05	0.02	0.01	0.02	0.02	0.07	0.04
Temp. of seawater to antisurge inlet	°C	mean	7.7	7.6	7.6	7.7	8.6	8.4	8.4	7.7	7.7	7.7	7.7	7.6	7.7	7.7	7.8	8.0
		stdev	0.02	0.006	0.02	0.01	0.17	0.11	0.02	0.008	0.03	0.05	0.01	0.02	0.01	0.02	0.07	0.06

[a] Uncertainty on the lean- and rich loading determination of 4%.
[b] Lean and rich loading not measured for case 1A-2.
[c] SRD is thermal energy consumption.
[d] LVC is electrical energy consumption.

Appendix H – TCM data for scenarios Shah1 to Shah5

Table 1. Phases of the campaign.

Condition	Phase A	Phase B	Phase C	Phase D	Phase E	Phase F
Flue gas flow [Sm^3/h]	40-47,000	50,000	50,000	67,000	67,000	59,000
Absorber packing height [m]	18	18	18	24	24	18
Stripper	CHP	CHP	CHP	RFCC	RFCC	RFCC
CO_2 capture rate [%][1]	85 - 96	90 - 91	89 - 93	95 - 99	98 - 99	90-91
Optimal SRD [GJ/ton CO_2][2]	**3.8** (85)	**3.6** (91)	**3.6** (91)	**3.7** (97)	**4.0** (98)	**3.7** (91)
MEA [wt%]	32	37	34 - 37	35 -36	35 -37	36 -38
CO_2 conc, wet [vol %]	3.6 - 4.2	4.0 – 4.2	3.8 – 4.2	4.0 – 4.2	3.9 – 4.2	4.1 – 4.2
Absorber water wash stages	2	1	1	1/2[3]	1	1
L/G [kg/Sm^3][4]	0.97 - 1.14	0.92 - 1.54	1.13 – 1.74	0.95 – 1.88	1.10 – 1,54	1.12 – 1.47
Flue gas temp [°C]	30	30	45	30	45	30
Rich solvent bypass [%]	0	20	20	20	20	20
Lean solvent temp [°C]	41.2	54.9	54.5	45.0	40.0	44.4
MEA emission [ppmv]	<1	<1	0.6	1.5	2.1	1.1

1: Capture rate is based on method 4 as described in the text. 2: SRD is Specific Reboiler Duty 3 as described in the text. Associated capture rate in parenthesis. 3: Second water wash stage was partially operated to manage emissions. 4: L/G is the ratio of lean solvent flow to flue gas flow into the absorber.

Table 3. Selected cases for economical evaluation [1-3]

#	Abs. pack [m]	MEA[1] [wt%]	Flue gas × 1000 [Sm^3/h]	L/G [kg/Sm^3]	Anti-foam [-]	Stripper bottom temp [°C]	Lean loading [mol/mol]	SRD [GJ/ton CO_2]	CO_2 Capture [%]
MEA-1	24	~ 30	47	1.17	No	119.3	0.23	4.1	~ 85
MEA-2	24	31/30	59	1	Yes	121.0	0.21	3.6	86
MEA-3	18	43/40	51.0	0.98	No	121.7	0.25	3.6	86
F2	18	36/34	59.0	1.29	No	121.0	0.26	3.8	90
B3-rep	18	37/35	50.0	1.13	No	121.4	0.24	3.6	91
D3-rep	24	36/34	67.0	1.12	No	122.5	0.21	3.7	97

1: Number given first is on MEA-water basis, second number is on MEA-water-CO_2 basis.

Table 4. Key cost parameters

	Adjusted abs. Pack [m]	Lean solvent flow [kg/kg CO_2 in]	Spec. packing volume [m^3/t CO_2, h]	Captured CO_2 [t/h]	CO_2 capture [%]
MEA-1[1]	~28	~16	~55	128	85
MEA-2[1]	25.5	14.5	50	128	86
MEA-3[1]	18.9	12.5	37	129	86
F2	16.6	17.5	37	135	90
B3-rep	19.5	14.5	36	136	91
D3-rep	19.6	15.5	34	146	97

Appendix I – Simulation flowsheet of TCM plant